

Oleksij Fomin  
Alyona Lovska



**IMPROVED MODELS AND CONSTRUCTS  
OF STRUCTURAL INTERACTION  
IN RAILWAY CONTAINER TRANSPORTATION**

**Tuculart Edition  
Czech Republic**



Oleksij Fomin, Alyona Lovska

**IMPROVED MODELS AND CONSTRUCTS  
OF STRUCTURAL INTERACTION  
IN RAILWAY CONTAINER TRANSPORTATION**

Tuculart s.r.o.  
Czech Republic, Ostrava  
2022

Fomin, O., & Lovska, A. (2022). Improved models and constructs of structural interaction in railway container transportation. Ostrava: Tuculart Edition.

ISBN 978-80-908353-6-8

DOI: 10.47451/book2022-02-01

The development of foreign economic cooperation of Ukraine as a transit country with European and Asian countries requires the introduction of combined transport systems. Today the most promising of them is the container transportation system due to mobility of a container, which can be transported by any transport facility.

As for railway transport, containers are carried by flat cars. And a lack of rolling stock units requires certain adaptation of the existing rail cars to transportation of some classes of freight. Therefore, the operational efficiency of railway transport can be increased at the modernization stage when the updated dynamic loads are taken into consideration in designing of the appropriate flat car constructs. This can further decrease damage in the elements of flat cars and containers, maintenance costs, increase the cost efficiency and compatibility of container transportation, etc.

The purpose of the monograph is to reveal the special aspects of the designed dynamic and computer models and the conceptual solutions intended for better interaction of the constructs of flat cars and containers during combined transportation. The monograph can be used as educational guidelines for graduate and undergraduate students of the related specialties.

Designed by Tuculart s.r.o., 2022.

Copyright © 2022 Oleksij Fomin  
Copyright © 2022 Alyona Lovska  
All rights reserved.

## CONTENTS

TERMS AND DIFINITIONS.....	5
LIST OF ABBREVIATIONS.....	6
ABSTRACT.....	7
PART 1 ANALYSIS OF THE RESEARCH INTO THE DETERMINATION OF LOADING OF FLAT CAR CONSTRUCTS DURING CONTAINER TRANSPORTATION.....	9
1.1 Special aspects of the loading on the bearing structure of a flat car in operation.....	9
1.2 Analysis of main scientific and engineering publications on the research into the dynamic loading and strength of flat cars and containers.....	12
Conclusions to Part 1.....	20
PART 2 DETERMINATION OF THE DYNAMIC LOADING OF FLAT CARS DURING SHUNTING IMPACTS.....	21
2.1 Mathematic modelling of the dynamic loading on the bearing structure of a flat car with dry-cargo containers during a shunting impact.....	21
2.2 Mathematic modelling of the dynamic loading on the bearing structure of a flat car with tank containers during a shunting impact.....	24
2.3 Computer modelling of the dynamic loading on the bearing structure of a flat car with dry-cargo containers during a shunting impact.....	28
2.4 Computer modelling of the dynamic loading on the bearing structure of a flat car with tank containers during a shunting impact.....	30
2.5 Theoretical substantiation of the introduction of elastic, viscous and elastic-viscous elements in the bearing structure of combined transport facilities to decrease the dynamic loading in operation.....	33
2.5.1 Theoretical substantiation of the introduction of elastic, viscous and elastic-viscous elements in the bearing structure of a dry-cargo container.....	33
2.5.2 Theoretical substantiation of the introduction of elastic, viscous and elastic-viscous elements in the bearing structure of a tank container.....	38

2.5.3 Designing of the computer model of the dynamic loading of containers located on the flat car during a shunting impact.....	41
2.5.4 Designing of a computer model of the dynamic loading of tank containers located on the flat car during a shunting impact.....	45
2.6 Determination of the strength of fixed fitting of a flat car during viscous and elastic-viscous interaction with a container/tank container....	48
Conclusions to Part 2 .....	56
<b>PART 3 EXPERIMENTAL RESEARCH INTO THE STRENGTH OF THE BEARING STRUCTURE OF A FLAT CAR DURING SHUNTING IMPACTS .....</b>	<b>59</b>
3.1 The experimental research into the strength of the bearing structure of a flat car in the standard diagram of interaction between fixed fittings and container fittings.....	59
3.2 Experimental research into the strength of the bearing structure of a flat car during elastic interaction between fixed fittings and container fittings.....	70
Conclusions to Part 3 .....	76
<b>GENERAL CONCLUSIONS .....</b>	<b>77</b>
<b>REFERENCES .....</b>	<b>79</b>
Appendix A. Program and procedure of testing on a flat car loaded with containers in the standard and improved diagrams of interaction between container fittings and fixed fittings .....	86

## TERMS AND DIFINITIONS

**Dynamic loading** is the process characterized by a rapid change of values, vectors, or points (areas) of the application of the dynamic loads and emergence of dynamic forces in the structural elements.

**Interoperability** is the ability of railway transport to maintain the safe and smooth motion of the rolling stock in compliance with the required operational quality according to the level of technical, technological, organizational and efficient support prescribed by the appropriate technical requirements for operational compatibility (Draft Law of Ukraine “On Railway Transport of Ukraine, No.9512).

**Train ferry** is a vessel intended for transportation of railway transport facilities.

**Strength** is the ability of material to resist failures resulting from the stresses due to external forces.

**Multi-functionality** is the principle according to which each element/unit performs more than one function simultaneously in the whole structure.

**Over-standardized mode** is the mode during which the bearing structure carries the loading which exceeds the normative values.

**Stress state** is the combination of normal and shear stresses emerging in different zones passing across the given point.

**Bearing structure of a rail car** is the combination of the structural elements which carry the main loading in operation.

**Rail car damage** is an event which impairs the normal state of a rail car while maintaining its operability.

**Operational mode** is the usage rate of a car according to the design parameters or those determined through its operation.

## LIST OF ABBREVIATIONS

FC	–	flat car
DL	–	dynamic loading
SE	–	state enterprise
TF	–	train ferry
IPT	–	isoparametric tetrahedron
TC	–	tank container
FEM	–	finite element method
SS	–	stress state
FE	–	finite element
FEM	–	finite element model
GMM	–	generic mathematical model



## ABSTRACT

The development of foreign economic cooperation of Ukraine as a transit country with European and Asian countries requires the introduction of combined transport systems. Today the most promising of them is the container transportation system due to mobility of a container, which can be transported by any transport facility.

As for railway transport, containers are carried by flat cars. And a lack of rolling stock units requires certain adaptation of the existing rail cars to transportation of some classes of freight. Therefore, the operational efficiency of railway transport can be increased at the modernization stage when the updated dynamic loads are taken into consideration in designing of the appropriate flat car constructs. This can further decrease damage in the elements of flat cars and containers, maintenance costs, increase the cost efficiency and compatibility of container transportation, etc.

The purpose of the monograph is to reveal the special aspects of the designed dynamic and computer models and the conceptual solutions intended for better interaction of the constructs of flat cars and containers during combined transportation.

The purpose was accomplished by the following tasks:

- to analyze the scientific research into the determination of the loading of flat car constructs in operation;
- to study the dynamic loading of containers and tank containers located on a flat car during a shunting impact;
- to build the mathematic models for the determination of the dynamic loading of containers and tank containers with elastic, viscous and elastic-viscous elements in the fittings;
- to test the strength of a flat car loaded with containers during a shunting impact.

*The subject of the research* is the processes of emerging, sustaining, and distributing the loads in flat car constructs and containers during their interaction.

*The scope of the research* is the functional models of flat car constructs and containers, and also the conceptual solutions to their improvements.

The monograph will be of interest to scientists and engineers concerned about the development of and research into the mechanics of the bearing

structure of freight cars and containers, and particularly, it will be of interest to scientists, designers, developers, doctoral and post-graduate students.

The monograph can be used as educational guidelines for graduate and undergraduate students of the related specialties.

Keywords: transport mechanics, railway transport, combine transportation, flat car, container, tank container, dynamic loading, strength, bearing structure.

**PART 1**  
**ANALYSIS OF THE RESEARCH INTO THE DETERMINATION**  
**OF LOADING OF FLAT CAR CONSTRUCTS DURING**  
**CONTAINER TRANSPORTATION**

**1.1 Special aspects of the loading on the bearing structure of a flat car in operation**

Railway transport can maintain the leading position in the transportation market only through the introduction of innovative rolling stock with improved technical and economic characteristics. It can be done at the designing stage by taking into account the updated dynamic loading which emerges during operational modes, particularly, over-standardized ones. The main and most frequent over-standardized operational modes of flat cars are:

- train ferry transportation of flat cars within combined trains; and
- shunting impacts of flat cars loaded with containers with consideration of technological gaps between the container fittings and fixed fittings.

If these loads are taken into account at the stage of designing constructs of flat cars and containers and if they are being improved, it may lead to fewer failures in operation, better traffic safety and ecological safety of freight transportation, better interoperability, etc.

In accordance with the data from the Ministry of Infrastructure for 2020 the volume of container transportation via the sea ports of Ukraine increased to 425000 TEU in comparison to 2019. And the containers transported are processed at the ports of Odessa, Chornomorsk, Yuzhny, and Olvia.

In comparison to 2019 the amount of containers transported by trains has also increased by 41%. In general 230000 TEU was transported by container trains. However, containers are transported not only by rail, but also by train ferries within combined trains.

At present train ferry routes connect Ukraine with Bulgaria, Georgia, and Turkey. Taking into account a rapid development of combined transportation the experts in the field forecast a growth of train ferry routes via the Black Sea.

Such an increase of freight transportation volume between European and Asian countries requires introduction of new transportation routes. One of the recent routes is the international transport corridor connecting European and

Asian countries. It was launched at the beginning of 2016 with the first combined train across the Black Sea to China.

In 2020 Ukrainian Railways (UZ) had 4330 flat cars for transportation of containers, among which five containers belonged to the Lviv Railways, 161 flat cars – to Refrigerated Wagon Company of UZ, and 3766 flat cars – to the center *Liski* of UZ.

At the moment of the research the inventory rolling stock of UZ had 111 flat cars for container transportation. And the volume of container transportation has been increasing all over the world.

The monograph deals with the determination of the amount of failures in fixed fittings during operations on the basis of data released by Ukrainian Railways. The results of the research are given in figure 1.1.

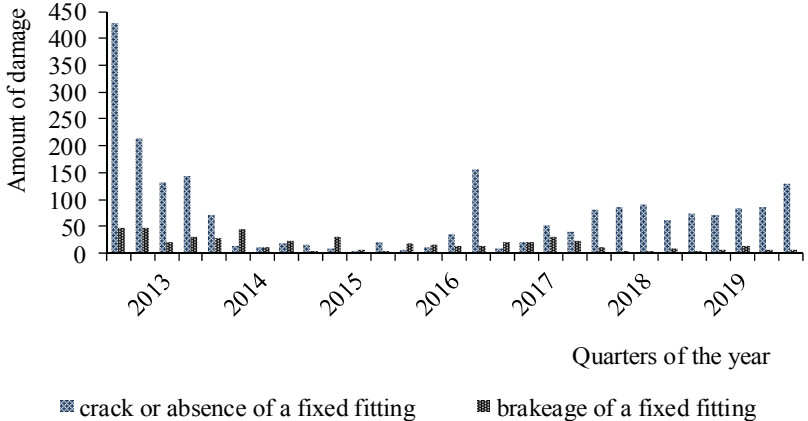


Figure 1.1 – Amount of failures in the fixed fittings of flat cars in operation

Figure 1.1 demonstrates that 2013 saw the maximum amount of such failures. This can be explained by intensive container transportation that period. Besides, when flat cars interacted with containers the latter suffer damage during transportation.

According to the information from open sources in Internet, the amount of damaged fixed fittings of flat cars on Russian Railways (RZD) is given in figure 1.2.

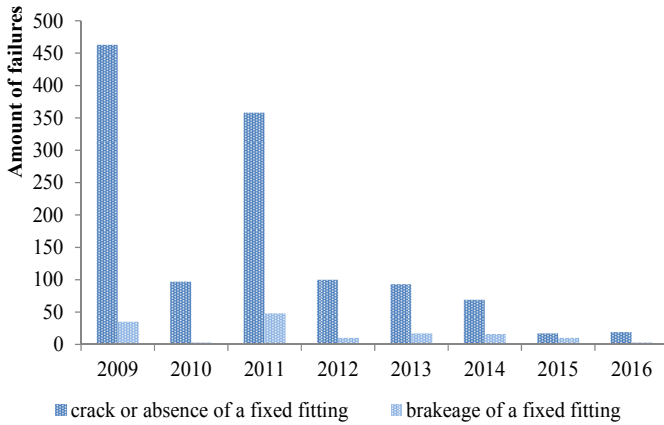
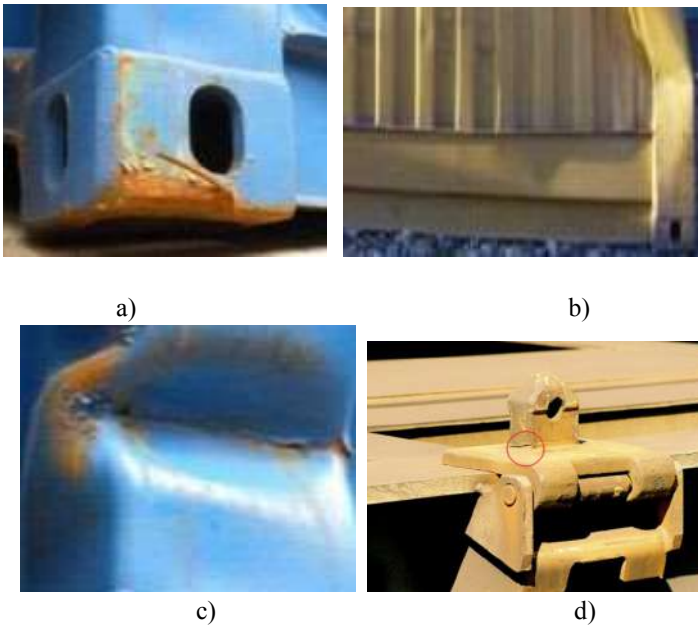


Figure 1.2 – Amount of failures in fixed fittings of flat cars on RZD

The most frequent failures in fixed fittings and container fittings are given in figure 1.3.



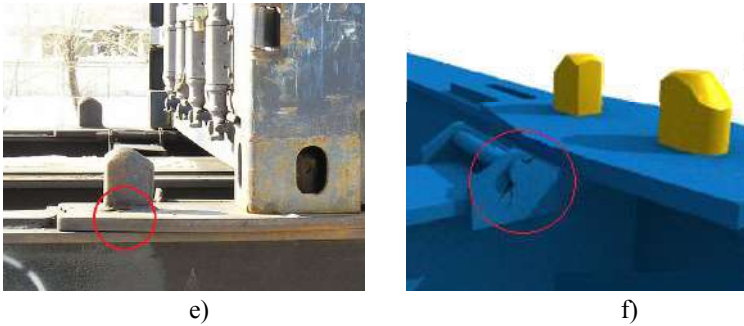


Figure 1.3 – Failures in container fittings and fixed fittings  
 a) distortion of a fitting; b) breakage of a post; c) deformation of a post;  
 d) e) cracks in a fixed fitting; f) failure in a fastening element

And the most frequent failures in fixed fittings are cracks in the structure, and in containers – cracks in the fittings and deformations of the bearing structure of a container. Therefore, it is important to create the measures for decreasing the dynamic loading of flat cars and containers in operation.

## 1.2 Analysis of main scientific and engineering publications on the research into the dynamic loading and strength of flat cars and containers

It is known that the main loads on a car in operation are classified by line of action, among which are vertical, transverse, and longitudinal. Generally, these forces act independently. The strength calculation of a rail car includes the least favorable combination of the forces according to the design modes [7, 26, 67].

Two main design modes (I and III) and one additional mode (II) are taken into account in the car building industry [8, 27, 69]. In operation mode I for freight cars includes such conditions: stoppage and restart; impact of cars during shunting operations, breaking-up on the hump; emergency braking at low speeds. This mode is characterized by a rare combination of extreme loads. The basic requirement for the strength calculation is to avoid residual deformation (failures) in a rail car unit. The allowable stresses are taken close

to the yield limit of the material with consideration of the loading type (quasi-static, impact) and the material properties.

Design mode III includes the common operational conditions of freight and passenger cars movement along straight and curved track sections, and over the switch points at an allowable speed with regular service braking. This case is characterized by relatively frequent combination of sufficient loads, natural for normal operation of a rail car in the moving train.

The main requirement in calculation is to avoid the damage in the car unit due to material fatigue. The allowable stresses are taken close to the endurance limit of the material with consideration of the combined action of quasi-static, vibration and impact loads, and corrosive effect.

Additional special mode II is used for certain types of cars as the combination of loads typical for these cars (e.g., loading/unloading works, repairs, etc.).

It should be noted that the existing standards do not completely cover special aspects of loading of the flat car with containers during shunting impacts with consideration of gaps between the container fittings and fixed fittings, loading of the bearing structure with elastic (viscous and elastic-viscous) elements during the operational modes, etc. The present stage of development of transport industry ultimately requires their consideration in designing innovative rolling stock.

It is known that one of the most required rail cars for international transportation is the flat car. The issues of development and improvement of the bearing structure of a flat car are considered by leading specialists of rail car building enterprises of the CIS countries.

A choice of the structural design diagram and parameters of the bearing structure of a flat car for transportation of high-capacity containers is considered in [34]. The authors described the structural features to be used for classification, and formed the generalized structural diagram for selecting the structural parameters of a long-base flat car. The study gives the parameterized FE model of the frame structure of a long-base flat car presented as the mesh with a variable step. The authors conducted the experimental research on a flat car sample in order to determine the validity of the technique suggested.

Shaitanova I.K. substantiated the possibility to use the standard 13-401 and 13-4012 flat cars for transportation of containers [68]. The study gives a comprehensive approach to rail car modernization based on the demand forecast for certain rail cars, and the analysis of the technical and economic

efficiency. On the basis of this approach the author demonstrated the possibility and efficiency of re-equipment of standard flat cars into container flat cars. The author substantiated the possibility to re-equip the standard 13-401 and 13-4012 flat cars for transportation of high-capacity containers.

The better strength characteristics of long-base flat cars by improving their structure and calculation methods are described in [62]. The study deals with the stress strain state estimation of the long-base flat car frame according to various operational loads. Besides, the study presents the determination of the rational parameters of the bearing structural elements of a long-base flat car with consideration of various loading diagrams.

A choice of structural solutions of articulated flat cars is given in [60]. The author described the promising engineering solutions for 1520-mm articulated flat cars, developed the computer modelling technique, and gave the description of how an articulated flat car for containers with turnstile supports and without them passed curved sections and humps in the sorting yards. Besides, the study presents the determination of the optimal dimensions of the structural elements which provide the safe traffic on such track sections.

Gurgi N.L. together with Prof. Miamlin S.V. conducted the research “Improved engineering characteristics of a section flat car by means of structural changes” [17]. The study presents the mathematical model for determination and estimation of the basic strength characteristics of a six-axle section flat car, and the mathematical model which describes the spatial oscillations of a section flat car. The author determined the dependencies of the dynamic loading of a section flat car on the elastic-dissipative parameters of a bogie, and improved the testing methods for determining the fatigue strength parameters of a flat car.

Study [22] deals with the methods to prolong the service life of special flat cars. The comparative estimation techniques proposed for the variants of how to prolong the service life of the flat car included the economic efficiency factor. The FE models of the improved flat cars included the changes after overhauls aimed at longer service life; the study also includes the strength calculation.

The structure and parameters of a long-base flat car for transportation of road-trains and high-capacity containers are substantiated in [43]. The study also deals with FE models of the flat car frames. The author developed the mathematical model of a long-base structure of a flat car with an optimal frame for determination of the basic dynamic characteristics. She also studied the



impact of the elasticity of a long-base flat car frame on the dynamic characteristics.

It should be noted that the research conducted did not include over-standardized loads on the bearing structure of a flat car, particularly, transportation of a flat car within a combined train by the train ferry.

Bogomaz G.I. studied the dynamics of a tank car (rail cars and containers) during the longitudinal impacts and transitional motion modes [3]. The author developed and substantiated the methods of modelling and study of the dynamic loading on the structural elements of tank cars with consideration of oscillations of the liquid freight during shunting impacts and transitional modes of trains; these methods are aimed at designing specialized rail cars and containers with improved technical and economical characteristics and reduced material capacity which can transport liquid freight (including hazardous).

Improvements in rail cars on the basis of detachable bodies are considered by Daukshi A.S. in her research [18]. The author studied the linear dimensions of detachable bodies and the technical and economical parameters of a rail car, and conducted a choice of the main types of bodies and their linear dimensions. The calculation of the required flat cars and detachable bodies included the seasonal changes in freight dispatches. The study also deals with the cost benefit analysis of the application of detachable bodies.

However, the designing of detachable bogies did not include potential loads during over-standardized operational modes.

A choice of the scientific substantiation of the structural solution aimed at provision of the strength of the main units of a tank container is presented in [66]. The author designed an improved mathematical model for the determination of the dynamic loading of a tank container transported by a flat car. They determined the dynamic loading on a tank container for various structural solutions. The authors developed the recommendations for the designing of a tank container and the optimal structural solutions, which are in conformance with the safety requirements for a tank container transported by rail.

The author proposed the engineering solutions to increase the strength of the fastening elements of the framework for the barrel of a tank container and a hatch. But these solutions are implemented through the reinforcement of the bearing structure of a tank container, but not through a decrease in the dynamic loading in operation.

In his work Arshintsev D.N. suggested the methods for increasing the

efficiency of the container transportation and ensuring the safe motion of container trains [2]. The author proved the efficiency of special trunked flat cars for transportation of containers loaded at two levels. The study presents the method for the calculation of containers located on the second level and the requirements for them. The experimental research was made for a 13-3124 flat car intended for transportation of high-capacity containers loaded by two levels.

The research into the stress strain state of high-capacity containers in operation is presented in the study by Kostritsa S.A. [31]. The finite element method used for the determination of the loading of a high-capacity container was presented as a spatial plate-framed system. The study presents the analysis of various calculation diagrams for estimation of the loading on the structural elements of a high-capacity container. It shows which calculation diagrams are more efficient for estimation of the strength of a container during a particular operational mode. The study also deals with the method for determination of the dynamic loading of a high-capacity container under the longitudinal loading. The calculation diagram “flat car – container – cargo” was used as a spatial plane-framed structure with non-linear elements. By solving the task, the non-linear mechanical system was presented as several linear forces connected by interaction forces simulating the non-linear links. The analysis demonstrated that the dynamic loading in the structural elements of a high-capacity container depended on the conditions of freight loading in the containers and the conditions of container allocation.

On the basis of the results of theoretical research the author made the recommendations for a selection of the optimal parameters for some structural elements of high-capacity containers and the method for their fastening on a flat car. As far as the re-equipment of flat cars with more efficient absorbing devices is rather energy-intensive, the author suggested some changes in the structure of units for fixation of containers on flat cars; this solution can reduce gaps between the fixed fittings and container fittings due to special absorbers.

The author proposed the measures for decreasing the dynamic loading of containers in operation; however the substantiation of these measures was not given. Besides, structurally, these improvements can be used for fixed fittings, not for container fittings.

The enhanced calculation method for fixation of freight during impacts of rail cars was considered in [32]. The author obtained the analytical formula for determining the vertical inertia force of the body; this force is transferred to the absorbers and the lashing devices at the moment of their maximum pressure on

the cargo during oscillations due to the natural oscillation frequency and the acceleration amplitudes which emerge during the oscillations of the cargo with its natural frequency and amplitude. The results of the experiments revealed a considerable influence of the pre-stressing forces in the spreaders on the loading distribution between fixation devices; the results made it possible to determine their optimal values.

However the issue of decreasing the dynamic loading of the spreaders during shunting impacts of a rail car was not studied.

The issue of situational adaptation of freight rail cars for international transportation was considered by Morchiladze I.G. [50]. The study deals with the method of situational adaptation of freight cars for international transportation; the method includes the weight-dimension limitations for transport corridors and compatibility of road, sea, and rail transport facilities for transferring heavy cargo. The author developed the algorithm to re-equip freight cars for international transportation. The author found the dependencies in changing strength, dynamic and aerodynamic characteristics of freight rail cars with various structural diagrams of bodies, frames, gear parts, and with consideration of one- and multi-level transportation of enlarged cargo units.

However, the author did not study the situational adaptation of rail cars for flat car transportation.

Improved calculation methods for the fatigue resistance of welded frames of long-base flat cars are studied in [10]. The study deals with the improved method for calculation of the fatigue resistance of welded joints of long-base flat car frames with determination of the efficient factor of stress concentrations with consideration of FE models of welded joints. The author built the FE models of various welded joints (T-like, lap-welded and butt joint) for the beams of long-base flat car frames with consideration of welded joint configuration, poor structural penetration, and thermal impact zone. The author experimentally determined the mechanical characteristics of the material in various welded areas.

The research included the normative values of the loads in a flat car in operation. Thus, the over-standardized loading modes on the bearing structure of a flat car in operation were not studied.

The structure of a car for intermodal transportation is analyzed in [83]. The special feature of such a car is a lowered middle part and reversible sectors. The car structure allows loading/unloading automobiles on/off by gravity.

The strength of the carrying capacity of a flat car with a motor semi-trailer was modeled in [5]. The study presents a design diagram with refined stress values in the bearing structure of a flat car.

Special features of a car for transportation of transport facilities and containers are presented in [85]. The car structure allows easy loading/unloading without any infrastructure or terminals. The study presents the dynamic characteristics obtained. The calculation was made in MSC Adams. It was found that the suggested solutions provided the needed strength of a rail car [75].

The strength of a flat car for the static and dynamic loading on the bearing structure is defined in [86]; the authors used experimental methods, in particular, strain measurement methods.

The spatial oscillations of a flat car with long items of cargo moving along the track with joint and harmonic irregularities in the horizontal and vertical planes are studied in [1]. The oscillations of the mechanic system are described with twenty-differential equations.

However, the calculation of the bearing structure of a rail car did not include the over-standardized loading modes in operation.

The issue of the determination of the dynamic loading and strength of the bearing structure of a container during operational modes was studied by many specialists.

The special features of the application of simplified measurement methods for the strain stress state of a container body with changeable capacity are described in [46, 47]. The authors presented the loading diagram and the measuring technique for longitudinal and transverse distortions in the container bodies.

The determination of the stress strain state of a container body with variable capacity is given in [48]. The calculation was made in ANSYS. The adequacy of the results obtained was checked experimentally for the transverse distortion of a container at small loads.

The research into the stress strain state of a container body during crane-lifting and drag-towing is presented in [21]. The theoretical determination of the strength characteristics was made in APM WinMachine. The experimental research was made by the strain gage measurement.

The special features of designing a container for transportation of fruit and vegetable products are described in [24]. The authors gave the requirements

for a container body, proposed the design of such a container, and presented the strength calculation with the finite element method.

The determination of the dynamic loading of a container during operational loading modes is given in [87]. The values of the dynamic loads obtained were included in the strength calculation of a container in ANSYS.

The peculiarities of the strength calculation of the floor for a 40-foot container in Abaqus/CAEv 6.1 are given in [72]. The study deals with the safety recommendations for such containers. The special features of designing the containers intended for transportation of long pipes by sea are presented in [55]. The authors presented the results of the strength calculation of the container framework during transportation of long pipes.

The determination of the dynamic loading of a flat car with containers is given in [71]. The model presented can be used for calculation of the displacements of a container during longitudinal loading on the flat car. Study [70] presents the determination of the dynamic loading of the bearing structure of a container located on a flat car during a shunting impact. The authors obtained the accelerations of a container during such an impact.

The dynamic stability of the freight during its loading into the container and transportation is presented in [73]. The research was conducted for package cargo. The measures for the loading and fixation of steel rolls in containers transported by rail and sea are considered in [4].

The special features of designing containers intended for transportation of long cargo are considered in [82]. The strength calculation for the bearing elements of a container under the loads from the pipes transported was conducted with the FEM. The impact of the gravity center of a flat car on the metacentric height of a ferry is studied in [63]. The authors suggested an algorithm for evaluation of the impact of the position of a container's gravity center on the stability of a container ship. However, in the above-mentioned works the authors did not raise the problem of improvements for the bearing structure of a container to decrease the dynamic loading in operation.

## **Conclusions to Part 1**

1. The monograph deals with the prospects of combined transport trains in international transportation and presents the statistic data on freight transportation by these trains. It was found that the volume of container transportation has been increasing.

2. The authors studied the statistic data on damage in the bearing structure of flat cars and containers in operation. The most frequent damage in the fixed fitting of flat cars is structural cracks and that of containers – cracks in container fittings and deformations in the bearing structure.

3. The authors also analyzed the main scientific publications dedicated to the research into the dynamic loading and strength of flat cars. It was found that great contribution to the theoretical foundations of the dynamic loading and strength of the bearing structure of rail cars was made by leading specialists from Ukraine, CIS, Check Republic, Slovakia and other countries.

The further development in the determination of the dynamic loading and strength of flat cars and their structural improvements is a rather important and challenging task.

The analysis of the existing standards on designing rail cars showed that they do not thoroughly cover over-standardized loading modes of rail cars in operation. It causes damage in the bearing structure of a car in operation, requires off-scheduled repairs, and can endanger the traffic safety.

## PART 2

### DETERMINATION OF THE DYNAMIC LOADING OF FLAT CARS DURING SHUNTING IMPACTS

#### 2.1 Mathematic modelling of the dynamic loading on the bearing structure of a flat car with dry-cargo containers during a shunting impact

The performance values of the dynamic loads on the bearing structure of a container located on the flat car during a shunting impact were calculated with the mathematical model given in [4]. The model included three tank containers located on a long-base flat car; the interconnection was simulated as elastic-frictional, i.e. each tank container had the degree of freedom in the vertical plane. It should be noted that in practice containers and tank containers are transported by flat cars which can accommodate two containers on the frame. Such cars have a shorter base, and, therefore, lower values of the displacements of the bearing structure under the vertical loads from the containers.

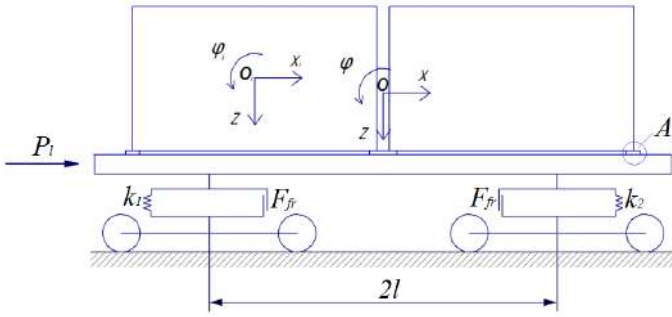
The diagram of the longitudinal force to a flat car loaded with containers with the friction forces between the container fittings and fixed fittings is given in figure 2.1.

The research was made for a 13-4085 flat car manufactured by DniproVahonMash (Ukraine) and for a 1CC container (according to ISO).

The container was considered as an adjacent mass relative to the flat car frame, longitudinally flexible due to the gaps between the fixed fittings located on the flat car and the container fittings. Thus, the container had the degree of freedom until the container fitting rested against the fixed fitting, and then the container repeated the movement pattern of the flat car. The interaction between the flat car frame and container fittings was simulated as frictional [76, 77, 78].

$$M'_{FC} \cdot \ddot{x}_{FC} + M_{FC} \cdot h \cdot \ddot{\varphi}_{FC} = P_l - \sum_{i=1}^2 F_{fr}^c, \quad (2.1)$$

$$\begin{aligned} I_{FC} \cdot \ddot{\varphi}_{FC} + M_{FC} \cdot h \cdot \ddot{x}_{FC} - g \cdot \varphi_{FC} \cdot M_{FC} \cdot h = \\ = l \cdot F_{fr} (\text{sign} \dot{\Delta}_1 - \text{sign} \dot{\Delta}_2) + l(k_1 \cdot \Delta_1 - k_2 \cdot \Delta_2), \end{aligned} \quad (2.2)$$



A (expanded)

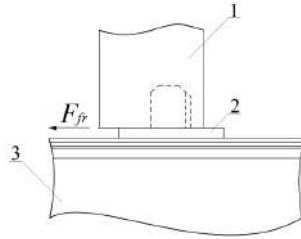


Figure 2.1 – Diagram of the longitudinal force on a flat car with containers  
 1 – container fitting; 2 – fixed fitting; 3 – longitudinal beam of a flat car

$$M_{FC} \cdot \ddot{z}_{FC} = k_1 \cdot \Delta_1 + k_2 \cdot \Delta_2 - F_{fr} (\text{sign} \dot{\Delta}_1 + \text{sign} \dot{\Delta}_2), \quad (2.3)$$

$$m_i \cdot \ddot{x}_i + (m_i \cdot z_{ci}) \cdot \ddot{\varphi}_i = -F_{fr}^c, \quad (2.4)$$

$$I_i \cdot \ddot{\varphi}_i + (m_i \cdot z_{ci}) \cdot \ddot{x}_i - g \cdot (m_i \cdot z_{ci}) \cdot \varphi_i = 0, \quad (2.5)$$

$$m_i \cdot \ddot{z}_{FC} = 0, \quad (2.6)$$

where

$$M'_{FC} = M_{FC} + 2 \cdot m_b + \frac{n \cdot I}{r^2}; \Delta_1 = z_{FC} - l \cdot \varphi_{FC}; \Delta_2 = z_{FC} + l \cdot \varphi_{FC},$$



where  $M_{FC}$  – mass of the bearing structure of a flat car;  $I_{FC}$  – inertia moment of a flat car relative to the longitudinal axle;  $P_l$  – value of the longitudinal impact force to the coupler;  $F_{fr}^c$  – friction force between the fixed fitting and container fitting during the longitudinal displacement of a container;  $m_b$  – bogie mass;  $I$  – inertia moment of a wheel set;  $r$  – radius of an average worn-out wheel;  $n$  – number of the bogie axles;  $l$  – half base of a flat car;  $F_{fr}$  – absolute value of the dry friction force in a spring group;  $k_1, k_2$  – rigidity of the springs in the spring group of a flat car;  $m_i$  – container mass;  $z_{ci}$  – height of the gravity center of a container;  $I_i$  – reduced inertia moment of the  $i$ -th container;  $x_{FC}, \varphi_{FC}, z_{FC}$  – coordinates corresponding to the longitudinal, angular (around the side axle), and the vertical displacements of a flat car;  $x_i, \varphi_i$  – coordinates corresponding to the longitudinal, transverse, and angular (around the transverse axle) displacements of a container.

Whereas  $x_i < 30$  mm [14, 15, 16], if  $x_i \geq 30$  mm, than  $x_i = x_{FC}$ .

The vertical displacements of a container relative to the flat car frame were neglected. The value of the longitudinal impact to the flat car was taken 3.5 MN.

The differential equations were solved with the Runge–Kutta method in MathCad [15, 16].

The results of the research demonstrated that with gaps between the fixed fittings and container fittings, the accelerations to the bearing structure were approximately 90 m/s<sup>2</sup> and 110 m/s<sup>2</sup>, respectively.

The accelerations to a flat car with containers during a shunting impact were determined with the mathematical model which included the absence of gaps between the fixed fittings and container fittings. This model was reduced to the following form

$$M'_{\text{III}} \cdot \ddot{x}_{\text{III}} + M_{\text{III}} \cdot h \cdot \ddot{\varphi}_{\text{III}} = S_a, \quad (2.7)$$

$$\begin{aligned} I_{\text{III}} \cdot \ddot{\varphi}_{\text{III}} + M_{\text{III}} \cdot h \cdot \ddot{x}_{\text{III}} - g \cdot \varphi_{\text{III}} \cdot M_{\text{III}} \cdot h = \\ = l \cdot F_{TP} (\text{sign} \dot{\Delta}_1 - \text{sign} \dot{\Delta}_2) + l (k_1 \cdot \Delta_1 - k_2 \cdot \Delta_2), \end{aligned} \quad (2.8)$$

$$M_{\text{III}} \cdot \ddot{z}_{\text{III}} = k_1 \cdot \Delta_1 + k_2 \cdot \Delta_2 - F_{TP} (\text{sign} \dot{\Delta}_1 + \text{sign} \dot{\Delta}_2), \quad (2.9)$$

$$m_i \cdot \ddot{x}_{\text{III}} + (m_i \cdot z_{ci}) \cdot \ddot{\varphi}_{\text{III}} = 0, \quad (2.10)$$

$$I_i \cdot \ddot{\phi}_{III} + (m_i \cdot z_{ci}) \cdot \ddot{x}_{III} - g \cdot (m_i \cdot z_{ci}) \cdot \varphi_{III} = 0, \quad (2.11)$$

$$m_i \cdot \ddot{z}_{III} = 0, \quad (2.12)$$

thus, it disregarded the friction forces between the fixed fitting and container fittings, and the inertia forces which emerged during the motion of a container relative to the flat car frame.

It was found that the maximum acceleration to a flat car and the containers located on it during a shunting impact was about 50 m/s<sup>2</sup>.

## **2.2 Mathematic modelling of the dynamic loading on the bearing structure of a flat car with tank containers during a shunting impact**

The analysis of the standards on the strength of tank containers in operation has demonstrated that the maximum dynamic loads on the bearing structure and fastening units are presented in GOST 31232 “Containers for transportation of dangerous freight. Operational safety requirements” [13]. According to these standards, the tank container structure must bear the own inertia forces emerging in motion, and also during a shunting impact of rail cars, including breaking-up on humps, emergency braking at low speeds and at the following accelerations: in the longitudinal direction  $P_{np} - 2g$ ; in the transverse direction  $P_n - 1g$ ; in the vertical direction  $P_e - 2g$ ; during shunting impacts: for a loaded container  $- 4g$ ; for an empty container (for an equipment check)  $- 5g$  [66].

The operational values of the dynamic loads on the bearing structure of a tank container placed on the flat car during a shunting impact were determined with the mathematical model developed by Prof. G. I. Bogomaz [4].

The research was conducted for a 13-4085 flat car manufactured by DniproVahonMash and for a TK25 tank container manufactured by Zarechensk Plant of Chemical Machine Building. It was a ICC container (ISO) intended for transportation of combustible and lubricating materials, petrol, diesel fuel, lubricants, motor oil, soot, solvent-naphtha, petroleum solvent and foaming agent.

The diagram of the longitudinal force to a flat car with containers is presented in figure 2.2.

The tank container was taken as an adjacent mass relative to the flat car frame, longitudinally flexible due to gaps between the fixed fittings and tank container fittings. Thus, the tank container had the degree of freedom up to the moment when the fitting rested against the fixed fitting, and then the tank container repeated the movement pattern of the flat car.

The interaction between the flat car frame and container fittings were simulated as frictional. Besides, it was taken into account that the tank containers located on the flat car were equally loaded with liquid freight [4, 77].

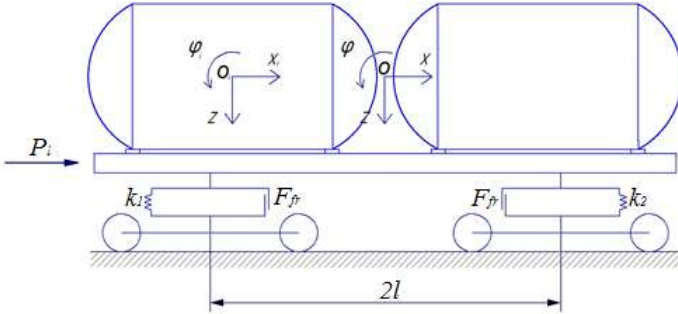


Figure 2.2 – Diagram of the longitudinal force to a flat car with containers

$$M'_{nl} \cdot \ddot{x}_{nl} + M_{nl} \cdot h \cdot \ddot{\varphi}_{nl} = S_a - \sum_{i=1}^2 S_i, \quad (2.13)$$

$$I_{nl} \cdot \ddot{\varphi}_{nl} + M_{nl} \cdot h \cdot \ddot{x}_{nl} - g \cdot \varphi_{nl} \cdot M_{nl} \cdot h = l \cdot F_{fp} (\text{sign} \dot{\Delta}_1 - \text{sign} \dot{\Delta}_2) + l(k_1 \cdot \Delta_1 - k_2 \cdot \Delta_2), \quad (2.14)$$

$$M_B \cdot \ddot{z}_B = C_1 + C_2 - F_{fp} (\text{sign} \dot{\Delta}_1 + \text{sign} \dot{\Delta}_2), \quad (2.15)$$

$$\left( m_i + \sum_{j=1}^k m_{ij} \right) \cdot \ddot{x}_i + \left( m_i \cdot z_{ci} + \sum_{j=1}^k m_{ij} \cdot c_{ij} \right) \cdot \ddot{\varphi}_i - \sum_{j=1}^k m_{ij} \cdot l_{ij} \cdot \ddot{\xi}_{ij} = S_i, \quad (2.16)$$

$$\left( I_{\theta_i} + \sum_{j=1}^k m_{ij} \cdot c_{ij}^2 \right) \cdot \ddot{\varphi}_i + \left( m_i \cdot z_{ci} + \sum_{j=1}^k m_{ij} \cdot c_{ij} \right) \cdot \ddot{x}_i + \sum_{j=1}^k m_{ij} \cdot c_{ij} \cdot l_{ij} \cdot \ddot{\xi}_{ij} - g \cdot \left( m_i \cdot z_{ci} + \sum_{j=1}^k m_{ij} \cdot c_{ij} \right) \cdot (\varphi_{nl} - \varphi_i) = 0, \quad (2.17)$$

$$\left( m_i + \sum_{j=1}^k m_{ij} \right) \cdot \ddot{z}_{iII} = 0, \quad (2.18)$$

$$I_{ij} \cdot \ddot{\xi}_{ij} - m_{ij} \cdot l_{ij} \cdot \ddot{x}_{ij} - m_{ij} \cdot c_{ij} \cdot l_{ij} \cdot \ddot{\varphi}_i + g \cdot m_{ij} \cdot l_{ij} \cdot \ddot{\xi}_{ij} = 0, \quad (2.19)$$

where

$$M'_{iII} = M_{iII} + 2 \cdot m_T + \frac{n \cdot I}{r^2}; \Delta_1 = z_{iII} - l \cdot \varphi_{iII}; \Delta_2 = z_{iII} + l \cdot \varphi_{iII}$$

$$S_i = f_{mp} \cdot \text{sign} \cdot (x_{iII} - x_i)'$$

where  $M_{iII}$  – mass of the bearing structure of a flat car;  $I_{iII}$  – inertia moment of a flat car relative to the longitudinal axle;  $S_a$  – value of the longitudinal impact force to the coupler;  $f_{mp}$  – amplitude value of the dry friction force;  $m_T$  – bogie mass;  $I$  – inertia moment of a wheel set;  $r$  – radius of an average worn-out wheel;  $n$  – number of the bogie axles;  $l$  – half base of a flat car;  $F'_{mp}$  – absolute value of the dry friction force in a spring group;  $k_1, k_2$  – rigidity of the springs of the spring suspension of bogies of a flat car;  $k$  – number of oscillation tones of the liquid freight;  $m_i$  – mass of the body equivalent to the  $i$ -th container with the part of the liquid freight not involved in the displacement relative to the barrel;  $m_{ij}$  – mass of the  $j$ -th pendulum in the  $i$ -th container;  $z_{ci}$  – height of the gravity center of a tank container;  $c_{ij}$  – distance from the plane  $z_i = 0$  to the point of fixation of the  $j$ -th pendulum in the  $i$ -th tank container;  $l_{ij}$  – length of the  $j$ -th pendulum;  $I_{ij}$  – reduced moment of the  $i$ -th tank container and the liquid freight not involved in the motion relative to the barrel;  $I_{ij}$  – inertia moment of the pendulum;  $x_{iII}, \varphi_{iII}, z_{iII}$  – coordinates corresponding to the longitudinal, angular (around the longitudinal axle), and vertical displacements of a flat car;  $x_i, \varphi_i$  – coordinates corresponding to the longitudinal and angular (around the longitudinal axle) displacements of a tank container;  $\xi_{ij}$  – angle of deflection of the  $j$ -th pendulum from the vertical position.

Whereas  $x_i < 30$  mm [14, 15, 16], if  $x_i \geq 30$  mm, than  $x_i = x_{iII}$ . Thus,

$$M'_{iII} \cdot \ddot{x}_{iII} + M_{iII} \cdot h \cdot \ddot{\varphi}_{iII} = S_a, \quad (2.20)$$

$$I_{\text{III}} \cdot \ddot{\varphi}_{\text{III}} + M_{\text{III}} \cdot h \cdot \ddot{x}_{\text{III}} - g \cdot \varphi_{\text{III}} \cdot M_{\text{III}} \cdot h = l \cdot F_{\text{TP}} (\text{sign} \dot{\Delta}_1 - \text{sign} \dot{\Delta}_2) + l(k_1 \cdot \Delta_1 - k_2 \cdot \dot{\Delta}_2), \quad (2.21)$$

$$M_{\text{III}} \cdot \ddot{z}_{\text{III}} = k_1 \cdot \Delta_1 + k_2 \cdot \Delta_2 - F_{\text{TP}} (\text{sign} \dot{\Delta}_1 + \text{sign} \dot{\Delta}_2), \quad (2.22)$$

$$\left( m_i + \sum_{j=1}^k m_{ij} \right) \cdot \ddot{x}_{\text{III}} + \left( m_i \cdot z_{ci} + \sum_{j=1}^k m_{ij} \cdot c_{yj} \right) \cdot \ddot{\varphi}_{\text{III}} - \sum_{j=1}^k m_{ij} \cdot l_{yj} \cdot \ddot{\xi}_{yj} = 0, \quad (2.23)$$

$$\left( I_{\theta i} + \sum_{j=1}^k m_{ij} \cdot c_{yj}^2 \right) \cdot \ddot{\varphi}_{\text{III}} + \left( m_i \cdot z_{ci} + \sum_{j=1}^k m_{ij} \cdot c_{yj} \right) \cdot \ddot{x}_{\text{III}} + \sum_{j=1}^k m_{ij} \cdot c_{yj} \cdot l_{yj} \cdot \ddot{\xi}_{yj} - g \cdot \left( m_i \cdot z_{ci} + \sum_{j=1}^k m_{ij} \cdot c_{yj} \right) \cdot \varphi_{\text{III}} = 0, \quad (2.24)$$

$$\left( m_i + \sum_{j=1}^k m_{ij} \right) \cdot \ddot{z}_{\text{III}} = 0, \quad (2.25)$$

$$I_{ij} \cdot \ddot{\xi}_{yj} - m_{ij} \cdot l_{yj} \cdot \ddot{x}_{yj} - m_{ij} \cdot c_{yj} \cdot l_{yj} \cdot \ddot{\varphi}_{\text{III}} + g \cdot m_{ij} \cdot l_{yj} \cdot \ddot{\xi}_{yj} = 0, \quad (2.26)$$

The vertical displacements of a tank container relative to the flat car frame were neglected. The yielding of the liquid freight relative to the tank walls was included in the calculation. The motion of the liquid freight was described by means of mathematical pendulums [4, 79]. The value of the longitudinal impact to a flat car was taken equal to 3.5 MN.

The hydrodynamic characteristics of the liquid freight were determined by the technique presented in [33]. The authors used petrol as the liquid freight. On the basis of the calculations for the case of the maximum potential loading of the tank container according to [56, 61], the authors obtained the following values:  $m_{ij} \approx 6.8 \text{ t}$ ,  $I_{ij} \approx 250 \text{ t} \cdot \text{m}^2$ .

The differential equations were solved with the Runge–Kutta method in MathCad.

The results of the research demonstrated that without gaps between the fixed fittings of a flat car and container fittings, the accelerations to the bearing structure of a tank container was approximately 40 m/s<sup>2</sup>. The maximum accelerations were obtained for a gap between the fixed fitting and container fitting of 30 mm with the accelerations being about 300 m/s<sup>2</sup>.

### 2.3 Computer modelling of the dynamic loading on the bearing structure of a flat car with dry-cargo containers during a shunting impact

The distributions fields of the accelerations to the bearing structure of a dry cargo container located on the flat car during a shunting impact were determined with the computer modelling. It was assumed that a longitudinal force of 3.5 MH was applied to the rear block of the coupler. The calculation was made with the FEM in CosmosWorks [37, 39, 40, 41].

The spatial model of the bearing structure of a flat car with containers is given in figure 2.3.

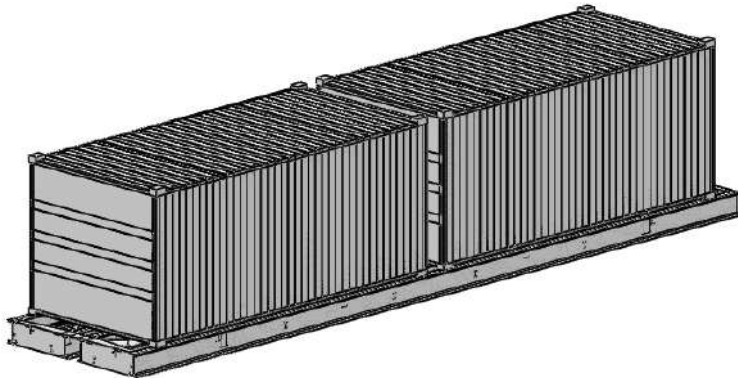


Figure 2.3 – Spatial model of a flat car with containers

The FE model consisted of spatial isoparametric tetrahedrons. The number of units in the mesh was 669705, and elements – 2010206. The maximum element size equaled 50 mm, the minimal element size – 10 mm. The minimum number of elements in the circle was 9; the element size gain ratio in the mesh was 1.7. The maximum side ratio was 16258; the percentage of elements with a side ratio of less than three was 47.6 and more than ten was 20.4.

The design diagram included, apart from the longitudinal force, the vertical force in the areas where the containers rested on the fixed fittings  $P_j^y$  (figure 2.4). The vertical force in the area where the container fitting rested upon the fixed fitting  $P_j^y$  affected the container. The computer model did not include an effect of the freight to the container's walls.

Steel 09C2Cu with the capacity limit  $\sigma_c=490$  MPa and the yield limit  $\sigma_y=345$  MPa was taken as the construction material of the bearing structure of the car and container.

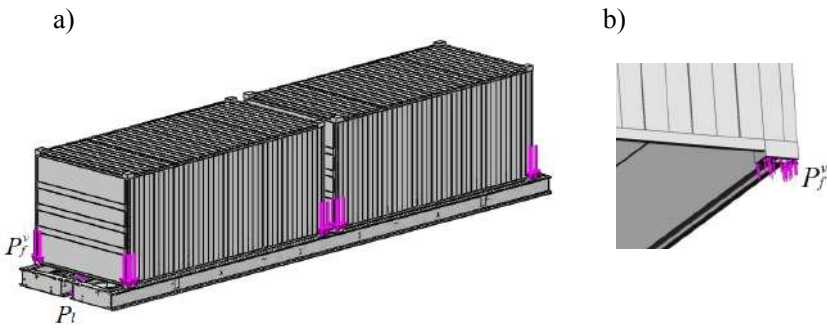


Figure 2.4 – Design diagram of a flat car with containers for the determination of the dynamic loading during a shunting impact  
 a) general view; b) vertical force to a container fitting from the support plane of a fixed fitting

The results of the calculation are given in figure 2.5.

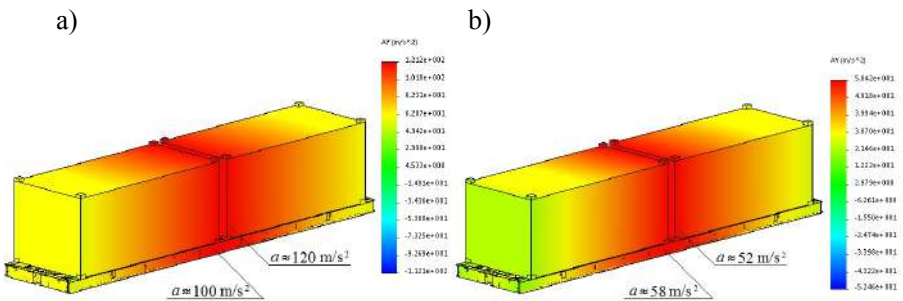


Figure 2.5 – Accelerations of a flat car with containers under the impact of a longitudinal force to the rear block of the coupler  
 a) with gaps between fixed fittings and container fittings; b) without gaps between fixed fittings and container fittings

The research conducted demonstrated that the maximum accelerations to a flat car with gaps of 30 mm between the fixed fittings and container fittings amounted to about  $100 \text{ m/s}^2$ , without gaps – about  $60 \text{ m/s}^2$ , for a container the

values of acceleration were about  $120 \text{ m/s}^2$  and  $50 \text{ m/s}^2$ , respectively.

The adequacy of the designed model was checked with an F-test. It was found that the model was linear and characterized a change in the accelerations of a flat car with containers due to the longitudinal force applied to the rear block of the coupler. The number of degrees of freedom at  $N = 5$  should be  $f_t = 3$ .

While determining the adequacy of the model with gaps between the fixed fittings and container fittings, it was found that with the error mean square  $S_y^2 = 2,5$  and the dispersion of adequacy  $S_{ad}^2 = 6,67$ , the actual F-test was  $F_p = 2.67$ , which was lower than its tabular value  $F_t = 5.41$ . Thus, the hypothesis on adequacy was not rejected. The approximation error amounted to about 4.27 %.

As it was found, without gaps between the fixed fittings and container fittings, at the error mean square  $S_y^2 = 2,5$  and the dispersion of adequacy  $S_{ad}^2 = 3,33$ , the actual value of the F-test was  $F_p = 0.24$ , which was lower than its tabular value  $F_t = 1.33$ . It implied that the hypothesis on adequacy was not rejected. The approximation error amounted to about 7.77 %.

This research showed that the values of accelerations to a flat car with containers during a shunting impact considerably exceeded the normative values, if all potential displacements of the container fittings relative to the fixed fittings were included [11, 12, 74]. Therefore, there is a need to improve the standards by introducing the values of maximum potential accelerations to a flat car with containers during a shunting impact, and also by including the improved values of the dynamic loading at the designing stage at car production facilities.

## **2.4 Computer modelling of the dynamic loading on the bearing structure of a flat car with tank containers during a shunting impact**

The distribution fields of the accelerations to the bearing structure of a tank container on the flat car during a shunting impact were determined with the computer modelling. A longitudinal force of 3.5 MH to the rear block of the coupler was included in the calculation. It was made with the FEM in CosmosWorks. The spatial model of the bearing structure of a flat car with a tank container is given in figure 2.6.



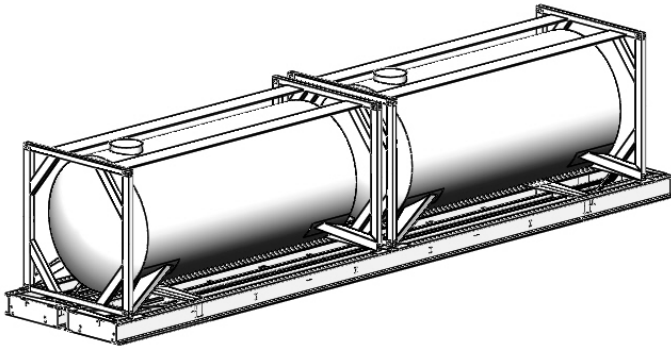


Figure 2.6 – Spatial model of a flat car with tank containers

The FE model consisted of spatial isoparametric tetrahedrons. The number of units in the mesh was 707359, and elements – 2150500. The maximum element size equaled 50 mm; the minimal element size was 10 mm. The minimum number of elements in the circle was 9; the element size gain ratio in the mesh was 1.7. The maximum side ratio was 689.01, the percentage of elements with a side ratio of less than three was 52.1, and more than ten was 4.75.

The design diagram included, apart from the longitudinal loads  $P_{y\partial}$ , the vertical loading in the areas of support of a tank container on the fixed fittings (figure 2.7). The following forces were applied to a tank container: vertical forces in the areas of support of a container fitting to the fixed fitting, inner pressure of the liquid freight  $P_{lf}$  to the tank head, longitudinal force  $P_h$  to the tank head during the displacement of the liquid freight due to the longitudinal force  $P_l$  to the rear block of the coupler, and the displacements of the container fittings relative to the fixed fittings.

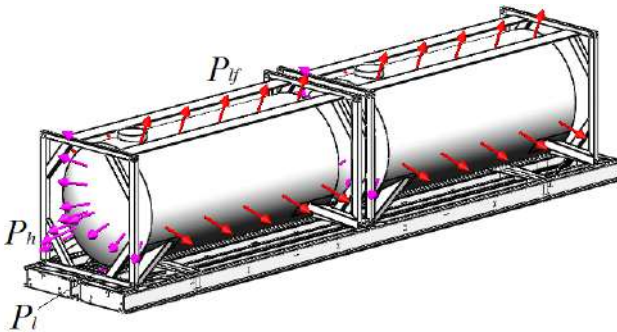


Figure 2.7 – Design diagram of a flat car with tank containers for the determination of the dynamic loading during a shunting impact

The model was secured in the areas of support of the bearing structure on the gearing parts. Steel 09C2Cu with the strength limit  $\sigma_S = 490$  MPa and the yield limit  $\sigma_Y = 345$  MPa was taken as the construction material of the flat car and tank container. The results of the calculation are given in figure 2.8.

The research conducted demonstrated that the maximum acceleration to the tank container was about  $320 \text{ m/s}^2$ .

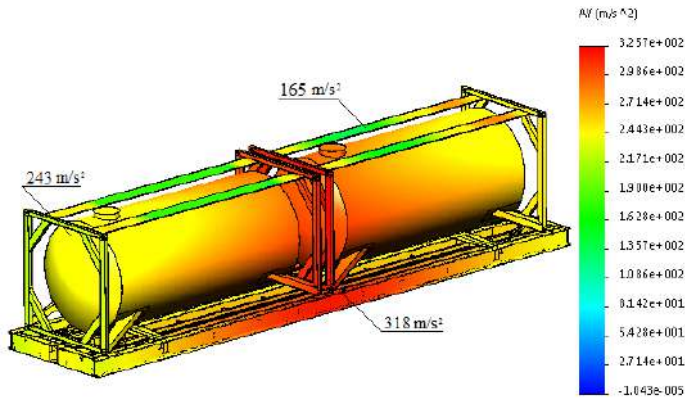


Figure 2.8 – Accelerations of a flat car with containers under the longitudinal force to the rear block of the coupler

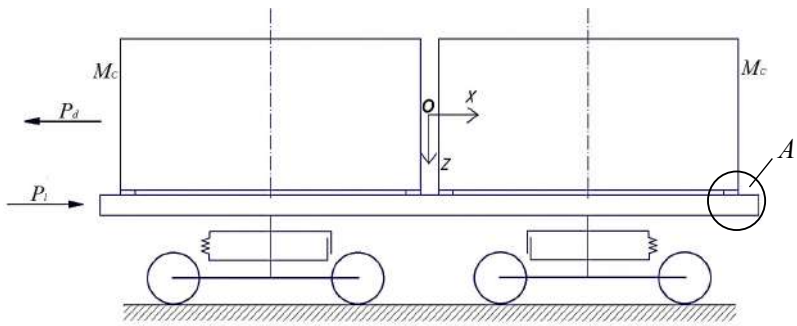
The adequacy of the designed model was checked with an F-test. It was found that the model under study was linear and it characterized a change in the accelerations of the tank container located on a flat car due to the longitudinal force to the rear block of the coupler. The number of degrees of freedom at  $N = 6$  was  $f_l = 4$ .

On the basis of the research it was found that the actual value of the criterion was  $F_p = 1.6$ , and it was lower than the tabular value  $F_t = 6.16$ . Therefore, the hypothesis on adequacy was not rejected.

**2.5 Theoretical substantiation of the introduction of elastic, viscous and elastic-viscous elements in the bearing structure of combined transport facilities to decrease the dynamic loading in operation**

**2.5.1 Theoretical substantiation of the introduction of elastic, viscous and elastic-viscous elements in the bearing structure of a dry-cargo container**

The authors suggested the application of elastic (viscous or viscous-elastic) elements between the container fittings and the fixed fittings of a flat car to decrease the impact loads between them for the cases when the impact load exceeds the friction force between the horizontal planes of the container fittings and the fixed fittings (figure 2.9).



A (expanded)

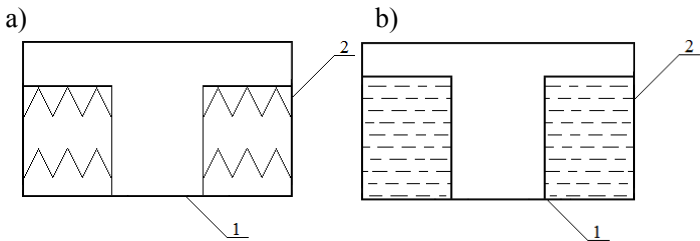


Figure 2.9 – Diagram of the longitudinal force to a flat car with containers

a) fitting with elastic elements; b) fitting with viscous elements

1 – fitting; 2 – elastic (viscous) element

The block-hierarchy diagram of an improved container structure is presented in figure 2.10.

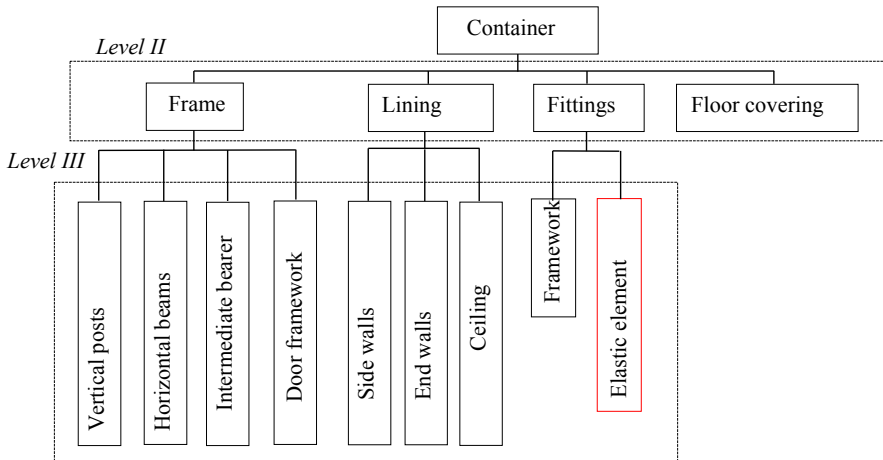


Figure 2.10 – Block-hierarchy diagram of a 1CC dry-cargo container structure

The container module is the 1<sup>st</sup> hierarchical level of the formal description. The components of the container module which form the 2<sup>nd</sup> hierarchy level are: frame, lining, fittings and wooden floor covering. The components of the 2<sup>nd</sup> level form the 3<sup>rd</sup> level.

The dynamic loading of a container during a shunting impact was determined with improved mathematical model (2.27), which included the displacements of a container on the flat car [39, 80, 81, 84].

A 13-4012M flat car was taken as the prototype car. The research was conducted for a 1CC container.

The diagram of forces between the container fitting and the fixed fitting on a flat car during a shunting impact is given in figure 2.11.

The model included the dry friction force which emerged during the displacement of the container fitting relative to the horizontal plate of the fixed fitting, and elastic links between the fixed fitting and container fitting [6, 28, 29, 35]. The research into the dynamic loading of a container was conducted in the plane coordinate system.

It was assumed that the container was loaded with conditional freight to the maximum loading capacity. Thus, the calculation included the gross container weight.

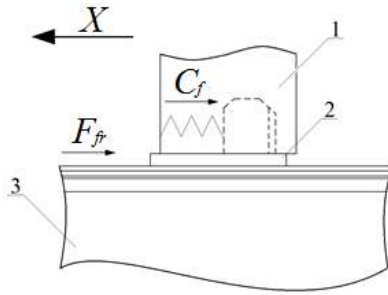


Figure 2.11 – Diagram of forces between the container fitting and the fixed fitting on a flat car during a shunting impact

1 – container fitting; 2 – fixed fitting; 3 – longitudinal beam of a flat car

As far as the impact force (3.5 MH, according to [11, 12, 74, 115]) was applied to the support surface of a rear block of the coupler from one side of a car, and it was balanced by the longitudinal inertia forces of the masses of car body, bogies, couplers and freight; the model did not include an absorber.

Differential equation system (2.27) in the normal form was integrated with the Runge–Kutta method. The initial conditions were taken equal to zero.

The calculation made it possible to obtain the acceleration to an improved container located on the flat car at a shunting impact (figure 2.12). This value was about  $50 \text{ m/s}^2$  ( $\approx 5g$ ), thus it exceeded the normative acceleration value by 60% [14].

$$\begin{cases} M_{\text{BIF}}^{\text{нон}} \cdot \ddot{q}_1 = P_{y0} - \sum_{i=1}^n (F_{TP} \cdot \text{sign}(\dot{q}_1 - \dot{q}_2) + C_{\phi} \cdot (q_1 - q_2)), \\ M_k \cdot \ddot{q}_2 = (F_{TP} \cdot \text{sign}(\dot{q}_1 - \dot{q}_2) + C_{\phi} \cdot (q_1 - q_2)), \end{cases} \quad (2.27)$$

where  $M_{\text{BIF}}^{\text{нон}}$  – gross weight of a flat car;  $P_{y0}$  – longitudinal force to the coupler;  $n$  – number of containers on a flat car;  $F_{mp}$  – friction force between the fixed fittings and container fittings;  $M_k$  – container mass;  $C_{\phi}$  – rigidity of elastic elements in the container fittings;  $q_1, q_2$  – coordinates corresponding to the displacements of a flat car and a container relative to the longitudinal axle, respectively.

Therefore, the elastic interaction between the container fittings and fixed fittings at the given design diagram does not fully compensate the value of

dynamic loading on the container. Therefore the authors studied the viscous interaction between the container fittings and fixed fittings of a flat car.

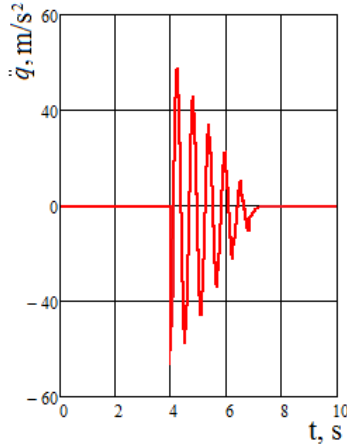


Figure 2.12 – Accelerations to a container with elastic links in the fittings, located on the flat car during a shunting impact

The mathematical model of the dynamic loading of a container with viscous links in the fittings during a shunting impact is given below.

$$\begin{cases} M_{\text{БЛ/Ф}}^{\text{нон}} \cdot \ddot{q}_1 = P_{y0} - \sum_{i=1}^n (F_{TP} \cdot \text{sign}(\dot{q}_1 - \dot{q}_2) + \beta_{\phi} (\dot{q}_1 - \dot{q}_2)), \\ M_k \cdot \ddot{q}_2 = (F_{TP} \cdot \text{sign}(\dot{q}_1 - \dot{q}_2) + \beta_{\phi} (\dot{q}_1 - \dot{q}_2)), \end{cases} \quad (2.28)$$

where  $\beta_{\phi}$  – coefficient of viscous resistance in the container fittings.

The accelerations to a container with viscous links in the fittings, located on the flat car during a shunting impact are given in figure 2.13.

At a given viscous resistance the acceleration in the container fittings was approximately  $20 \text{ m/s}^2$  ( $\approx 2g$ ), thus it did not exceed the normative value [14]. At that the viscous resistance to the displacements of a container should be within a range of  $10 - 50 \text{ kN}\cdot\text{s/m}$ .

The possibility to decrease the dynamic loading of a container on the flat car at a shunting impact was also studied for elastic-viscous links in the fittings.

The mathematical model for the determination of the dynamic loading of a container is given below.

$$\begin{cases} M_{B1\Gamma\Phi}^{noou} \cdot \ddot{q}_1 = P_{y0} - \sum_{i=1}^n (F_{TP} \cdot \text{sign}(\dot{q}_1 - \dot{q}_2) + C_\phi(q_1 - q_2) + \beta_\phi(\dot{q}_1 - \dot{q}_2)), \\ M_k \cdot \ddot{q}_2 = (F_{TP} \cdot \text{sign}(\dot{q}_1 - \dot{q}_2) + C_\phi \cdot (q_1 - q_2) + \beta_\phi(\dot{q}_1 - \dot{q}_2)). \end{cases} \quad (2.29)$$

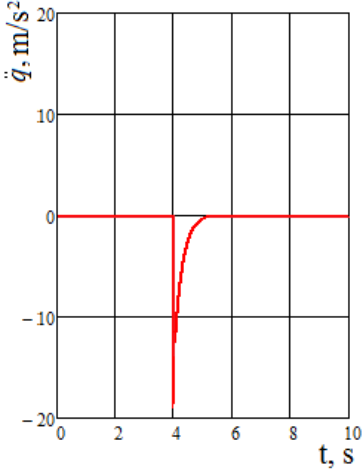


Figure 2.13 – Accelerations to a container with viscous links in the fittings, located on the flat car during a shunting impact

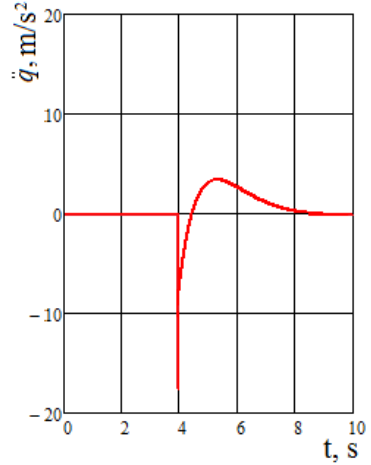


Figure 2.14 – Accelerations to a container with elastic-viscous links in the fittings, located on the flat car during a shunting impact

The results of the calculation demonstrated that at the rigidity of an elastic element 20 kN/m, and the viscous resistance coefficient 30 kN·s/m the accelerations to a container on the flat car at a shunting impact were about 20 m/s<sup>2</sup> ( $\approx 2g$ ), (figure 2.14); they were within the admissible values [14].

### 2.5.2 Theoretical substantiation of the introduction of elastic, viscous and elastic-viscous elements in the bearing structure of a tank container

The dynamic loading of a tank container with viscous links in the fittings during a shunting impact was determined with mathematical model (2.30). The design diagram is presented in figure 2.15.

$$\begin{cases} M_{\text{БПФ}}^{\text{нобн}} \cdot \ddot{q}_1 = P_{y0} - \sum_{i=1}^n (F_{TP} \cdot \text{sign}(\dot{q}_1 - \dot{q}_2) + C_{\phi} (q_1 - q_2)), \\ M_k \cdot \ddot{q}_2 = \sum_{i=1}^n (F_{TP} \cdot \text{sign}(\dot{q}_1 - \dot{q}_2) + C_{\phi} \cdot (q_1 - q_2) + M_M \cdot l \cdot q_3), \\ I_{\text{HB}} \cdot \ddot{q}_3 = M_M \cdot l \cdot \ddot{q}_2 - g \cdot M_M \cdot l \cdot q_3, \end{cases} \quad (2.30)$$

where  $M_{\text{БПФ}}^{\text{нобн}}$  – gross weight of a flat car;  $P_{y0}$  – value of the longitudinal force to the coupler;  $F_{mp}$  – friction force between the fixed fittings and container fittings;  $M_k$  – tank container mass;  $C_{\phi}$  – rigidity of elastic elements in the tank container fittings;  $M_M$  – mass of the pendulum simulating the displacement of the liquid freight in a tank container;  $l$  – length of the pendulum hanger;  $I_{\text{HB}}$  – inertia moment of the pendulum;  $q_1, q_2, q_3$  – coordinates corresponding to the displacements of flat car, tank container, and liquid freight relative to the longitudinal axle, respectively.

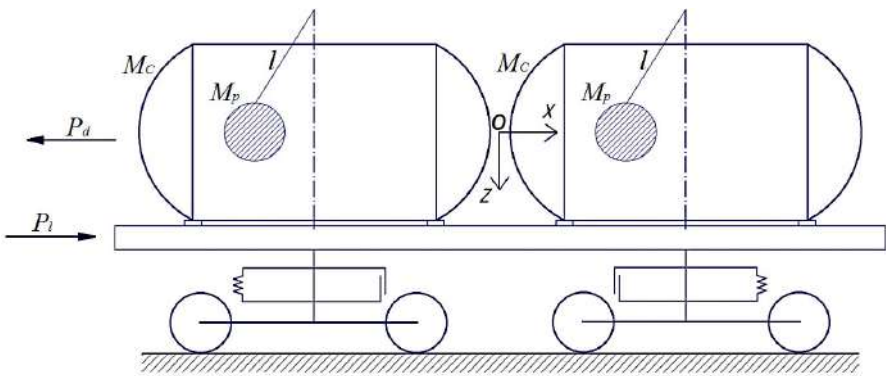


Figure 2.15 – Diagram of the longitudinal force to a flat car with tank containers



Petrol was taken as the liquid freight. The hydrodynamic characteristics of the liquid freight were determined with consideration of the maximum allowable capacity of the tank container barrel in accordance with [56]. The motion of the liquid freight was described by means of a system of mathematical pendulums [4].

Mathematical model (2.30) was solved in the MathCad [20, 25]. It was reduced to the normal Cauchy form. The differential equation system was integrated in the normal form with the Runge–Kutta method. The initial conditions were taken equal to zero.

On the basis of the calculation the authors obtained the accelerations to an improved tank container on the flat car at a shunting impact (figure 2.16). This value of acceleration was about  $40 \text{ m/s}^2$  ( $\approx 4g$ ); thus it was within the allowable values [13]. And the total rigidity of the elastic elements for one tank container should be within a range of  $420 - 530 \text{ kN/m}$ .

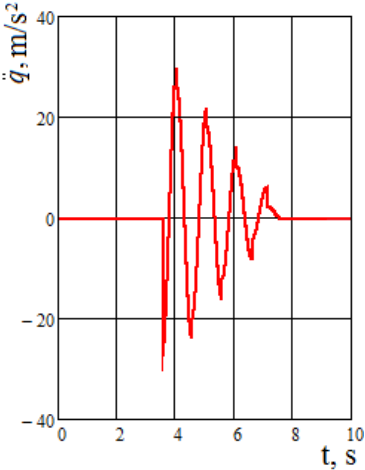


Figure 2.16 – Accelerations to a tank container with elastic links in the fittings, located on the flat car during a shunting impact

The possibility to decrease the dynamic loading of a tank container on the flat car at a shunting impact was studied with consideration of fittings with elastic-viscous links. The mathematical model of the dynamic loading of a tank container during a shunting impact with consideration of viscous links in the fittings is given below.

$$\begin{cases} M_{\text{BII}\phi}^{\text{non}} \cdot \ddot{q}_1 = P_{y_0} - \sum_{i=1}^n (F_{TP} \cdot \text{sign}(\dot{q}_1 - \dot{q}_2) + \beta_{\phi}(\dot{q}_1 - \dot{q}_2)), \\ M_k \cdot \ddot{q}_2 = \sum_{i=1}^n (F_{TP} \cdot \text{sign}(\dot{q}_1 - \dot{q}_2) + \beta_{\phi}(\dot{q}_1 - \dot{q}_2) + M_M \cdot l \cdot \dot{q}_3), \\ I_{HB} \cdot \ddot{q}_3 = M_M \cdot l \cdot \dot{q}_2 - g \cdot M_M \cdot l \cdot q_3, \end{cases} \quad (2.31)$$

$\beta_{\phi}$  –coefficient of viscous resistance in the container fittings.

Differential equation system (2.31) in the normal form was integrated by the Runge–Kutta method. The accelerations to a tank container with viscous links in the fittings, located on the flat car during a shunting impact are given in figure 2.17.

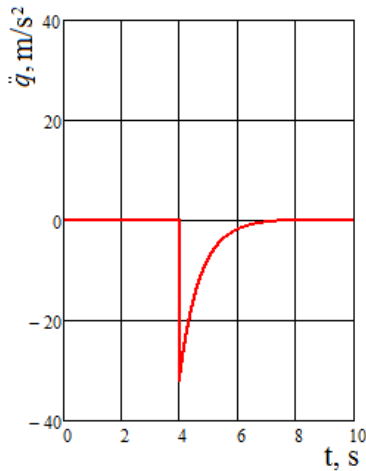


Figure 2.17 – Accelerations to a tank container with viscous links in the fittings, located on the flat car during a shunting impact

At a given viscous resistance in the tank container fittings the acceleration was approximately  $40 \text{ m/s}^2$  ( $\approx 4g$ ); it did not exceed the normative value [13].

And the total viscous resistance to the displacement of one tank container should be within a range from 9 to 54  $\text{kN}\cdot\text{s/m}$ .

The authors also considered the variant with elastic-viscous links between the container fittings and fixed fittings. The mathematical model has the form:

$$\begin{cases} M_{BII\Phi}^{no\Phi} \cdot \ddot{q}_1 = P_{yo} - \sum_{i=1}^n (F_{TP} \cdot \text{sign}(\dot{q}_1 - \dot{q}_2) + c(q_1 - q_2) + \beta_{\phi}(\dot{q}_1 - \dot{q}_2)), \\ M_k \cdot \ddot{q}_2 = \sum_{i=1}^n (F_{TP} \cdot \text{sign}(\dot{q}_1 - \dot{q}_2) + c(q_1 - q_2) + \beta_{\phi}(\dot{q}_1 - \dot{q}_2) + M_M \cdot l \cdot q_3), \\ I_{HB} \cdot \ddot{q}_3 = M_M \cdot l \cdot \ddot{q}_2 - g \cdot M_M \cdot l \cdot q_3, \end{cases} \quad (2.32)$$

The accelerations to a tank container with consideration of elastic-viscous links in the fittings are given in figure 2.18.



Figure 2.18 – Accelerations to a tank container with elastic-viscous links in the fittings, located on the flat car during a shunting impact

The rigidity of an elastic element was taken equal to 480 kN/m, and the viscous resistance coefficient – 30 kN·s/m. The maximum acceleration was about 40 m/s<sup>2</sup> ( $\approx 4g$ ) and it did not exceed the normative value [13].

### ***2.5.3 Designing of the computer model of the dynamic loading of containers located on the flat car during a shunting impact***

The dynamic loading of an improved tank container was studied through the computer modelling with the FEM in CosmosWorks [38, 58]. Spatial isoparametric tetrahedrons were used as the finite elements, the optimal number

of which was determined by the graphic analytical method. The number of units in the mesh was 285189, and the number of elements was 853256. The maximum element size was 100 mm; the minimal element size was 20 mm. The minimum number of elements in the circle was 9; the element size gain ratio in the mesh was 1.7. The maximum side ratio was 306.67; the percentage of elements with a side ratio of less than three was 29.6 and more than ten was 21.2.

The design diagram for the determination of the dynamic loading of a flat car with containers during a shunting impact is given in figure 2.19.

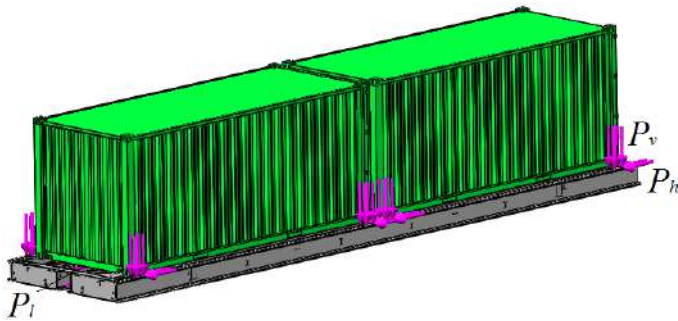


Figure 2.19 – Design diagram for the determination of the dynamic loading of a flat car with containers during a shunting impact

The model included the horizontal loading  $P_h$  from the vertical surface of the rear block of the coupler, the impact force  $P_i$ , and the vertical forces in the areas of support of the container fittings on the fixed fittings  $P_v$ . The model did not include the pressure from the freight to the container walls. The container was secured in the areas where it rested on the flat car. It was taken into account that during the horizontal loading  $P_h$  the container moved relative to the initial position by 30 mm.

While designing the dynamic loading of a container with viscous links in the fittings, the total viscous resistance to the displacement of one container was taken within a range of 10 – 50 kN·s/m. Steel 09C2Cu was taken as the structural material. The results of the calculation are given below.

The maximum accelerations to a container with viscous interaction of the container fittings and fixed fittings emerged in the end walls of the end frame parts of a flat car; they amounted to about  $20 \text{ m/c}^2$  (figure 2.20). In the middle

part of a container the accelerations were  $15 \text{ m/s}^2$ . The lowest acceleration was in the end walls of a container across the frame center of the flat car; it was about  $8 \text{ m/s}^2$ . The maximum accelerations to the bearing structure of a flat car were in the end parts and amounted to about  $38 \text{ m/s}^2$ ; the accelerations across the bolster sections of the frame were about  $30 \text{ m/s}^2$ . The accelerations in the middle section of the center sill were  $21.4 \text{ m/s}^2$ . The lowest accelerations were in the middle parts of the main longitudinal beams of the flat car frame; they were  $7.2 \text{ m/s}^2$ . During the modelling of the dynamic loading of a container with elastic-viscous links in the fittings the rigidity of the elastic element was taken  $20 \text{ kN/m}$  and the coefficient of viscous resistance –  $30 \text{ kN}\cdot\text{s/m}$ .

The results of the calculation demonstrated that the maximum accelerations to the bearing structure of a container on the flat car were  $19.7 \text{ m/s}^2$  and  $38.4 \text{ m/s}^2$ , respectively.

The research showed that the maximum accelerations to a container with elastic-viscous links between the container fittings and fixed fittings did not exceed the allowable values [14].

The natural oscillation frequencies of an improved container on the flat car during a shunting impact were determined with the modal analysis in CosmosWorks. The numerical values of the natural oscillation frequencies are given in table 2.1.

The research conducted demonstrated that the values of the natural oscillation frequencies were within the allowable values [11, 12, 74, 115].

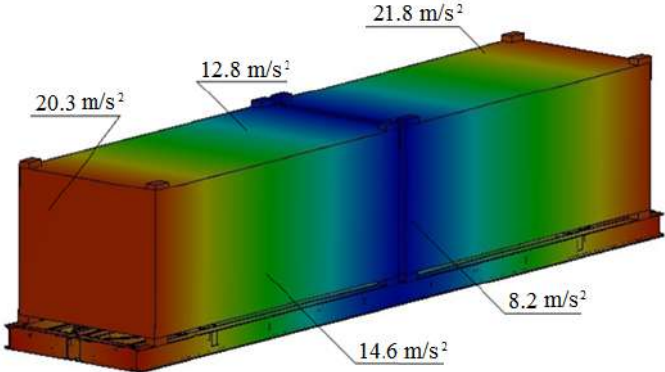


Figure 2.20 – Distribution of accelerations to a flat car with containers during a shunting impact

The models were verified with an F-test. The input parameter of the mathematical and computer models of the dynamic loading was the impact

force to the coupler of a flat car, and the output parameter was the accelerations to a container located on the flat car (table 2.2). The results of the calculation showed that for viscous interaction of the container fittings and fixed fittings at the error mean square  $S_y=2.83$  and the dispersion of adequacy  $S_{ad}^2=3.1$ , the actual value  $F_p=1.09$ , which was lower than the tabular value  $F_r=3.07$ . Thus, it implies that the hypothesis on adequacy was not rejected.

Table 2.1 – Numerical values of the natural oscillation frequencies of an improved container

Form of oscillations	Interaction in the fittings			
	Viscous		Elastic-viscous	
	Frequency, rad/s	Frequency, Hz	Frequency, rad/s	Frequency, Hz
1	72.97	11.61	74.26	11.82
2	104.41	16.62	105.84	16.85
3	114.25	18.18	115.16	18.33
4	133.75	21.29	135.69	21.6
5	134.74	21.44	137.65	21.91
6	135.11	21.5	137.85	21.94
7	135.22	21.52	139.07	21.13
8	138.3	22.0	139.87	22.26

Table 2.2 – Numerical values of the accelerations to a container on the flat car at a shunting impact

Impact force to the coupler, MN	Acceleration value, g			
	Mathematical model		Computer model	
	Viscous link	Elastic-viscous link	Viscous link	Elastic-viscous link
1	2	3	4	5
2.6	14.6	14.2	15.1	14.8
2.7	15.1	14.8	15.7	15.4
2.8	15.7	15.4	16.2	15.9
2.9	16.2	15.9	16.8	16.6
3.0	16.8	16.7	17.4	17.5
3.1	17.4	17.2	18	17.8
3.2	17.8	17.8	18.5	18.1
3.3	18.5	18.3	19.2	18.6
3.4	19	18.8	19.7	19.2
3.5	19.6	19.3	20.3	19.7

During the elastic-viscous interaction of the container fittings and fixed fittings the error mean square was  $S_y=2.7$  and the dispersion of adequacy was

$S_{\alpha\alpha}=3.0$ . The actual value of an F-test was  $F_p=1.11$ , which was lower than the tabular value  $F_{\bar{r}}=3.07$ . It implies that the hypothesis on adequacy was not rejected.

#### ***2.5.4 Designing of a computer model of the dynamic loading of tank containers located on the flat car during a shunting impact***

The distribution fields of the acceleration relative to the bearing structure of a flat car with containers were determined with the computer modelling. The design model is presented in figure 2.21. It included the horizontal load  $P_h$  from the vertical surface of the rear block of the coupler, the impact force  $P_i$ , and the vertical reactions in the areas of support of the container fittings on the fixed fittings  $P_v$ . The design diagram also included the pressure from the liquid freight to the barrel  $P_{lf}$ , and the pressure  $P_p$  to the tank head due to the longitudinal impact to the rear block of the coupler of a flat car and the displacements of the container fittings relative to the fixed fittings.

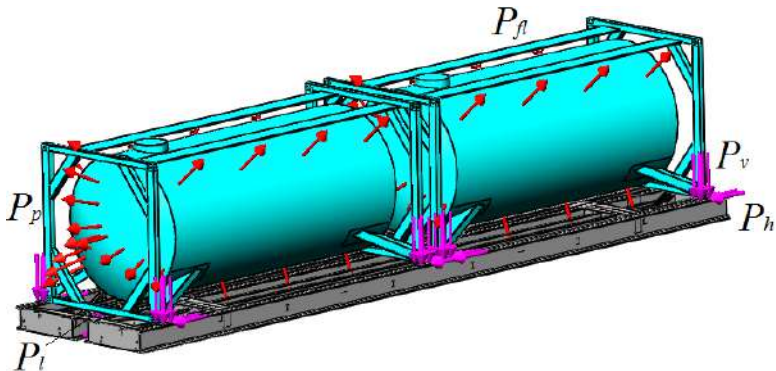


Figure 2.21 – Design diagram for the determination of the dynamic loading of a flat car with tank containers during a shunting impact

The container was secured in the areas of support on the flat car. It was taken into account that due to the dynamic loading the container fittings moved at 30 mm from the initial position. The fittings of a tank container had elastic elements with a rigidity of 420 kN/m.

Steel 09C2Cu was taken as the structural material. The results of the calculation are given below.

The maximum accelerations to a tank container with viscous interaction between the container fittings and fixed fittings were in the frame at the end walls of the bearing structure of a flat car; they were about  $40 \text{ m/s}^2$  (figure 2.22). In the middle part of a tank container the accelerations were  $28.6 \text{ m/s}^2$ . The lowest accelerations were in the flat car frame in the central symmetry plane of the bearing structure of a flat car; they were about  $16 \text{ m/s}^2$ . The maximum accelerations to the bearing structure of a flat car were in the end parts and they amounted to about  $41 \text{ m/s}^2$ . In the middle part of the center sill the accelerations were  $37.8 \text{ m/s}^2$ . The lowest acceleration was in the middle part of the main longitudinal beams of the flat car frame; it was  $8.4 \text{ m/s}^2$ .

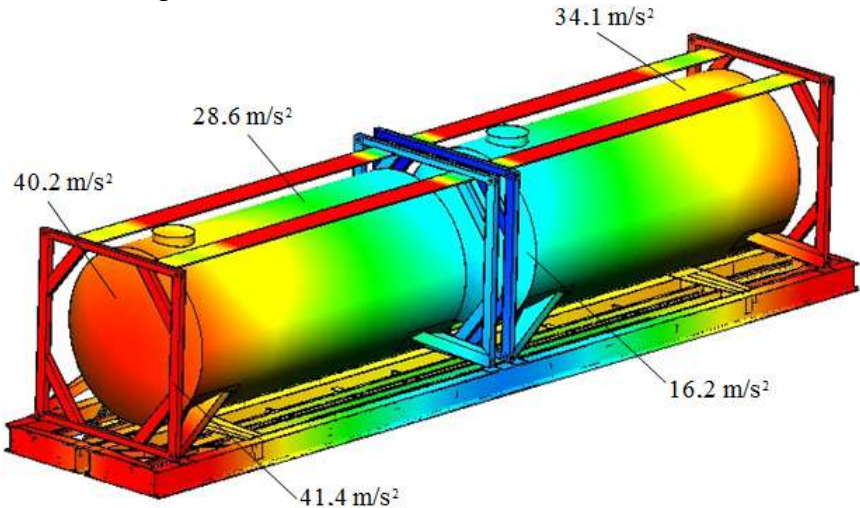


Figure 2.22 – Distributions of the accelerations to the flat car with tank containers during a shunting impact

While modelling the dynamic loading of a tank container with viscous links in the fittings, the viscous resistance to the displacement of one tank container must be in a range of  $9 - 54 \text{ kN}\cdot\text{s/m}$ .

The results of the modelling of the dynamic loading for a tank container with elastic-viscous interaction between the container fittings and fixed fittings demonstrated that the maximum accelerations to the bearing structure of a tank container were  $39.2 \text{ m/s}^2$ , and for a flat car –  $40.5 \text{ m/s}^2$ .

Thus, the maximum accelerations to a tank container with viscous interaction between the container fittings and fixed fittings did not exceed the



allowable values [13].

On the basis of the design diagram the natural oscillations frequencies of a tank container were determined (table 2.3). The results of the calculation demonstrated that the natural oscillations frequencies did not exceed the admissible values [11, 12, 74, 115].

Table 2.3 – Numerical values of the natural oscillation frequencies of an improved tank container

Form of oscillations	Interaction in fittings			
	Viscous		Elastic-viscous	
	Frequency, rad/s	Frequency, Hz	Frequency, rad/s	Frequency, Hz
1	52.25	8.32	53.18	8.47
2	53.65	8.53	54.82	8.73
3	57.18	9.1	58.25	9.28
4	145.6	23.17	146.3	23.29
5	146.81	23.37	147.15	23.43
6	150.07	23.88	151.1	24.1
7	202.65	32.25	203.23	32.36
8	221.87	35.31	222.16	35.38

The models were verified with an F-test. The input parameter of the mathematical and computer models of the dynamic loading of a tank container was the impact force to the coupler of a flat car, and the output parameter was the acceleration to a tank container located on the flat car (table 2.4). The amount of the statistic data required was determined with Student's test [30].

At the mathematic expectation 33.6, dispersion 31.7, mean square deviation 5.63, it was found that the optimal number of measurements was six. Thus, the number of measurements conducted was sufficient to obtain the reliable estimation of the results.

The results of the calculation showed that for viscous interaction of the container fittings and fixed fittings at the error mean square  $S_y=8.5$  and the dispersion of adequacy  $S_{ao}^2=11.15$ , the actual value of an F-test was  $F_p=1.3$ , which was lower than the tabular value  $F=3.07$ . Thus, it implies that the hypothesis on adequacy was not rejected.

Table 2.4 – Numerical values of the acceleration to a tank container located on the flat car during a shunting impact

Impact force to the coupler, MN	Acceleration value, g			
	Mathematical model		Computer model	
	Viscous interaction	Elastic-viscous interaction	Viscous interaction	Elastic-viscous interaction
2.6	28.9	33.1	31.8	33.5
2.7	29.5	33.6	32.6	34.1
2.8	30	34.1	33.1	34.8
2.9	31	34.6	34.2	35.4
3.0	32.1	35.2	35.5	36.1
3.1	33	35.9	36.7	36.8
3.2	34.2	36.5	37.9	37.4
3.3	35.2	37.1	39	38.0
3.4	36	37.7	40.2	38.6
3.5	37.4	38.4	41.4	39.2

With the elastic-viscous interaction of the container fittings and fixed fittings the error mean square was  $S_y=3.22$  and the dispersion of adequacy was  $S_{ad}^2=3.73$ . The actual value of an F-test was  $F_p=1.16$ , which was lower than the tabular value  $F_r=3.07$ . Thus, the hypothesis on adequacy was not rejected.

## **2.6 Determination of the strength of fixed fitting of a flat car during viscous and elastic-viscous interaction with a container/tank container**

The strength of the fixed fittings of a flat car with viscous and elastic-viscous interaction with containers was calculated with the FEM in CosmosWorks. A 13-401 flat car model was taken as the basic model. It included the impact force  $P_l$  (figure 2.23) to the flat car, the vertical force  $P_v$  from the containers to the fixed fittings, and the horizontal force  $P_h$  due to the displacements of the fittings relative to the fixed fittings (figure 2.24).

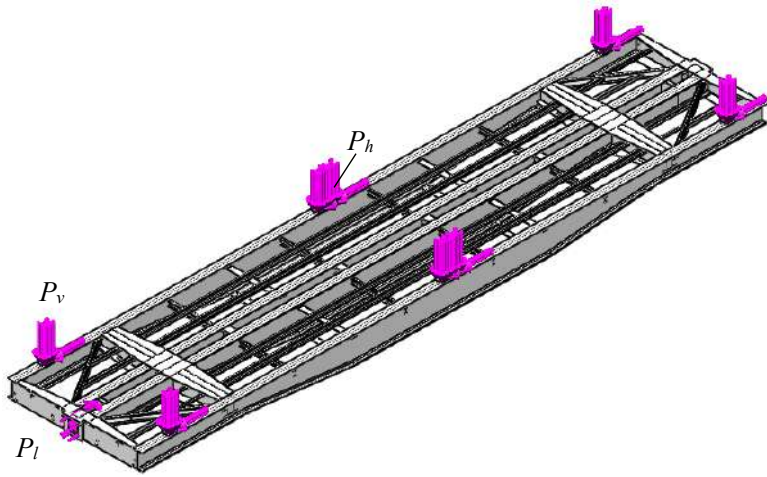


Figure 2.23 – Design diagram of the bearing structure of a flat car

Isoparametrical tetrahedrons were taken as the finite elements. The number of units in the mesh was 311601, and the number of elements –932166. The maximum element size was 80 mm, the minimal element size –16 mm. The minimum number of elements in the circle was 9; the element size gain ratio in the mesh was 1.7. The maximum side ratio was 470.8; the percentage of elements with a side ratio of less than three was 41.5 and more than ten was 8.17.

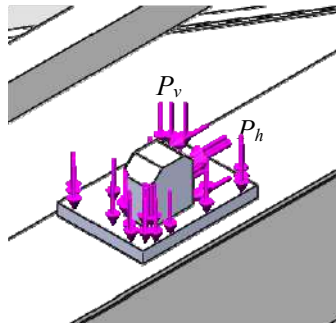


Figure 2.24 – Design diagram of the fixed fitting of a flat car

The results of the calculation are given in figures 2.25 – 2.27. It was found that with viscous interaction between the container fittings and fixed

fittings during a shunting impact of a flat car, the maximum equivalent stresses were about 270 MPa (figures 2.25 and 2.26); they were concentrated in the zone of interaction of the center sill and the body bolster beam. The maximum displacements were in the middle parts of the main longitudinal beams of the flat car frame; they amounted to 12.1 mm (figure 2.27).

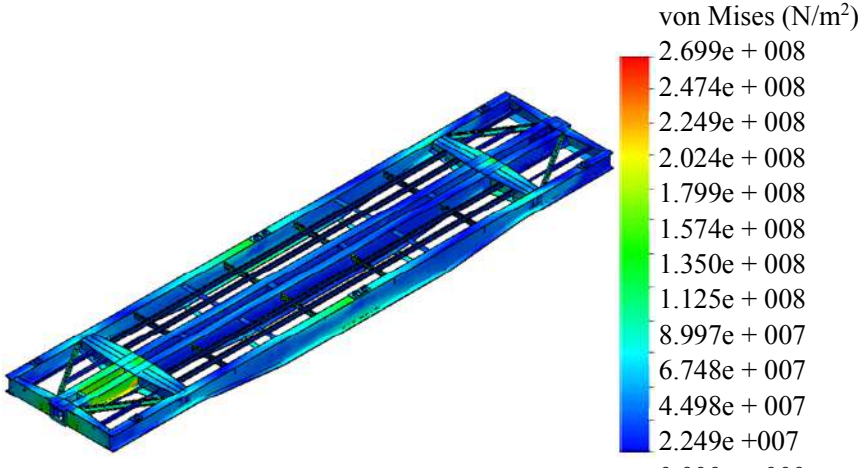


Figure 2.25 – Stress state of the bearing structure of a flat car during viscous interaction of the container fittings and fixed fittings (side view)

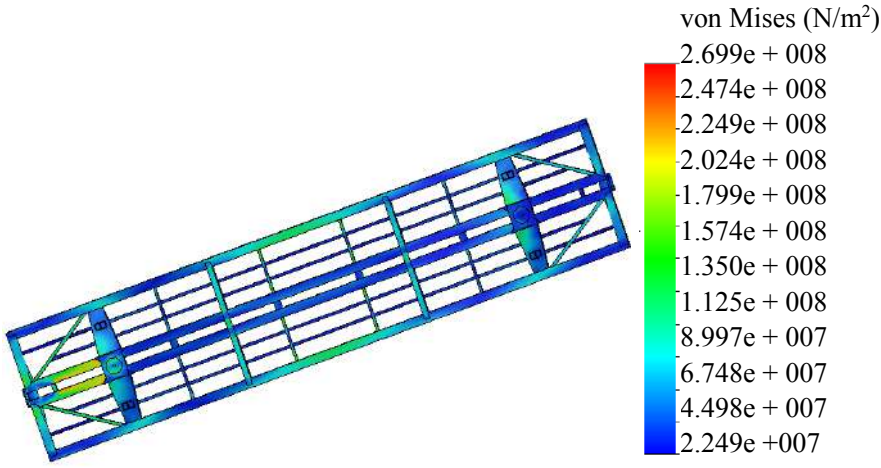


Figure 2.26 – Stress state of the bearing structure of a flat car during viscous interaction of the container fittings and fixed fittings (bottom view)

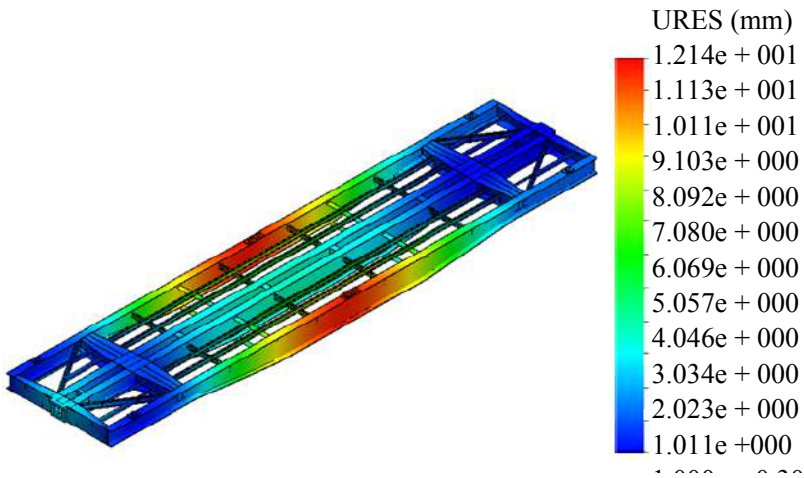


Figure 2.27 – Displacements in the units the bearing structure of a flat car during viscous interaction of the container fittings and fixed fittings

With elastic-viscous interaction of the container fittings and fixed fittings during a shunting impact of a flat car, the maximum equivalent stresses were about 260 MPa (figures 2.28 and 2.29); they were concentrated in the zone of interaction between the center sill and the body bolster beam.

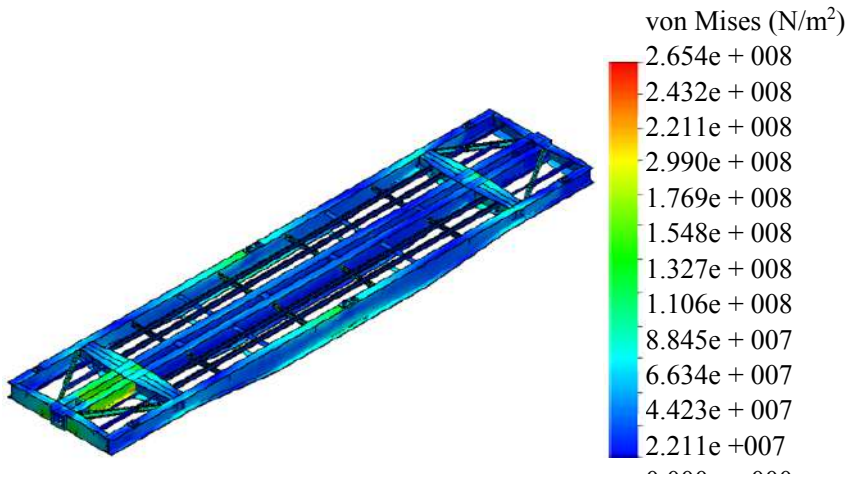


Figure 2.28 – Stress state of the bearing structure of a flat car during viscous interaction of the container fittings and fixed fittings (side view)

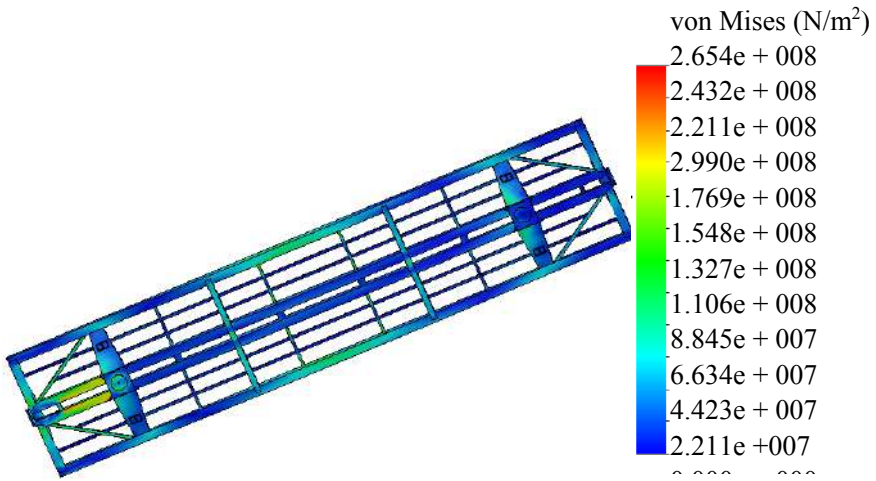


Figure 2.29 – Stress state of the bearing structure of a flat car during elastic-viscous interaction of the container fittings and fixed fittings (bottom view)

The maximum displacements were in the middle parts of the main longitudinal beams of the flat car frame; they amounted to 11.0 mm (figure 2.30).

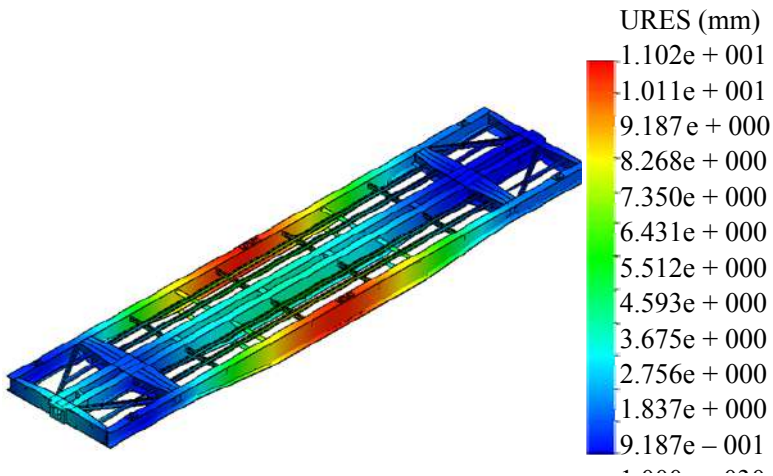


Figure 2.30 – Displacements in the units of the bearing structure of a flat car during elastic-viscous interaction of the container fittings and fixed fittings

The measures proposed for improving the diagrams of interaction between the flat car and containers can decrease the maximum equivalent stresses in the fixed fittings almost one third (figure 2.31), and in the container fittings – almost seven times (figure 2.32).

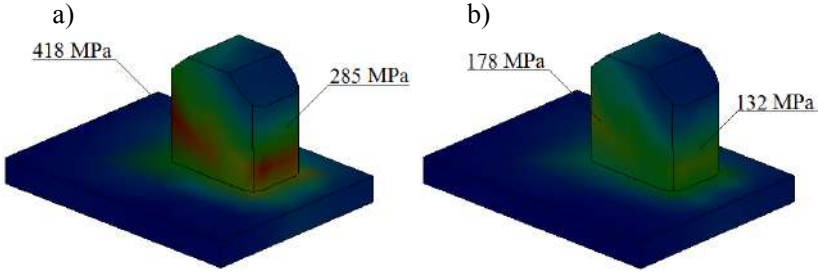


Figure 2.31 – Stress state of the fixed fitting of a flat car  
 a) standard interaction diagram; b) improved interaction diagram

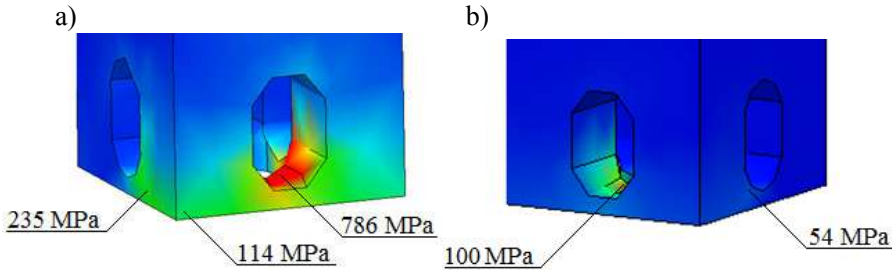


Figure 2.32 – Stress state of the container fitting  
 a) standard interaction diagram; b) improved interaction diagram

The strength of a flat car with viscous and elastic-viscous interaction between the fixed fittings and container fittings during a shunting impact was calculated with FE model in CosmosWorks.

The results of the calculation are given in figures 2.33 – 2.35. It was found that with viscous interaction between the container fittings and fixed fittings during a shunting impact of a flat car, the maximum equivalent stresses were about 270 MPa (figures 2.33 and 2.34); they were concentrated in the zone of interaction between the center sill and the body bolster beam. Thus, the maximum equivalent stresses in the bearing structure of a flat car did not exceed the allowable values [11, 12, 74, 115].

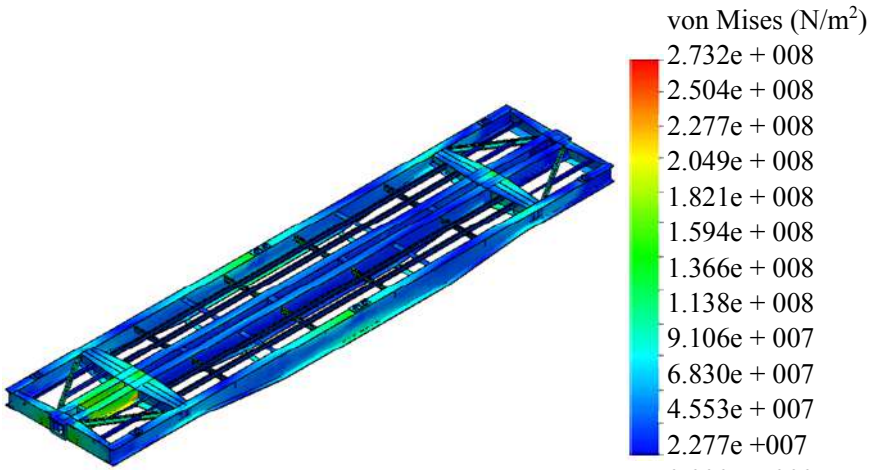


Figure 2.33 – Stress state of the bearing structure of a flat car with viscous interaction between the container fittings and fixed fittings (side view)

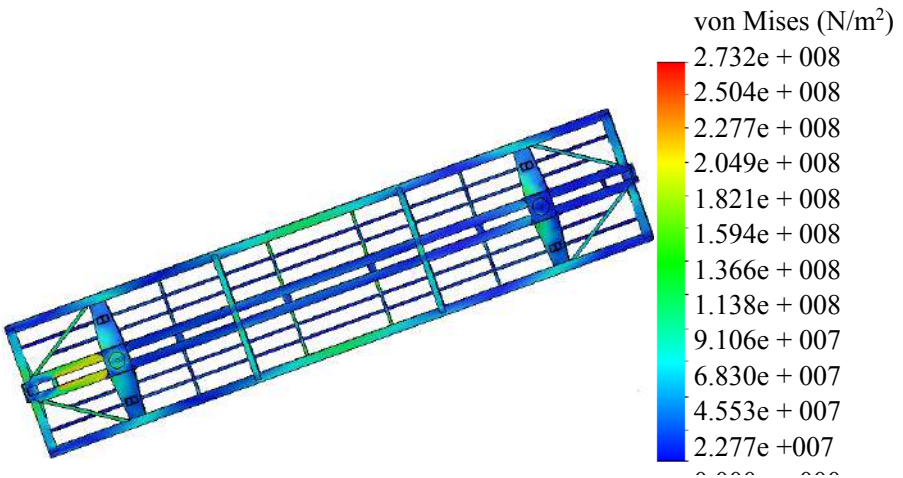


Figure 2.34 – Stress state of the bearing structure of a flat car with viscous interaction of the container fittings and fixed fittings (bottom view)

The maximum displacements were in the middle parts of the main longitudinal beams of the flat car frame; they amounted to 12.1 mm (figure 2.35).



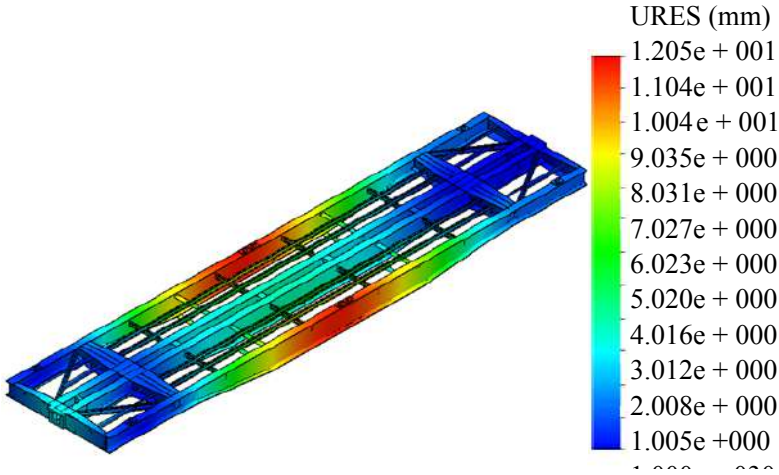


Figure 2.35 – Displacements in the units of the bearing structure of a flat car with viscous interaction of the container fittings and fixed fittings

With elastic-viscous interaction between the container fittings and fixed fittings the maximum equivalent stresses in the bearing structure of a flat car were about 260 MPa. The maximum displacements were 11.8 mm. The measures proposed for improving the diagrams of interaction between the flat car and containers can decrease the maximum equivalent stresses in the fixed fittings almost three times (figure 2.36), and in the tank container fittings – almost seven times.

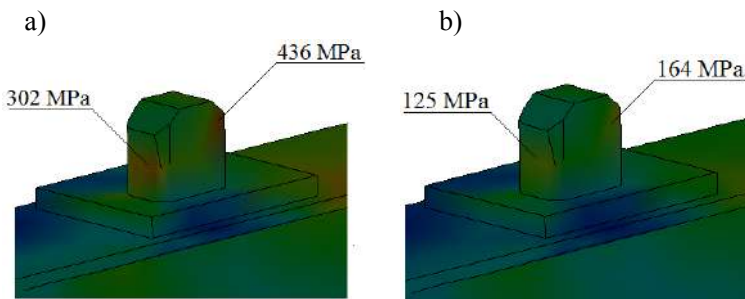


Figure 2.36 – Stress state of the fixed fittings of a flat car  
 a) standard interaction diagram; b) improved interaction diagram

## Conclusions to Part 2

1. The research deals with the mathematic modelling of the dynamic loads on the bearing structure of a flat car with dry-freight containers during a shunting impact. The research was made in the plane coordinates. The value of the longitudinal impact to a flat car was taken 3.5 MN.

It was found that with gaps between the container fittings and fixed fittings, the accelerations to the bearing structures of a flat car and the containers were approximately  $90 \text{ m/s}^2$  and  $110 \text{ m/s}^2$ , respectively.

Without gaps between the container fittings and fixed fittings, the maximum acceleration to a flat car and containers during a shunting impact was about  $50 \text{ m/s}^2$ ;

2. The research also deals with the mathematic modelling of the dynamic loads on the bearing structure of a flat car with a dry-freight container during a shunting impact. It was found that without gaps between the container fittings and fixed fittings, the accelerations to the bearing structure of a tank container was approximately  $40 \text{ m/s}^2$ . The maximum accelerations were obtained for a gap between the container fitting and the fixed fitting of 30 mm. They amounted to about  $300 \text{ m/s}^2$ ;

3. The research also presents the mathematic modelling of the dynamic loads on the bearing structure of a flat car with dry-freight containers during a shunting impact. The maximum accelerations on a flat car with gaps of 30 mm between the fixed fittings and container fittings were about  $100 \text{ m/s}^2$ , without gaps – about  $60 \text{ m/s}$ , for the container the values of acceleration were about  $120 \text{ m/s}^2$  and  $50 \text{ m/s}^2$ , respectively. The developed models were checked for adequacy. It was found that the hypothesis on adequacy was not rejected.

4. The research deals with the computer modelling of the dynamic loads on the bearing structure of a flat car with a dry-freight container during a shunting impact. The research demonstrated that the maximum acceleration on the tank container was about  $320 \text{ m/s}^2$ .

5. The authors theoretically substantiated the introduction of elastic, viscous, and elastic-viscous links in the bearing structure of combined transport facilities in order to decrease the dynamic loading in operation. It was done with the mathematic model which included elastic, viscous, and elastic-viscous interaction between the container fittings and fixed fittings.

It was found that the accelerations to the container with viscous interaction in the fittings, located on the flat car during a shunting impact were

about  $20 \text{ m/s}^2$  ( $\approx 2g$ ); thus it did not exceed the normative value. And the viscous resistance to the displacements of the container should be within a range of  $10 - 50 \text{ kN}\cdot\text{s/m}$ .

With elastic-viscous interaction between the container fittings and fixed fittings the accelerations to a container on the flat car during a shunting impact were about  $20 \text{ m/s}^2$  ( $\approx 2g$ ). The rigidity of an elastic element was taken  $20 \text{ kN/m}$ , and the viscous resistance coefficient –  $30 \text{ kN}\cdot\text{s/m}$ .

The authors built the computer model of the dynamic loading of a container located on the flat car during a shunting impact. The maximum accelerations to a container with viscous interaction of the container fittings and fixed fittings were about  $20.3 \text{ m/s}^2$ ; with elastic-viscous interaction the maximum accelerations were  $19.7 \text{ m/s}^2$ .

The models of the dynamic loading of a container on the flat car during a shunting impact were verified with an F-test. It was found that the hypothesis on adequacy was not rejected.

It was found that the accelerations to a tank container with viscous interaction in the fittings located on the flat car during a shunting impact were about  $40 \text{ m/s}^2$  ( $\approx 4g$ ); they did not exceed the normative value.

Here, the total viscous resistance to the displacements of one tank container should be within a range from  $9$  to  $54 \text{ kN}\cdot\text{s/m}$ .

With consideration of elastic viscous interaction of the container fittings and fixed fittings the maximum acceleration was about  $40 \text{ m/s}^2$  ( $\approx 4g$ ). And the rigidity of an elastic element was taken  $480 \text{ kN/m}$ , and the viscous resistance coefficient –  $30 \text{ kN}\cdot\text{s/m}$ .

The authors built the computer model of the dynamic loading of a tank container located on the flat car during a shunting impact. The maximum accelerations to the tank container with consideration of viscous interaction between the container fittings and fixed fittings were in the frame at the end walls of the bearing structure of a flat car; they amounted to about  $40 \text{ m/s}^2$ . In the middle part of a tank container the accelerations were  $28.6 \text{ m/s}^2$ .

The results of the modelling of the dynamic loading of a tank container with elastic-viscous interaction between the container fittings and fixed fittings demonstrated that the maximum accelerations to the bearing structure of a tank container were  $39.2 \text{ m/s}^2$ .

The models of the dynamic loading of a tank container on the flat car during a shunting impact were verified with an F-test. It was found that the hypothesis on adequacy was not rejected.

6. The research deals with the determination of the strength of the fixed fittings on the flat car with viscous and elastic-viscous interaction with the tank container. It was found that with viscous interaction of the dry-freight container fittings and fixed fittings during a shunting impact of the flat car, the maximum equivalent stresses were about 270 MPa; they were concentrated in the zone of interaction between the center sill and the body bolster beam. The maximum displacements were in the middle parts of the main longitudinal beams of the flat car frame; they amounted to 12.1 mm.

It was found that with viscous interaction of the dry-freight container fittings and the fixed fittings during a shunting impact of the flat car, the maximum equivalent stresses were about 260 MPa; they were concentrated in the zone of interaction between the center sill and the body bolster beam.

The measures proposed for improving the interaction diagram between a flat car and a container can decrease the maximum equivalent stresses in the fixed fittings almost three times, and in the container fittings – almost seven times.

With viscous interaction of the container fittings and fixed fittings during a shunting impact of a flat car, the maximum equivalent stresses were about 270 MPa; they were concentrated in the zone of interaction between the center sill and the body bolster beam. The maximum displacements were in the middle parts of the main longitudinal beams of the flat car frame; they amounted to 12.1 mm.

With elastic-viscous interaction of the tank container fittings and fixed fittings the maximum equivalent stresses in the bearing structure of a flat car were about 260 MPa. The maximum displacements were 11.8 mm.

The measures proposed for improving the interaction diagram between the flat car and container can decrease the maximum equivalent stresses in the fixed fittings almost three times, and in the tank container fittings – almost seven times.

### PART 3

## EXPERIMENTAL RESEARCH INTO THE STRENGTH OF THE BEARING STRUCTURE OF A FLAT CAR DURING SHUNTING IMPACTS

### 3.1 The experimental research into the strength of the bearing structure of a flat car in the standard diagram of interaction between fixed fittings and container fittings

The strength of the bearing structure of a flat car during a shunting impact was determined by means of full-scale tests in accordance with the “Program and procedure of testing” (Appendix A).

The purpose of the experiments was to determine the maximum equivalent stresses in the bearing structure of a flat car in the standard diagram of interaction between the container fittings and fixed fittings.

The subject of the experiments was a 13-401-17 flat car modernized with fixed fittings on the frame (figure 3.1). During the experiments the flat car was loaded with coiled steel.



Figure 3.1 – Flat car 13-401-17

The technical state of the flat car was diagnosed as satisfactory [9, 54, 64, 65]. It was found that the geometric parameters of the main bearing elements of the frame were within the allowable values. The measurements were conducted with an electronic caliper (figure 3.2) and a ranging laser (figure 3.3).



Figure 3.2 – Measurements of the parameters of the main bearing elements of the flat car



Figure 3.3 – Ranging laser

The maximum equivalent stresses in the bearing structure of the flat car were determined by the strain gage method [42, 44, 46, 49]. The research was conducted by certified specialists from the Center for Diagnostics of Transport Facilities together with the fellows of the Department of Wagon Engineering and Product Quality of Ukrainian State University of Railway Transport (UkrSURT).

The layout diagram of the strain gages on the flat car is presented in figure 3.4. The locations of the gages were determined on the basis of the fields of stress distribution obtained with the FEM.a)

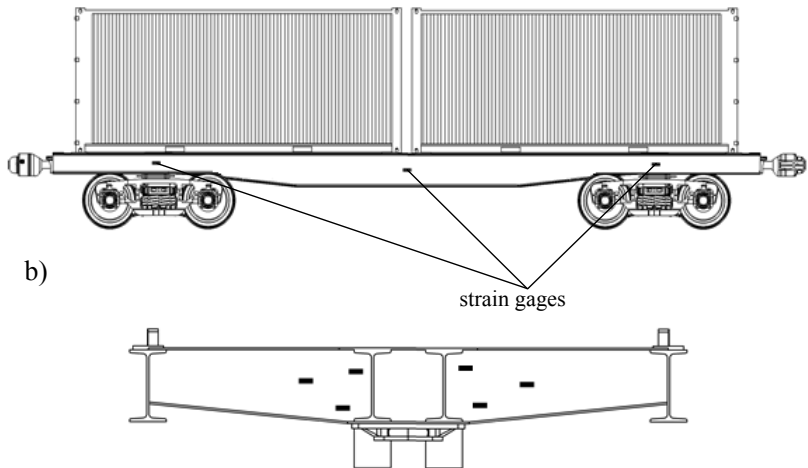


Figure 3.4 – Layout diagram of the strain gages on the bearing structure of the flat car

a) on the main longitudinal beam of the frame; b) on the body bolster beam

The measurements were made with the strain gages with a measuring grid length of 10 mm and a resistance of 200 Ohm. The resistance of the strain gages was checked before testing. The resistance difference of the strain gages was no more than 3 Ohm.

Before the experiments the strain gages were calibrated (figure 3.5 and 3.6).



Figure 3.5 – Calibration of the strain gages



Figure 3.6 – Mounting of the strain gages on the calibrating beam

The strain gages were mounted on the prepared surfaces which were cleaned and treated with alcohol in advance. The prepared surface and the strain gage were treated with a thin coat of glue, when the glue dried they were coated with glue again, and, after that, the strain gage was attached to the surface of the bearing structure.

The strain gages were glued with cyanoacrylate-based thermosetting adhesive. The strain gages were pressed to the surface, and the remaining glue was removed. The outputs of the strain gages were connected to the measuring equipment; some time was spent on glue drying. Before the strain gages were mounted, the surface of the bearing structure of the flat car was dried with a heat gun. The bitumen tape was used for securing the plates with compensating strain gages (figure 3.7).



Figure 3.7 – Plate with a compensating strain gage

Insulation tapes were glued under the outputs of the strain gages to prevent the contact between the outputs and the plates.



The connection diagram of the strain gages is given in the technical description and the manual for the 32-channel strain gage amplifier (figure 3.8).



Figure 3.8 – 32-channel strain-gage amplifier

The strain gages were joined by the dual element connector diagram (figure 3.9), [23].

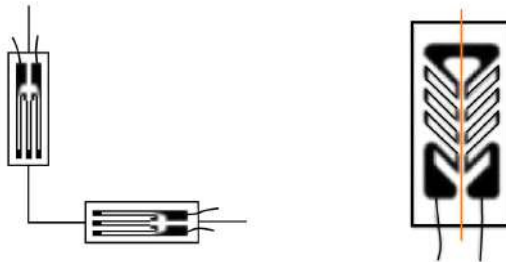


Figure 3.9 – Connection diagram of the strain gages

The layout diagram of the strain gages on the bearing structure of the flat car is presented in figures 3.10 – 3.12.

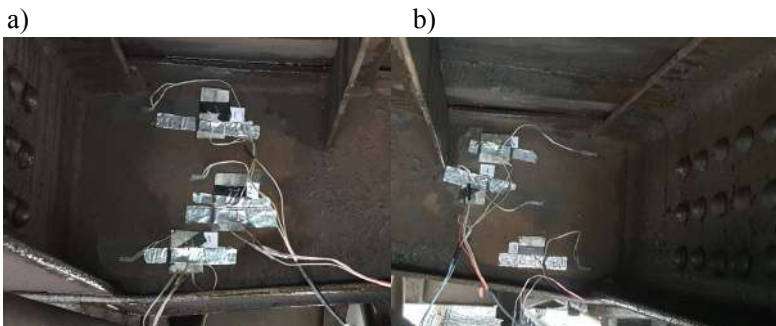


Figure 3.10 – Layout of strain gages on the body bolster of the flat car  
a) left vertical sheet; b) right vertical sheet

Some strain gages were mounted on the automatic coupler in order to determine the impact force (figure 3.12, a). Besides, the accelerations of the bearing structure of the flat car, and, therefore, the impact force, were determined with an acceleration indicator attached to the bearing structure of the flat car (figure 3.12, b).

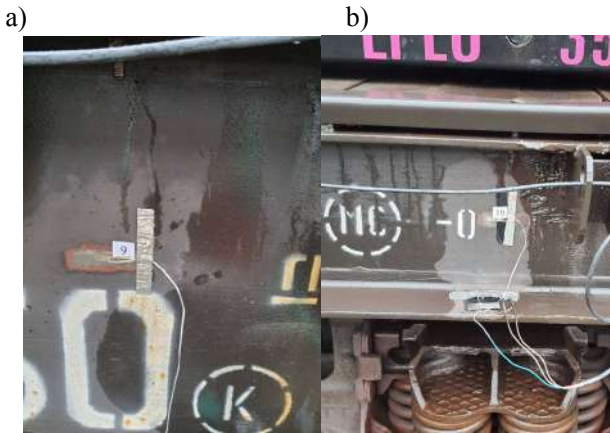


Figure 3.11 – Layout of strain gages on the main longitudinal beam of the flat car

a) middle part of the beam; b) end part of the beam

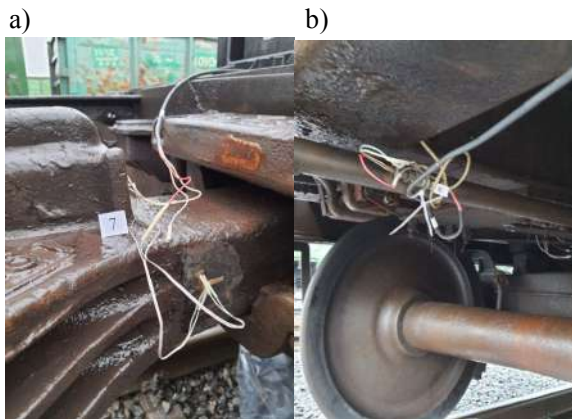


Figure 3.12 – Location of measuring devices on the flat car  
a) strain gages on the automatic coupler; b) acceleration indicator

The strength tests on the flat car were conducted in the dynamic mode at various impact speeds in the intervals and conditions specified in the standards [11, 12, 19]. The first test stage included the determination of the maximum equivalent stresses in the bearing structure of the flat car in the standard diagram of interaction of the container fittings and fixed fittings. The flat car was placed on the horizontal section of a sorting track (figure 3.13), [57, 59]

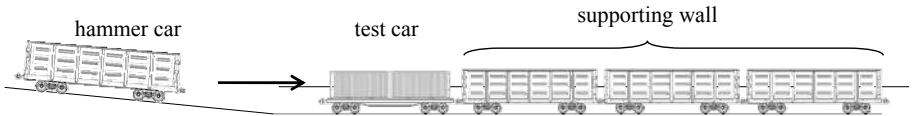


Figure 3.13 – Rail car impact diagram

Some chalk marks on the flat car indicated the location of the fittings before an impact. The impact tests for the research car were carried out with a set of stationary retaining cars (supporting wall) loaded to the full load capacity. The supporting wall consisted of seven open cars coupled to each other and put on hold with a pneumatic brake (figure 3.14).



Figure 3.14 – Location of the flat car coupled to the retaining cars

The car which was the first from an impact was additionally fixed with two brake shoes [57, 59]. The total mass of the retaining cars exceeded 650 tons. The difference in the levels of the couplers of the hammer car and the research car, and that of the retaining cars and the research car was 0.05 m. The hammer car rolled off the sorting hump and impacted with the research flat car (figure 3.15). The rolling-off speed and the impact force were recorded. The mass of the hammer car was about 100 tons.



Figure 3.15 – Rolling of the hammer car off the hump

The pre-impact speed of the car was calculated by the formula

$$V = \frac{36}{t}, \quad (3.1)$$

where  $t$  – time during which the car passed the control section, s.

The time was measured with a stopwatch. After each impact, the flat car was inspected for damage. The displacements of the fittings relative to their initial position were chock marked before and after the impact. 17 impacts were made on a straight track section one after another as presented in table 3.1 [11, 12, 59].

Table 3.1 – Impact modes of the flat car

Mode No.	Impact speed range, km/h	Number of impacts
1	3 – 6	7
2	6 – 10	7
3	over 10	3

All those participating in the experiments observed the safety requirements [9, 52, 53, 57].

The maximum equivalent stresses were recorded by strain gage No. 5. The test results are given in table 3.2. Table 3.2 – Maximum equivalent stresses in the bearing structure of the flat car

Test No.	Maximum equivalent stresses, MPa		
	Impact speed, km/h		
	3 – 6	6 – 10	over 10
1	69.5	82.9	98.5
2	71.6	84.5	91.4
3	72.4	88.4	95.3
4	76.8	84.7	
5	78.8	88.6	
6	71.2	82.5	
7	74.5	85.4	
Average value	73.5	85.3	95.1

Figures 3.16 and 3.17 show the dependency of the maximum equivalent stresses in the bearing structure of the flat car on time. The results recorded by strain gages No. 2 and No. 5 can serve as an example.

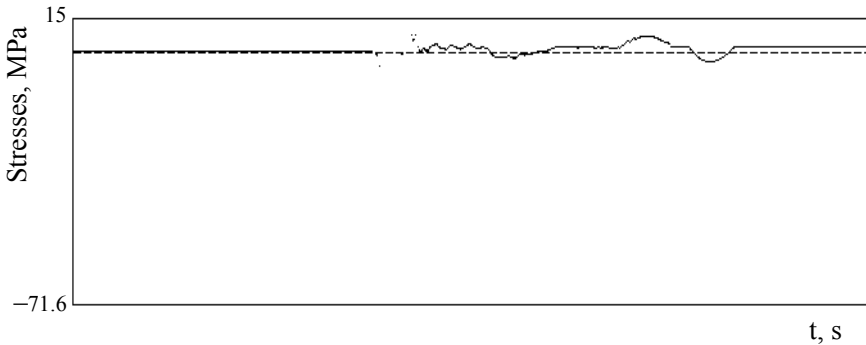


Figure 3.16 – Maximum equivalent stresses (strain gage No. 2)

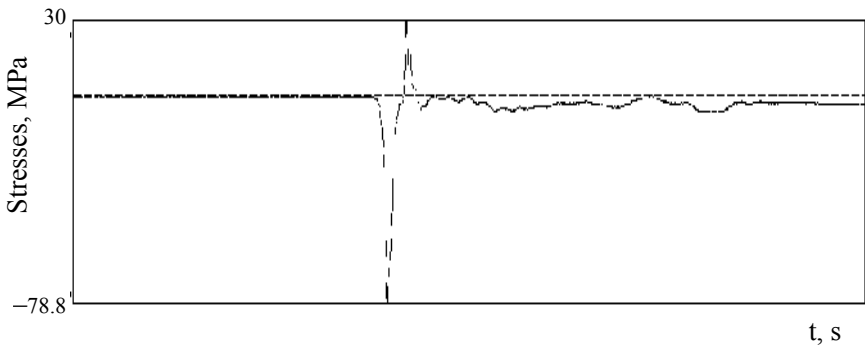


Figure 3.17 – Maximum equivalent stresses (strain gage No. 5)

It was found that the maximum stresses in the bearing structure of the flat car emerged in the moment of impact and had a negative value.

The comparative analysis of the stress values in the bearing structure of the flat car obtained theoretically and experimentally is presented in table 3.3. The maximum difference between the test results was 17.0%.

Table 3 – Comparative analysis of the theoretical and experimental stresses in the bearing structure of the flat car (strain gage No. 5)

Impact speed, km/h	Stresses, MPa		Relative difference, %
	theoretical	experimental	
3 – 6	90.1	78.8	14.4
6 – 10	103.7	88.6	17.0
over 10	111.6	98.5	13.3
Average value			14.9

The acceleration indicator installed on the bearing structure of the flat car recorded the accelerations during an impact (figure 3.18). The maximum value of acceleration was about 98 m/s<sup>2</sup>. The difference between the theoretical value of acceleration obtained in Part 3 and the experimental value was about 8%.

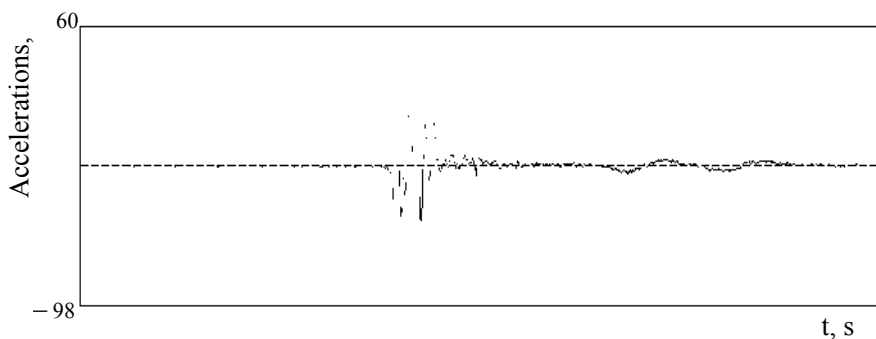


Figure 3.18 – Accelerations to the bearing carrying structure of the flat car during an impact

The loading models of the flat car were verified with an F-test. It was assumed that the model under consideration was linear, i.e., a single-factor

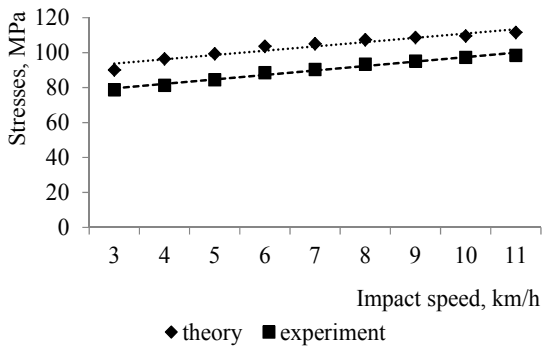
model, and it characterized a change of the stresses in the bearing structure of the flat car according to the impact speed.

The calculation was made for strain gage No. 5 in a speed range of 3 – 11 km/h. The results of the measurements are showed in table 3.4 and figure 3.19. The theoretical values of the stresses in the bearing structure of the flat car were determined according to the design scheme given in Part 3.

Table 3.4 – Stresses in the bearing structure of the flat car during an impact (strain gage No. 5)

Impact speed, km/h	Stresses, MPa	
	theoretical	experimental
3	90.1	78.8
4	96.5	81.3
5	99.4	84.5
6	103.7	88.6
7	105.1	90.4
8	107.4	93.4
9	108.7	95.2
10	109.6	97.3
11	111.6	98.5

On the basis of the calculation at  $f_1 = 7$  and  $f_2 = 9$  the authors obtained the value  $F_p = 1.01$ , which was lower than  $F_t = 3.29$ . Thus, with a significance level of  $p = 0.05$  the hypothesis on adequacy of the model designed was not



rejected.

Figure 3.19 – Dependency of the stresses in the bearing structure of the flat car on impact speeds

### 3.2 Experimental research into the strength of the bearing structure of a flat car during elastic interaction between fixed fittings and container fittings

The purpose of the experiments was to determine the maximum equivalent stresses in the bearing structure of the flat car during elastic interaction of the container fittings and fixed fittings, and prove the efficiency of the measures suggested.

The maximum equivalent stresses in the bearing structure of the flat car with elastic interaction of the container fittings and fixed fittings were determined in the course of full-scale experiments.

A spring with a given rigidity was mounted between the fixed fitting and the inner surface of the container fitting (figure 3.20).

The total rigidity of the springs for one container was 1700 kN/m; it was determined through the mathematic modelling demonstrated in Part 2.

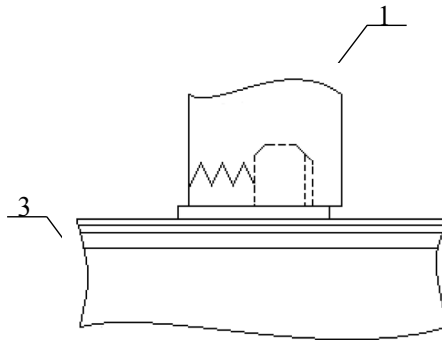


Figure 3.20 – Diagram of interaction between the container fitting and fixed fitting

1 – container fitting; 2 – fixed fitting; 3 – longitudinal beam of the flat car

The geometric characteristics of the springs were calculated in advance in accordance with the geometric parameters of the container fittings [16] and fixed fittings (album of drawings of flat cars for transportation of containers).

The diameter of a spring coil was determined according to [8]



$$c = \frac{G \cdot d^4}{8D^3 \cdot n_p}, \quad (3.4)$$

where  $c$  – spring rigidity;

$d$  – coil diameter;

$D$  – average spring diameter;

$G$  – shear modulus;

$n_p$  – number of the spring's working coils.

From where

$$d = \sqrt[4]{\frac{c \cdot 8 \cdot D^3 \cdot n_p}{G}}. \quad (3.5)$$

The average spring diameter was determined according to the geometric characteristics of the container fitting.

The geometric parameters of the spring are given in figure 3.21. The physical models of the springs were built according to the geometric parameters obtained (figure 3.22). During the tests the end parts of the springs were rested on the vertical parts of the fixed fittings of the flat car and the container fittings (figure 3.23).

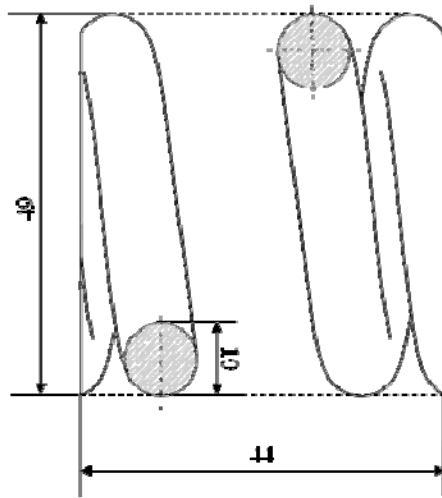


Figure 3.21 – Geometrical parameters of the spring



Figure 3.22 – Fitting springs

The consequence of the tests was identical to that mentioned above. The test results are given in table 3.5.

Figures 3.16 and 3.17 show the dependency of the maximum equivalent stresses in the bearing structure of the flat car on time (strain gages No. 2 and No. 5).

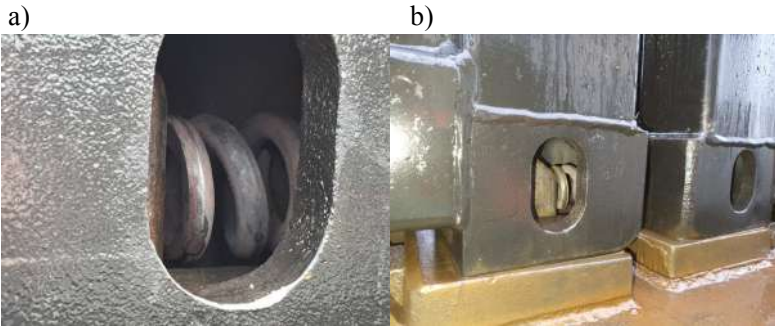


Figure 3.23 – Location of springs in the fittings

a) front fitting on the side of an impact; b) rear fitting on the side of an impact

Table 3.5 – Maximum equivalent stresses in the bearing structure of the flat car during elastic interaction of the container fittings and fixed fittings

Test No.	Maximum equivalent stresses, MPa		
	Impact speed, km/h		
	3 – 6	6 – 10	over 10
1	55.5	72.3	81.8
2	61.2	74.4	81.3
3	61.7	75.6	81.5
4	66.3	76.7	
5	68.5	78.3	
6	67.2	73.8	
7	64.5	76.5	

Average value	63.6	75.4	81.5
---------------	------	------	------

The stresses in the bearing structure of the flat car appeared in the moment of an impact and had a negative value (the same as in the previous diagram described).

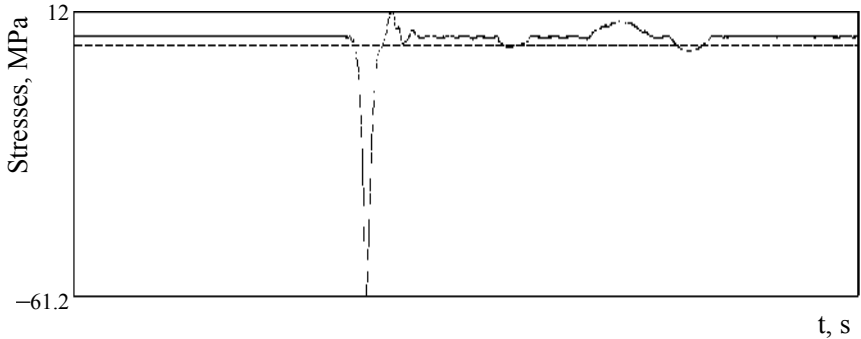


Figure 3.24 – Maximum equivalent stresses (strain gage No. 2)

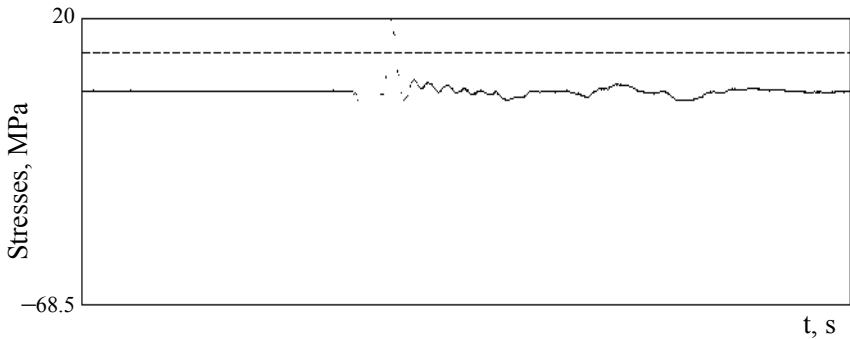


Figure 3.25 – Maximum equivalent stresses (strain gage No. 5)

The comparative analysis of the theoretical and experimental stresses in the bearing structure of the flat car is presented in table 3.6. The maximum difference between the test results was 17.5%. The maximum acceleration was about 60 m/s<sup>2</sup>. The difference between the theoretical acceleration value obtained in Part 2 and the experimental value was about 16%.

Table 3.6 – Comparative analysis of the theoretical and experimental values of the stresses in the bearing structure of the flat car (strain gage No. 5)

Impact speed, km/h	Stresses, MPa		Relative difference, %
	theoretical	experimental	
3 – 6	79.7	68.5	16.3
6 – 10	91.7	78.3	17.1
over 10	99.1	81.8	17.5
Average value			16.97

The graphical time dependency of the accelerations of the bearing structure of the flat car is given in figure 3.26.

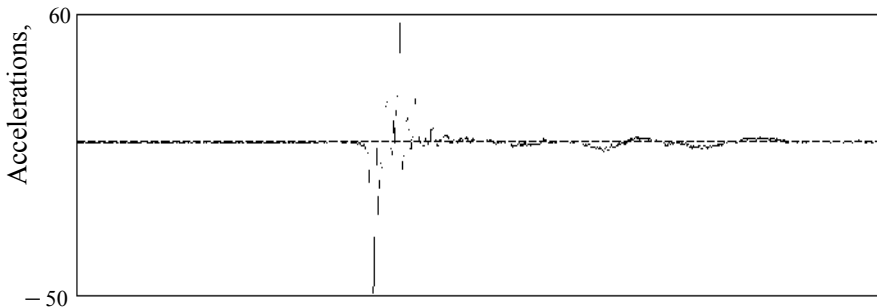


Figure 3.26 – Accelerations to the bearing structure of the flat car at a shunting impact

The loading models of the flat car were verified with an F-test. The calculation was made for strain gage No. 5 in a speed range of 3 – 11 km/h. The test results are given in table 3.7. The dependency of the stresses in the bearing structure of the flat car on impact speeds is presented in figure 3.27.

On the basis of the calculation at  $f_1 = 7$  and  $f_2 = 9$  the authors obtained the value  $F_p = 1.45$ , which was lower than  $F_t = 3.29$ . Thus, with a significance level of  $p = 0,05$  the hypothesis on adequacy of the model designed was not rejected. Table 3.7 – Stresses in the bearing structure of the flat car during an impact (strain gage No. 5)

Impact speed, km/h	Stresses, MPa	
	theoretical	experimental
3	79.7	68.5
4	83.5	72.4
5	88.4	75.2
6	91.7	78.3
7	92.3	79.2
8	92.7	79.9
9	93.6	80.5
10	94.4	81.1
11	95.8	81.5

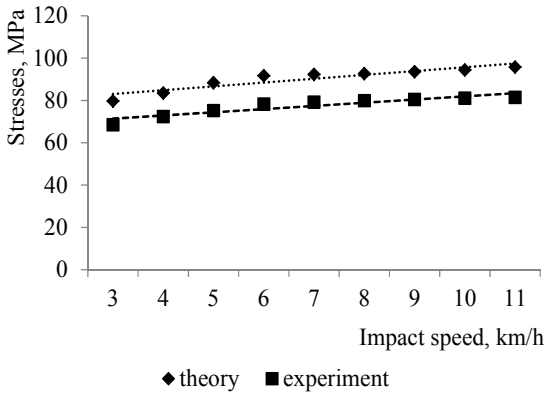


Figure 3.27 – Dependency of the stresses in the bearing structure of the flat car on impact speeds

### Conclusions to Part 3

1. The research deals with the study into the strength of the bearing structure of the flat car during a shunting impact in the standard diagram of interaction between the container fittings and fixed fittings. The tests were conducted by the strain-gage method. The following range of impact speeds was taken into account: 3 – 6 km/h, 6 – 10 km/h, and over 10 km/h.

It was found that the maximum equivalent stresses in the vertical sheet of the body bolster beam were about 98.5 MPa at an impact speed of over 10 km/h. The maximum difference between the results of mathematical and physical experiments was 13.3%.

The models of loading on the bearing structure of the flat car were verified in the standard diagram of interaction of the container fittings and fixed fittings with an F-test. On the basis of the calculation at  $f_1 = 7$  and  $f_2 = 9$  the authors obtained the value  $F_p = 1.01$ , which was lower than  $F_t = 3.29$ . Thus, with the level of significance  $p = 0.05$ , the hypothesis on adequacy of the models designed was not rejected.

2. The research deals with the study into the strength of the bearing structure of the flat car during a shunting impact with elastic interaction of the container fittings and fixed fittings. Some springs were designed on the basis of the geometrical dimensions of the container fitting and fixed fitting, and mounted between them.

The research had the same sequence as in the standard diagram of interaction between the container fittings and fixed fittings.

It was found that the maximum equivalent stresses in the vertical sheet of the body bolster beam were 81.8 MPa. The maximum difference between the results of mathematical and physical experiments was 17.5%.

The models of loading on the bearing structure of the flat car with elastic interaction of the container fittings and fixed fittings were verified with an F-test.

On the basis of the calculation at  $f_1 = 7$  and  $f_2 = 9$  the authors obtained the value  $F_p = 1.45$ , which was lower than  $F_t = 3.29$ . Thus, with the level of significance  $p = 0.05$ , the hypothesis on adequacy of the model designed was not rejected.

## GENERAL CONCLUSIONS

1. The research included the analysis of scientific works dedicated to the determination of the loading of flat car constructs in operation. It was found that the issue of determination of the dynamic loading of a flat car during over-standardized modes has not been thoroughly studied. The analysis of existing standards on designing flat cars showed that they do not cover all over-standardized loading modes for rail cars. It can cause failures in the bearing structure of a flat car in operation and, thus, require off-schedule repairs.

2. The research presents the study into the dynamic loading of containers and tank containers located on the flat car during a shunting impact. It was found that the accelerations to the bearing structure were approximately  $90 \text{ m/s}^2$  and  $110 \text{ m/s}^2$  if there were gaps between the container fittings and fixed fittings. As for the longitudinal loading on a flat car with tank containers, the maximum accelerations were obtained for a gap between the fixed fitting and container fitting of 30 mm. They amounted to about  $300 \text{ m/s}^2$ .

3. The authors built the mathematical models for the determination of the dynamic loading of containers and tank containers with elastic, viscous, and elastic-viscous interaction in the fittings; these models were used for obtaining the dependencies of their dynamic loading during a shunting impact. They also developed the new method which included over-standardized loading modes for the bearing structure of a flat car loaded with containers and tank containers with elastic, viscous and elastic viscous elements in the fittings during a shunting impact. The results of the research demonstrated that the accelerations to a container and a tank container with viscous and elastic-viscous interaction in the fittings, located on the flat car during a shunting impact were about  $20 \text{ m/s}^2$  and  $40 \text{ m/s}^2$ ; they did not exceed the normative values. The measures proposed for improving the interaction diagram between a flat car and containers can decrease the maximum equivalent stresses in the fixed fittings almost three times, and in the container fittings – almost seven times.

4. The strength of the rail cars during over-standardized loading modes was researched by means of experiments. The full-scale testing was based on the strain gage measurement.

Two diagrams of interaction between the container fittings and fixed fittings were studied: standard and elastic. The maximum difference between the results of the mathematic and physical experiments in the standard interaction diagram between the container fittings and fixed fittings was 17.0%, and for the elastic diagram – 17.5%. The models of the dynamic loading on the bearing structure of the flat car were verified with an F-test. It was found that the hypothesis on adequacy was confirmed.



## REFERENCES

1. Anisimov P. Model prostranstvennyh kolebanij platformy s dlinomernym gruzom. Mir transporta. 2013. № 4. S. 6–13.
2. Arshincev D. N. Sposoby povysheniya effektivnosti kontejnernih perevozok i obespechenie bezopasnosti dvizheniya kontejnernih poezdov: avtoref. dis. ... kand. tekhn. nauk: 05.22. Moskva, 2010. 24 s.
3. Bogomaz G. I. Dinamika cistern (vagonov i kontejnerov) pri prodol'nyh udarah i perekhodnyh rezhimah dvizheniya poezdov: avtoref. dis. ... dokt. tekhn. nauk: 05.22.07. Leningrad, 1990. 31 s.
4. Bogomaz G. I., Mekhov D. D., Pilipchenko O. P., Chernomashenceva Yu. G. Nagruzhenost' kontejnerov-cistern, raspolozhennyh na zheleznodorozhnoj platforme, pri udarah v avtoscepku. Zbirnik naukovih prac' "Dinamika ta keruvannya ruhom mekhanichnih sistem". 1992. S. 87 – 95.
5. Bondar A. I., Panin A. Yu. Teoreticheskaya i eksperimentalnaya ocenka prochnosti vagona-platformy dlya perevozki avtomobilnyh polupricepov. Transport Rossijskoj federacii. 2014. № 3. S. 33–35.
6. Vagon-platforma zchlenovanogo tipu dlya perevezennya kontejneriv: pat. 145433 Ukraïna, MPK (2020.01) B61D 3/00, B61D 3/08 (2006.01), B61F 1/08 (2006.01). u2020 04117; zayavl. 07.07.20; opubl. 10.12.20, Byul. № 23.
7. Vagon-platforma zchlenovanogo tipu dlya perevezennya kontejneriv: pat. 122328 Ukraïna, MPK B61D 3/08 (2006.01), B61D 3/10 (2006.01), B61D 3/20 (2006.01), B60P 7/13 (2006.01), B60P 7/08 (2006.01), B61F 1/08 (2006.01), B61F 1/02 (2006.01). a2017 04241; zayavl. 28.04.17; opubl. 26.10.20, Byul. № 20.
8. Vagony / Shadura L. A. i dr.; pod red. L. A. Shadura. Moskva: Transport, 1980. 139 s.
9. Vagony-platformy dlya perevozki krupnotonnazhnyh kontejnerov massoj brutto do 36 t. Tipovaya metodika ispytanj. M., 2016.
10. Vasilenko D. A. Sovershenstvovanie metodov rascheta soprotivleniya ustalosti svarnyh soedinenij ram dlinnobaznyh vanonov-platform: avtoref. dis. ... kand. tekhn. nauk: 05.22.07. Sankt-Peterburg, 2010. 16 s.
11. GOST 33788-2016. Vagony gruzovye i passazhirskie. Metody ispytanj na prochnost' i dinamicheskie kachestva. [25.05.2016]. Moskva: Standartinform, 2016. 40 s.
12. GOST 33211-2014. Vagony gruzovye. Trebovaniya k prochnosti i dinamicheskim kachestvam. [22.12.2014]. Moskva: Standartinform, 2016. 54 s.
13. GOST 31232. Kontejnery dlya perevozki opasnyh gruzov. Trebovaniya po ekspluatacionnoj bezopasnosti. [28.03.2005]. Minsk: NP RUP "Belorusskij

gosudarstvennyj institut standartizacii i sertifikacii (BelGISS)”, 2005. 6 s.

14. GOST 20259-80. Kontejnery universal'nye. Obshchie tekhnicheskie usloviya. [07.2002]. Moskva: IPK standartov, 2002. 17 s.

15. GOST 18477-79. Kontejnery universal'nye. Tipy, osnovne parametry i razmery. [11.2004]. Moskva: IPK standartov, 2004. 11 s.

16. GOST 20527-82. Fitingi uglovyje krupnotonnazhnyh kontejnerov. Konstrukcija i razmery. [26.10.2004]. Moskva: IPK standartov, 2004. 9 s.

17. Gurzhi N. L. Polinshennya tekhnichnih karakteristik sekcijnogo vagonu-nlatformi shlyahom vdoskonalennya konstrukcii: avtoref. dis. ... kand. tekhn. nauk: 05.22.07. Dnipropetrovs'k, 2010. 20 s.

18. Dauksha A. S. Sovershenstvovanie vagonov na osnove ispol'zovaniya s'emnyh kuzovov: avtoref. dis. ... kand. tekhn. nauk: 05.22.07. Sankt-Peterburg, 2018. 16 s.

19. DSTU 7598:2014. Vagoni vantazhni. Zagal'ni vimogi do rozrahunkiv ta proektuvannya novih i modernizovanih vagoniv kolii 1520 mm (nesamohidnih). [01.07.2015]. Kiïv, 2015. 162 s.

20. Dyakonov V. MATHCAD 8/2000: specialnyj spravochnik. SPb.: Piter, 2000. 592 c.

21. Eremin V., Semennikova L. Issledovanie napryazhenno-deformirovannogo sostoyaniya kuzov-kontejnera s pomoshchyu programmnogo kompleksa ARM WinMachine. SAPR i grafika. 2004. №7. S. 23–28.

22. Zharova E. A. Obosnovanie variantov prodleniya srokov sluzhby specializirovannyh vagonov-platform: avtoref. dis. ... kand. tekhn. nauk: 05.22.07. Sankt-Peterburg, 2008. 16 s.

23. Zabrodin V. P., Seregin A. A., Suhanova M. V., Portakov A. B. Eksperimentalnye metody opredeleniya napryazhenij i deformacij: uchebnoe posobie. Zernograd: Azovo-Chernomorskij inzhenernyj institut FGBOU VO Donskoj GAU, 2017. 104 s.

24. Ibragimov N. N., Rahimov R. V., Hadzhimuhamedova M. A. Razrabotka konstrukcii kontejnera dlya perevozki plodoovoshchnoj produkcii. Molodoj uchenyj. 2015. №21(101). S. 168–173.

25. Kiryanov D. V. Mathcad 13. SPb.: BHV. Peterburg, 2006. 608 c.

26. Kobzar A. I. Prikladnaya matematicheskaya statistika. Moskva: Fizmatlit, 2006. 816 s.

27. Konstruirovaniye i raschet vagonov / Lukin V.V i dr.; pod. red. V. V. Lukina. Moskva: UMK MPS Rossii, 2000. 731 s.

28. Kontejner-cisterna: pat. 135552 Ukraïna, MPK (2019.01) B65D 88/12 (2006.01), B61D 3/00, B61D 3/20 (2006.01). u2018 12989. zayavl. 27.12.18; opubl. 10.07.19, Byul. № 13.

29. Kontejner-cisterna: pat. 134400 Ukraina, MPK (2019.01) B61D 3/00, B61D 3/20 (2006.01), B61D 5/00, B65D 88/06 (2006.01), B65D 88/12 (2006.01). u2018 12988; zayavl. 27.12.18; opubl. 10.05.19, Byul. № 9.

30. Kosmin V.V. Osnovy nauchnyh issledovaniy. Moskva: GOU “Uchebno-metodicheskij centr po obrazovaniyu na zheleznodorozhnom transporte”, 2007. 271 s.

31. Kostrica S. A. Napryazhenno-deformirovanoe sostoyanie krupnotonnazhnyh kontejnerov v usloviyah ekspluatacii: avtoref. dis. ... kand. tekhn. nauk: 05.22.07. Dnepropetrovsk, 1987. 17 s.

32. Koroleva D. Yu. Sovershenstvovanie metoda rascheta krepleniya gruzov pri soudareniiyah vagonov: avtoref. dis. ... kand. tekhn. nauk: 05.22.08. Novosibirsk, 2001. 17 s.

33. Krivovyazyuk Yu. P. Ocenka ekvivalentnoj nagruzhennosti chetyrekhosnyh zheleznodorozhnyh cistern s zhidkimi gruzami razlichnoj plotnosti pri prodol'nyh udarah: dis. ... kand. tekhn. nauk: spec. 05.22.07, Dnepropetrovsk, 1986. 157 s.

34. Kyakk K. V. Vybory konstruktivnoj skhemy i parametrov nesushchej konstrukcii zheleznodorozhnoj platformy dlya perevozki krupnotonnazhnyh kontejnerov: avtoref. dis. ... kand. tekhn. nauk: 05.22.07. Sankt-Peterburg, 2007. 16 s.

35. Lovska A. O. Vyznachennya navantazhenosti kontejnera, rozmishchenogo na vagoni-platformi pri pruzhno-vyazkij vzaemodii fittingiv z fittingovimi uporami. Zbirnik naukovih prac UkrDUZT. 2019. Vip. 184. S. 6–19.

36. Lovska A. O. Doslidzhennya dinamichnogo navantazheniya vagona-platformi z kontejnerami, rozmishchenimi na nomu pri manevrovomu spivudaryanni. Innovacii infrastrukturi transportno-logistichnih sistem. Problemi, dosvid, perspektivi: zb. tez mizhnarodnoi naukovo-praktichnoi konferencii. (Truskavec, 11–17 kvitnya 2016 r.). Truskavec: SNU im. V. Dalya, 2016. S. 108–110.

37. Lovska A. O. Doslidzhennya dinamichnoi navantazhenosti kontejneriv z pruzhno-vyazkimi zvyazkami u fittingah pri ekspluatsijnih rezhimah. Vagoni novogo pokolinnya: iz XX v XXI storichchya: Tezi dopovidej II Vseukrainskoi konferencii. (Harkiv, 23–25 kvitnya 2019 r.). Harkiv: UkrDUZT, 2019. S. 13–14.

38. Lovska A. O. Kompyuterne modelyuvannya navantazhenosti kontejnera-cisterni pri ekspluatsijnih rezhimah. Logistichne upravlinnya ta bezpeka ruhu na transporti: zbirnik naukovih prac naukovo-praktichnoi konferencii studentiv ta molodih vchenih. (Kyiv, 16–17 listopada 2018 r.). Kyiv: SNU im. V. Dalya, 2018. S. 114–116.

39. Lovska A. O. Osoblivosti kompyuternogo modelyuvannya navantazhenosti kontejnera z pruzhno-vyazkimi zvyazkami u fittingah pri ekspluatsijnih rezhimah. Zbirnik naukovih prac Derzhavnogo universitetu infrastrukturi ta tekhnologij

Ministerstva osviti i nauki Ukraini: Seriya «Transportni sistemi i tehnologii». 2019. Vip. 33. T. 2. S. 28–37.

40. Lovska A. O. Osoblivosti modelyuvannya dinamichnoi navantazhenosti vagona-platformi zchlenovanogo tipu z kontejnerami. Visnik Skhidnoukrainskogo nacionalnogo universitetu imeni V. Dalya. 2017. №4(234). S. 138–145.

41. Lovska A. O., Ravlyuk V. G. Doslidzhennya dinamichnoi navantazhenosti nesuchih konstrukcij kontejneriv pri perevezenni na vagonah-platformah. Dynamikanaukovykh budań-2017:

materialy XIII międzynarodowej naukowipraktycznej konferencji. (Przemyśl, 07–15 lipca 2017 roku). Przemyśl: Nauka studia, 2017. S. 24–26.

42. Makarov R. A. Tenzometriya v mashinostroenii. Moskva: Mashinostroenie, 1975. 288 s.

43. Manueva M. V. Obosnovanie struktury i parametrov dlinnobaznyh vagonov-platform dlya perevozki avtopoezdov i krupnotonnazhnyh kontejnerov: avtoref. dis. ... kand. tekhn. nauk: 05.22.07. Bryansk, 2012. 17 s.

44. Metodika vypolneniya izmerenij staticheskikh i dinamicheskikh deformacij pri ispytaniyah izdelij mashinostroeniya. Mariupol, 1998.

45. Mekheda V. A. Tenzometricheskij metod izmereniya deformacij: uchebnoe posobie. Samara: Izdatelstvo Samarskogo gosudarstvennogo aerokosmicheskogo universiteta, 2011. 56 s.

46. Mishuta D. V., Mihajlov V. G., Algin V. B. Metodika razrabotki shtabnoj mashiny s kuzovom-kontejnerom. Mekhanika mashin, mekhanizmov i materialov. 2013. No. 3 (24). S. 13 – 19.

47. Mishuta D. V., Algin V. B., Mihajlov V. G. Ocenka napryazhenno-deformirovannogo sostoyaniya kuzova-kontejnera peremennogo obema. Vestnik Belorussko-Rossijskogo universiteta. 2012. №4(37). S. 61–68.

48. Mishuta D. V. Uproshchennye metody izmereniya napryazhenno-deformirovannogo sostoyaniya kuzova-kontejnera peremennogo obema. Pribory i metody izmerenij. 2012. №2(5). S. 100–103.

49. Moroz V.I. Suranov O.V., Bratchenko O.V., Logvinenko O.A. Osoblivosti viniknennya pogrishnostej tenzometruvannya v doslidzhennyh mekhanizmv gazorozpodilu chotiritaktnih dizeliv. Zbirnik naukovih prac Ukrainskoi derzhavnoi akademii zaliznichnogo transportu. 2001. Vip. 49. S. 85–90.

50. Morchiladze I. G. Situacionnaya adaptaciya vagonov dlya mezhdunarodnyh perevozok gruzov: avtoref. dis. ... dokt. tekhn. nauk: 05.22.07. Sankt-Peterburg, 2006. 55 s.

51. Normy dlya rascheta i proektirovaniya vagonov zheleznyh dorog MPS kolei 1520 mm (nesamohodnyh). Moskva: GosNIIV – VNIIZhT, 1996. 319 s.

52. NPAOP 60.1-1.48-00. Pravila bezpeki dlya pracivnikov zaliznichnogo transportu na elektrifikovanih liniyah. [31.05.2000]. Kyiv: Devalta, 2014. 159 s.

53. NPAOP 40.1-1.21-98. Pravila bezpečnoї ekspluataciji elektroustanovok spozhivachiv. [20.02.1998]. Kyiv: Derzhnaglyadohoronpraci, 1998. 91 s.

54. OST 32.55-96. Sistema ispytanyj podvizhnogo sostava. Trebovaniya k sostavu, soderzhaniyu, oformleniyu i poryadku razrabotki programm i metodik ispytanyj i attestaciji metodik ispytanyj. [11.07.1996]. Moskva: VNIIZhT, 1996. 22 s.

55. Panasenko N. N., Yakovlev P. V. Proektirovanie kontejnerov dlya morskoy perevozki dlinnomernyh trub. Vestnik Astrahanskogo gosudarstvennogo tekhnicheskogo universiteta. Seriya: Morskaya tekhnika i tekhnologiya. 2014. №3. S. 97–107.

56. Pravila perevozok opasnyh gruzov. K soglasheniyu o mezhdunarodnom zheleznodorozhnom gruzovom soobshchenii. Tom 3. OSZhD, 2011. 531 s.

57. Programa viprobuvan vagoniv-platform modelej 13-7138, 13-7138-01. Kremenchuk: UkrNDIV, 2020.

58. Proektirovanie podemnyh barabanov v SolidWorks Simulation / K. Zabolotnyj, A. Zhupiev, E. Panchenko, I. Protynyak, S. Kalyuzhnyj, Yu. Ovchinnikov. SAM–SISTEMY. 2010. № 1. S. 16 – 21.

59. RD 24.050.37-95. “Vagony gruzovye i passazhirskie. Metody ispytanyj na prochnost i hodovye kachestva”, GosNIIV, 1995.

60. Taniecheva N. A. Vybor konstruktivnyh reshenij sochlenennyh gruzovyh vagonov-platform: avtoref. dis. ... kand. tekhn. nauk: 05.22.07. Sankt-Peterburg, 2013. 16 s.

61. Tekhnicheskie usloviya razmeshcheniya i krepleniya gruzov v vagonah i kontejnerah. M., 2017.

62. Fedosov-Nikonov D.V. Pokrashchennya micnisnih yakostej dovgobaznih vagoniv-platform shlyahom udoskonalennya ih konstrukcij ta metodiv rozrahunkiv: avtoref. dis. ... kand. tekhn. nauk: 05.22.07. Kyiv, 2018. 23 s.

63. Carik R. S., Akmajkin D. A. Ocenka vliyaniya polozheniya centra tyazhesti kontejnera na metacentricheskuyu vysotu kontejnerovoza. Vestnik Gosudarstvennogo universiteta morskogo i rechnogo flota imeni admirala S. O. Makarova. 2016. №6(40). S. 58–70.

64. CV-0142. Vagoni vantazhni zaliznic Ukraini kolii 1520 (1524) mm. Nastanova z depovskogo remontu. [26.12.2013]. Kyiv: Devalta, 2014. 159 s.

65. CV-0016. Vantazhni vagoni zaliznic Ukraini kolii 1520 mm. Pravila kapitalnogo remontu. [20.06.2006]. Kyiv, 2006. 173 s.

66. Cyganskaya L. V. Vliyanie konstruktivnyh reshenij kontejnerov-cistern na ih nagruzhennost pri transportirovke zheleznodorozhnym transportom: avtoref. dis. ... kand. tekhn. nauk: 05.22.07. Sankt-Peterburg, 2008. 16 s.

67. Chepurnoj A. D., Litvinenko A. V., Shejchenko R. I., Graborov R. V., Chuban M. A. Hodovye prochnostnye i dinamicheskie ispytaniya vagona-platformy.

Visnik Nacionalnogo tekhnichnogo universitetu "Harkivs'kij politekhnichnij institut". 2015. Vip. 31 (1140). S. 111–128.

68. Shajtanova I. K. Vybor napravlenij modernizacii universalnyh vagonov-platform: avtoref. dis. ... kand. tekhn. nauk: 05.22.07. Sankt-Peterburg, 2005. 20 s.

69. Shevchenko V. V., Gorbenko A. P. Vagony promyshlennogo zheleznodorozhnogo transporta. Kyiv: Vishcha shkola, 1980. 224 s.

70. Andrew Nikitchenko, Viktor Artiukh, Denis Shevchenko, Raghu Prakash. Evaluation of Interaction Between Flat Wagons and Container at Dynamic Coupling of Flat Wagonss. MATEC Web of Conferences. 2016. Vol. 7, 04008. DOI: 10.1051/mateconf/2016 TPACEE-201 6

71. Antipin D.Ya., Racin D.Yu., Shorokhov S.G. Justification of a Rational Design of the Pivot Center of the Open-top Wagon Frame by means of Computer Simulation. Procedia Engineering. 2016.Vol. 150. P. 150–154.

72. Arkadiusz Rzeczycki, Bogusz Wisnicki. Strength analysis of shipping container floor with gooseneck tunnel under heavy cargo load. Solid State Phenomena. 2016.Vol. 252.P. 81–90.

73. Chandra Prakash Shukla, P. K. Bharti. Study and Analysis of Doors of BCNHL Wagons. International Journal of Engineering Research & Technology (IJERT). 2015. Vol. 4. Issue 04.P. 1195–1200.

74. EN 12663–2. Railway applications – structural requirements of railway vehicle bodies– Part 2: Freight wagons.[01.07.2010]. Bulgaria: BIS, 2010. 54 c.

75. Evandro C. Bracht, Thiago A. de Queiroz, Rafael C. S. Schouery, Flávio K. Miyazawa. Dynamic cargo stability in loading and transportation of containers. IEEE International Conference on Automation Science and Engineering (CASE). 2016, 21 – 25 Aug.

76. Fomin O., Gerlici J., Lovska A., Kravchenko K., Fomina Yu., Lack T. Determination of the strength of the containers fittings of a flat wagon loaded with containers during shunting. IOP Conference Series: Materials Science and Engineering. 2019. Vol. 659. 012056. doi:10.1088/1757-899X/659/1/012056.

77. Fomin Oleksij, Gerlici Juraj, Lovska Alyona, Kravchenko Kateryna, Fomina Yuliia, Lack Tomas. Determination of the strength of the containers fittings of a flat wagon. Research and Development of Mechanical Elements and Systems, IRMES 2019: Book of Abstracts for the 9th International Scientific Conference [on]. (Kragujevac, 5–7 September 2019.). Kragujevac, 2019. P. 228–229.

78. Fomin Oleksij, Lovska Alyona, Gorobchenko Oleksandr, Turpak Serhii, Kyrychenko Iryna, Burlutski Oleksii. Analysis of dynamic loading of improved construction of a tank container under operational load modes. EUREKA: Physics and Engineering. 2019. 2. P. 61–70.

79. Fomin Oleksij, Lovska Alyona, Daki Olena, Bohomia Volodymyr, Tymoshchuk Olena, Prokopenko Pavlo. The substantiation of the concept of creating

containers with viscous-elastic connections in fitting. *ARPN Journal of Engineering and Applied Sciences*. 2019. Vol. 14, No. 15. P. 2771–2776.

80. Fomin O., Lovska A., Kulbovskiy I., Holub H., Kozarchuk I., Kharuta V. Determining the dynamic loading on a semi-wagon when fixing it with a viscous coupling to a ferry deck. *Eastern-European Journal of Enterprise Technologies*. 2019. № 2/7 (98). P. 6–12.

81. Fomin O., Lovska A., Masliyev V., Tsymbaliuk A., Burlutski O. Determining strength indicators for the bearing structure of a covered wagon's body made from round pipes when transported by a railroad ferry. *Eastern-European Journal of Enterprise Technologies*. 2019. № 1/7 (97). P. 33–40.

82. Khadjimukhametova Matluba Adilovna, Rakhmatov Zafar Xasanovich. Development of improved technical means for transportation fruits and vegetables. *European science review*. 2016. P. 175 – 177.

83. Krason W., Niezgodna T. Fe numerical tests of railway wagon for intermodal transport according to PN-EU standards. *Bulletin of the Polish Academy of Sciences Technical Sciences*. 2014. Vol. 62. Iss. 4. P. 843–851.

84. Lovska Alyona. Research of dynamic loading of a container located on a flat wagon at visco-elastic interaction between fittings and fitting stops. *Globalization of scientific and educational space. Innovations of transport. Problems, experience, prospects: Theses of international scientific and practical conference*. (Salou (Spain), 4–11 May 2019). Salou (Spain): Volodymyr Dahl East Ukrainian National University, 2019. P. 57–58.

85. Pavol Šťastniak, Pavol Kurčik, Alfréd Pavlík. Design of a new railway wagon for intermodal transport with the adaptable loading platform. *MATEC Web of Conferences*. 2018. Vol. 235(2). 00030.

86. Sapronova S., Tkachenko V., Fomin O., Gatchenko V., Maliuk S. Research on the safety factor against derailment of railway vehicles. *Eastern-European journal of enterprise technologies*. 2017. Vol. 6, Issue 7 (90). P. 19–25. doi: 10.15587/1729-4061.2017.116194

87. Tomasz Kuczek, Bartosz Szachniewicz. *Topology Optimization of Railcar Composite Structure*. Inderscience Enterprises Ltd. 2014, January.

## **Appendix A**

**Program and procedure of testing on a flat car loaded with containers  
in the standard and improved diagrams of interaction between  
container fittings and fixed fittings**



## Contents

Introduction	374
1 Field of application	375
2 Purpose and task of testing	375
3 Test objects and their selection	376
4 Types and procedure of the tests	381
5 Characteristics to be determined	382
6 Testing environment	385
7 Testing procedure	388
8 Test interpretation	394
9 Requirements for personnel	402
10 Responsibilities and accountability	403
11 Safety requirements	404
References	405

## Introduction

The development of foreign economic cooperation of Ukraine as a transit country with European and Asian countries requires the introduction of combined transport systems. Today the most promising of them is the container transportation system. It is explained by the mobility of a container which can be transported by any transport facility.

The growth of container transportation is accompanied by a growth of failures in both containers and flat cars in operation. The most frequent failures in containers are cracks in container fittings and deformation of the bearing structure; most frequent failures in flat cars are cracks in fixed fittings.

In order to decrease these failures in the bearing structures of a flat car and container it is important to take into account improved loading values at the production stage. It is also of great importance to take innovative solutions aimed at a decrease in the dynamic loading in the least favourable operational diagrams, particularly, during shunting impacts. One of the possible variants to achieve the purpose is to implement improved container fittings with elastic, viscous, or viscous-elastic elements between container fittings and fixed fittings.

These measures can decrease the number of failures in flat cars and containers in operation, and reduce the costs of off-schedule repairs. Therefore, this program and procedure of testing is aimed at the determination of the dynamic characteristics and the strength of the bearing structures of a flat car and containers during operational loading modes, including elastic interaction between the fixed fittings and container fittings.

## 1 FIELD OF APPLICATION

1.1 The Program describes the consequence and procedure of the testing on flat cars and dry-freight containers.

1.2 The work is performed by specialists of the Center for Diagnostics of Transport Facilities and experienced fellows of the Department of Wagon Engineering and Product Quality of the UkrSURT (Certificate of Conformance of Measurement System to the Requirements of DSTU ISO 10012:2005, №01-0171/2019 on December 10, 2019).

1.3 The field of application is railway transport and freight rail cars.

## 2 PURPOSE AND TASK OF TESTING

### *Flat car*

2.1 According to the Program it is possible to conduct experiments within the scope of scientific and research work.

2.2 The purpose of the testing on flat cars is to determine the characteristics of strength and dynamics of the bearing structures of a flat car in the standard diagram of interaction between the fixed fittings and container fittings under operational modes in accordance with the existing standards [1], [2], [3], and also on flat cars improved with elastic elements.

2.3 The task of the wedge testing is to estimate the natural oscillation frequencies and dynamic loads in the bearing structure elements of a flat car.

2.4 The task of the standard strength testing during an impact is to determine and estimate the dynamic loads and deformations in the bearing structure of a flat car and container when the normative impact forces are applied through the coupling equipment.

2.5 The task of the dynamic testing is to determine the dynamic characteristics of a flat car moving along the rail track at various operational speeds with different train consist diagrams.

2.6 The task of strength testing on the bearing structure of a flat car with elastic interaction between the container fittings and fixed fittings is to determine the stresses and deformations in the bearing structures of a flat car and container.

### *Container*

2.7 The purpose of the testing is to verify the conformity with the strength and structural rigidity of a container during the operational loading, including also elastic interaction between the container fittings and fixed fittings.

2.8 The main task of the testing is to check the endurance characteristics of the container, examine how it can bear the normative dynamic loads, and estimate the stress state of the container structure during shunting impacts, including elastic interaction between the container fittings and fixed fittings.

### 3 TEST OBJECTS AND THEIR SELECTION

3.1 The research objects are a 13-401M1 flat car and ICC containers. If needed, other flat car types can be used. The flat cars and containers are selected out of those used at the station; they are checked for the remnants of freight, cleaned, and examined for arrangement of the certificates of selection and identification.

Representatives of the Department of Commercial Work and UkrSURT select the flat car and containers, two parallel track sections, retaining cars, hammer car, locomotive, and a locomotive crew for the testing (by order/instruction of the UZ Administration). The flat car and containers selected for the testing should be completely repaired and meet the requirements presented in [4 – 6]. The basic technical characteristics of the flat car are given in table 1 [7], and those of the container – in table 2.

Table 1 – Basic technical characteristics of a 13-401M1 flat car

Rail car type	Units	Value
Loading capacity	ton	70.0
Tare weight (min/max)	ton	18.0/20.0
Design speed	km/h	120
Size	–	0 – BM (01 – T)
Car base	mm	9720
Length along the coupler pulling faces	mm	14620
Height from the rail head top to the floor level (max)	mm	1310

Number of axles	–	4
Model of double-axle bogie	–	18-100
Transition zone	–	no
Hand brake	–	yes
Body length in the middle	mm	13300
Body width in the middle	mm	2770

3.2 The samples are identified before the testing in accordance with standards, physical form, and structure (for the flat car and container), configuration, and marking.

3.3 The flat car and containers are transported and stored according to the requirements prescribed in the standards or manuals.

Table 2 – Basic technical characteristics of a ICC container

Gross weight, t		24.00	
Cargo weight, t		21.75	
Tare weight, t		2.25	
Interior useful capacity, m <sup>3</sup>		32.70	
Dimensions, mm	External	Length	6058
		Width	2438
		Height	2591
	Internal	Length	5867
		Width	2330
		Height	2350
Doorway opening, mm		Width	2286
		Height	2261

3.4 The flat car and containers with the set of normative, technical (design) documentations, and the certificate for selection are sent to the Osnova Wagon Depot (UZ regional department) and submitted to the specialists of UkrSURT for testing.

The flat car and containers selected and received by the specialists of UkrSURT for the testing must be identified by the following characteristics:

- object name;

- object model;
- manufactory number;
- manufacturer;
- owner;
- date of production;
- type of absorbing equipment (for the flat car).

3.5 The 13-401M1 flat car (figure 1) is intended for high-capacity containers (heavy freight).

The flat car has a welded frame. The center sill consists of two I-profiles similar to the beam of the equal bending resistance. The main longitudinal beams also consist of I-profiles of constant height throughout the length. The center sill and main longitudinal beams are connected with two box-section end beams (roll-formed angle and sheet), by two box-section bolster beams, two cross-bearers, and four roll-formed I-section transverse beams.

The floorboards between the center sill and side beams are supported with additional longitudinal I-section beams rested on the frame cross bearers. The top elements of the frame cross bearers are located lower than the upper elements of the center beam and side beams at the height of additional longitudinal elements which provide the allocation of the floorboards.

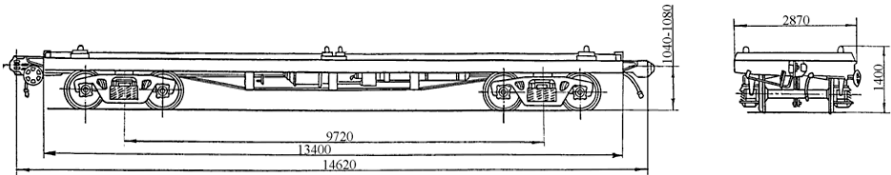


Figure 1 – Flat car 13-401M1

The end beam has a handle for a shunting master and strikers cast together with the front block of the coupler. The bearing elements are made of Steel 09C2Cu.

The bearing structure of the flat car is equipped with fixed fittings (stationary or folding) for container transportation.

3.6 The container is a disposable transportation unit which can accommodate and store the cargo transported by one or several transport means. The container can be loaded, unloaded, and transshipped mechanically, and transport a wide range of freight standardized by gross weight, dimensions, structure, and marking.

The container consists of bearing elements, top and bottom beams, and hinged door (figure 2). The information about tare, number, loading capacity, volume, and date of production is marked on the hinged door. The floor is made of wood, typically, plywood. The container is equipped with the pockets for a fork loading/unloading device. Loaded containers can be unloaded only if they have special marking. The forklift pockets are used only for 20-foot containers; they are located in the middle of the sidewalls.

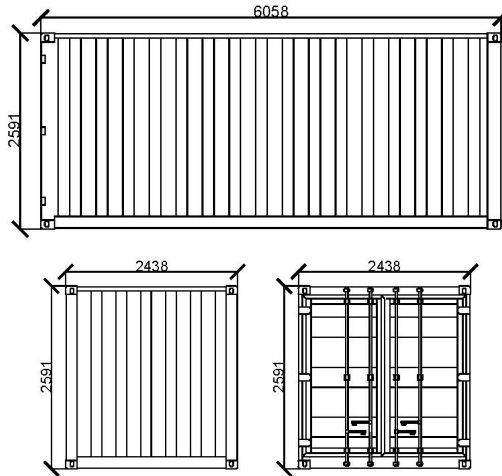


Figure 2 – Container ICC

The cast angle fittings are located on the angles of the framework; they are used for unloading with a spreader, a special device for grabbing containers. The top and bottom sidewall beams, and the angle posts (in the middle) have special rings intended for up to 1000 kg used for fixation of the freight.

The container consists of the steel frame of two roll profiles with corner fittings.

The frame consists of corner posts, top/bottom side rails, and top/bottom end rails.

The floor consists of profiled steel side rail with welded 28-mm-width cross bearers, water-proof glued plywood as the floor covering with cross members bolted and hermetically sealed in the longitudinal and transverse joints.

The sidewalls consist of a 1.5-mm profiled steel sheet, with a depth of 36 mm, water-proof and welded to the frame.

The roof is a water-proof profiled steel sheet with a depth of 2 mm, welded to the frame.

The standard container doors consist of the frame formed by empty square profiles. All external and internal surfaces are lacquered with an expendable paintwork material, with 80-  $\mu\text{m}$  internal and 110-  $\mu\text{m}$  external coating thickness.

#### 4 TYPES AND PROCEDUR OF THE TESTS

The flat car testing goes in the following order: inspection, selection and identification; wedge tests, impact tests (standard and resource); running dynamic tests; strength tests on the bearing structure of the flat car with elastic interaction of the container fittings and fixed fittings.

The tests for the container also include the dynamic testing.

The Program is designed for three testing variants for containers:

- testing in accordance with the Standards ... [6];
- testing in accordance with the Standards ... [8];
- strength testing for the bearing structure of a container with elastic interaction of container fittings and fixed fittings.

The container can be tested by one or two test variants. The results of the tests are registered in the Testing Worksheet.

The testing on containers should be in conformity to the requirements of Standards ... considered separately and approved by appropriate structural divisions; it is not within the scope of this Program.

#### 5 CHARACTERISTICS TO BE DETERMINED

5.1 During inspection, selection, and identification of the flat car and containers, they are checked for failures, such as: deformations, breaks, worn-outs, bends, deflections, corrosion, breakages, unfastening of units and details, eruptions, and cracks.

5.2 The frequency and stresses are tested during wedge tests.

5.3 During the standard impact tests the following characteristics are measured [1], [2], [3]: leading speed of the hammer car; impact force to the coupler; number of cycles before the hard fault; stresses in the flat car elements under study.



5.4 During the running dynamic tests on the car the following characteristics are measured: vertical and horizontal (transverse) accelerations of the sprung weights of the car in the area of the center bowl; dynamic side (frame) forces to the wheel-set boxes; coefficients of vertical dynamics of sprung and unsprung weights; coefficient of horizontal dynamics (ratio of the side frame force to the axial loading); and traffic speed. The values characterizing the running dynamics of freight cars are given in table 3 [1, 2, 8].

Table 3 – Running dynamic characteristics of freight cars

Motion estimation	Coefficient of vertical dynamics		Frame forces in parts of the axial loading $P_0$		Vertical $[a_z]$ and horizontal $[a_r]$ accelerations in parts g			
	$k_{zB}$ , less than		$[H_p/P_0]$ less than		$[a_z]$ less than		$[a_r]$ less than	
	empty	loaded	empty	loaded	empty	loaded	empty	loaded
Sprung weight of a car bogie								
Excellent <sup>[1]</sup> <sub>[2]</sub>	0.50	0.20	-	-	0.50	0.20	0.20	0.10
	0.50	0.20	-	-	0.50	0.20	0.20	0.10
Good <sup>[1]</sup> <sub>[2]</sub>	0.60	0.35	-	-	0.60	0.35	0.25	0.15
	0.60	0.35	-	-	0.60	0.35	0.25	0.15
Satisfactory <sup>[1]</sup> <sub>[2]</sub>	0.70	0.40	-	-	0.70	0.45	0.40	0.30
	0.70	0.40	-	-	0.70	0.45	0.40	0.30
Allowable <sup>[1]</sup> <sub>[2]</sub>	0.75	0.65	-	-	0.75	0.65	0.55	0.45
	0.75	0.65	-	-	0.75	0.65	0.55	0.45
Unsprung elements in the frame of a car bogie								
Excellent <sup>[1]</sup> <sub>[2]</sub>	0.60	0.50	0.25	0.20	0.65	0.55	0.30	0.25
	0.60	0.50	0.25	0.20	0.65	0.55	0.30	0.25
Good <sup>[1]</sup> <sub>[2]</sub>	0.75	0.70	0.30	0.25	0.80	0.75	0.35	0.30
	0.75	0.70	0.30	0.25	0.80	0.75	0.35	0.30
Satisfactory <sup>[1]</sup> <sub>[2]</sub>	0.85	0.80	0.38	0.30	0.90	0.85	0.50	0.35
	0.85	0.80	0.38	0.30	0.90	0.85	0.50	0.35
Allowable <sup>[1]</sup> <sub>[2]</sub>			0.40	0.38	0.98	0.90	0.55	0.45
			0.40	0.38	0.98	0.90	0.55	0.45

\*– the numerator includes the value for unloading, the nominator includes the value for additional loading.

1 – DSTU 7598:2014 Freight cars. General requirements for calculation and design of new and modernized 1520-mm cars (unpowered).

2 – DSTU GOST 33211:2017 “Freight cars. Requirements for strength and dynamic characteristics”.

The strain gages are located on the bearing structures of the test flat car and containers and chosen according to the appropriate diagrams [1], [2], [3].

5.5 The strength testing on the bearing structure of the flat car with elastic interaction of the container fittings and fixed fittings is conducted for measuring the stresses in the bearing structure of the flat car.

5.6 The dynamic tests on the container are conducted for measuring the characteristics presented in table 4.

Table 4 – Characteristics under control during impacts for various dynamic tests on the container

Characteristics to be measured	Conditions of control
	“Standards ...”
The leading speed of the flat car with containers under study to the supporting wall, and the hammer car – to the flat car	+
The force to the coupler of the flat car with the test container during an impact	+
Longitudinal accelerations of the container during an impact, measured on the bottom fittings	–
Deformations in the container elements	+

Identification marking: “+” – mandatory control;  
“–” – not under control.

5.7 The strength tests on the bearing structure of the flat car with elastic interaction between the container fittings and fixed fittings are carried out for measuring the stresses in the bearing structure of the flat.

## 6 TESTING ENVIRONMENT

### *Flat car*

6.1 The visual control of the technical state can reveal deformations, breaks, worn-outs, deflections, bends, corrosion, unfastened units and details, eruptions, cracks in frame elements, flat car body, and containers.

6.1.1 If it is impossible to visually detect obvious defects (e.g., cracks), the magnetic particle and capillary methods of non-destructive control are used [1], [2], [3].

6.2 The factors which can stop the tests are

- completing the testing program;
- obtaining the critical values which may put the safety of further testing at risk;
- failures, breakages of some parts of the test car; and
- obtaining the whole set of experimental data prescribed by the Program.

6.3 The natural oscillation frequencies are estimated by the results of the wedge testing. The strain gages are mounted on the frame of the flat car according to the diagram of the control points. The wedges are placed under the wheels according to the natural oscillation frequencies under study, the car is rolled on the wedges and after that the wedges are removed.

6.4 The standard impact tests for the determination of the strength of the structural elements of the car should be conducted during the daytime on the horizontal track section with a locomotive. Apart from the locomotive the following equipment is used:

- a hammer car with a mass exceeding the mass of the test car;
- three or four braked retaining freight cars with the total mass exceeding 300 tons; they cannot move due to brake shoes; and
- a dynamometric test car (on the adjacent track).

6.5 The difference between the axle levels of the couplers for the test car and hammer car should not exceed 50 mm.

6.6 During impacts of the cars the largest longitudinal force to the coupler should be within a range of the normative force values.

6.7 The running dynamic tests are conducted on the cars equipped according to the appropriate technical documentations with the appropriate certificates of selection and identification.

The testing should be approved by the UZ Administration and the administration of the Southern Railway.

The running dynamic tests should be conducted during testing runs in real operational conditions during the daytime; the dynamic processes are being registered in the control points.

6.8 The strength tests on bearing structure of the flat car with elastic interaction of the container fittings and fixed fitting are used for determination

of the strength of the structural elements of the car during the daytime on the straight horizontal track section. The impact is made with a locomotive. Apart from the locomotive the following equipment is used:

- a hammer car with a mass exceeding the mass of the test car;
- three or four braked retaining freight cars with the total mass exceeding 300 tons; their motion is restricted by rail shoes; and
- a dynamometric test car (on the adjacent track).

6.9 The difference between the axle levels of the couplers of the car under study and the hammer car should not exceed 50 mm.

6.10 During impacts of the cars the largest longitudinal force to the coupler should be within a range of the normative force values.

6.11 The sequence and technology used for preparation of the object for the testing should be convenient and comply with the safety requirements for all the program procedures.

6.12 The condition of the test beginning means the completion of the mounting of the measuring indicators and diagrams, installation of the appropriate equipment, and the readiness of the technical means for the testing.

#### *Container*

6.13 The containers are tested for dynamic characteristics.

6.14 The dynamic tests are conducted on a straight track section during the daytime at the environment temperature and air humidity which ensure the stable operation of the measuring equipment.

6.15 The strength tests on the bearing structure of the container with elastic interaction of the container fittings and fixed fitting are used for the determination of the strength of the structural elements of the container during the daytime. The containers are located on the flat car. The tests are conducted on a straight horizontal track section. The impact is fulfilled by means of the locomotive.

6.16 The condition of the completion of the testing is the obtaining of all experimental data prescribed by the Program.

6.17 The condition for stoppage of the tests is failures in the container structure, which can put further testing at risk.

6.18 The sequence and technology of the testing must ensure the fulfillment of the tasks and the achievement of the objectives of the testing on the full scale basis with maximum convenience and safety.

## 7 TESTING PROCEDURE

*Flat car*

7.1 Wedge tests.

The car is rolled with the locomotive to the wedges (height is over 25 mm, length – 350 mm, and width – 50 mm). The wedges are mounted in turn (table 5):

- 1) under all the wheels of the car (simulation of bouncing);
- 2) under the wheels of one bogie on the right side and the wheels of the other bogie on the left side (simulation of torsion);
- 3) under all the wheels of one bogie (simulation of galloping);
- 4) under the wheels on one side of the car (simulation of side rolling).

Table 5 – Diagram of wedges mounted under the car wheels

№	Type of oscillations	No. of a wheel set			
		1	2	3	4
1	Bouncing				
2	Torsion of the body				
3	Galloping				
4	Side rolling				

According to the number of the wedges and their locations under the appropriate car wheels, deflections, frequencies and stresses during a run and wedge tests are determined.

The whole cycle of the testing includes three tests for each wedge diagram.

7.2 The procedure of the standard impact tests includes the following:

- loading the car to the nominal load capacity;
- weighing of the loaded car;
- equipping the car with a special coupler-dynamometer, previously calibrated with application of the static loading to 3 – 3.5 MN;
- putting the car on the test track section and the stake for the determination of the rolling speed of the hammer car;
- impact testing;
- measuring deformations, rolling speed, and impact force of the hammer car with the measuring equipment; and
- examining the structures after each 3-5 impacts during the standard impact tests.

The impact tests are conducted by rolling the hammer car with the locomotive to the test car supported or unsupported. The supported state: the test car is coupled to the supporting wall; the unsupported state: the test car is not coupled to the supporting wall, its location being at a one-meter distance from the retaining cars.

The support is formed of 3-4 braked loaded freight cars with the total weight exceeding 300 tons; their motion is additionally restricted with brake shoes.

The impacts of the freight cars during the standard tests are made at the speeds given in table 6.

Table 6 – Number of impacts of the flat car in each speed interval when the cars are supported/not supported during the standard tests

Range of impact speed, km/h	Number of impacts	
	Supported	Unsupported
From 3 to 6	7	7
From 6 to 10	7	7
From 10 to 12	3	3

#### 7.4 The sequence of running dynamic tests.

7.4.1 The test freight cars must be equipped with the primary measuring transmitters and devices for measuring the values under study and the processes according to the requirements. The recommended mounting diagrams of these devices are given in figures 3 and 4.

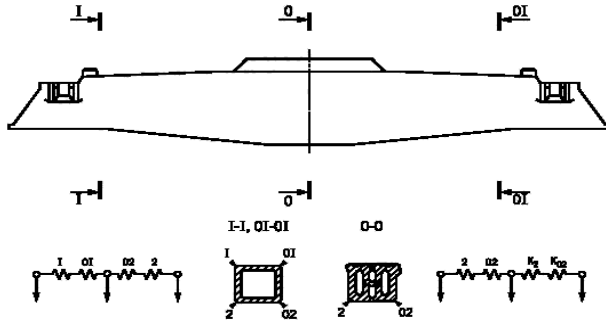


Figure 3 – Diagram of mounting and connecting the strain gages for the determination of the vertical dynamic coefficients in the bolster beam sections of the freight car bogie

$K_2, K_{O2}$  – compensating strain gages

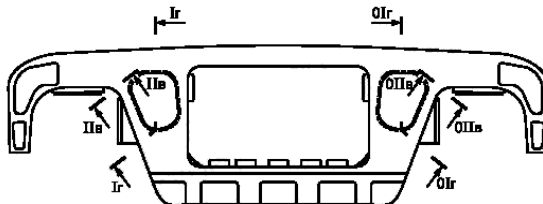
The 13-401 flat car is tested for two bogie variants:

- bogies without deviations in the units and details; and
- bogies with deviations.

The constant multiplier, installations and devices for recording and processing the test data are located in the dynamometric car.

7.4.2 The control check of the measuring values recorded should be done daily before the beginning and after the completion of each cycle of test runs, or more frequently, if needed.

7.4.3 The actual values of static deflections in the spring suspension, stresses in the bogie elements during the static loading from the gravity force of the car tare are determined, the sensitivity of the measuring diagrams is checked, etc, with the control lifting of the car bodies up to the full unloading of bogies.



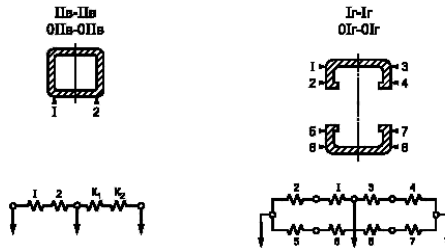


Figure 4 – Diagram of mounting and connecting the strain gages for measuring horizontal (frame) forces (section with index “I”) and vertical forces (section with index “B”) on the bogie frame of the freight car.

$K_1, K_2$  compositing strain gages

\* – size for information

7.3 The sequence of the impact tests with elastic interaction of the container fittings and fixed fittings.

The tests are made in the dynamic mode at various impact speeds in the interval and conditions specified in the standards [1 – 3]. The stresses in the bearing structure of the flat car with elastic interaction of the container fittings and fixed fittings are also determined (figure 5).

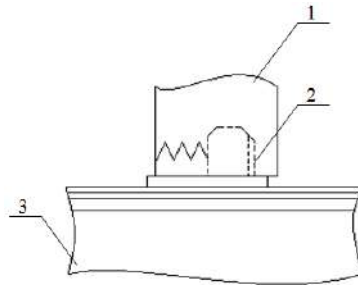


Figure 5 – Diagram of interaction between the container fitting and fixed fitting  
 1 – container fitting; 2 – fixed fitting; 3 – longitudinal beam of the flat car

A spring with a given rigidity is mounted between the fixed fitting and the inner surface of the container fitting. The total rigidity of the springs for one container should be more than 1700 kN/m. The geometric parameters of the spring are given in figure 6.

The side part of the fitting is cut and the springs are mounted between it and the fixed fitting. The end parts of the spring are rested on the vertical part of the fixed fitting of the flat car and the container fitting.



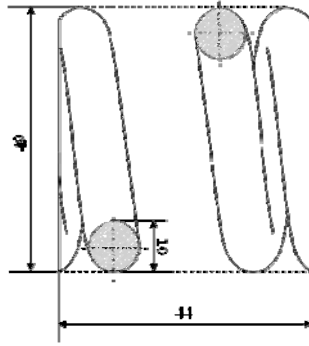


Figure 6 – Geometrical dimensions of the spring

### *Container*

7.4 The container is tested according to ПД 24.050.37 – 95 and “Standards ...”.

The dynamic testing (impact tests) are conducted on the container loaded to the full capacity and located on the technological flat car according to [8].

The hammer car is rolled on the flat car with the container (at first within the supporting wall, and then in a free state at a distance of 1.0 – 1.5 m from the supporting wall).

The impacts are fulfilled at the speeds from 3 km/h to the speed which generates the impact force from 6 to 10 km/h and over 10 km/h; generally no less than seven impacts at each interval should be performed. More than three impacts should be performed at the maximum impact load. The maximum impact force should not exceed the maximum design force according to the Standards ... more than at 10%.

The difference between the levels of the couplers should not exceed 50 mm.

The state of the container and the flat car should be monitored. When the longitudinal force reaches 2.5 MN, the examination should be made after each impact.

The characteristics presented in item 5 are measured during the testing.

Typically, the deformations are measured at the spacer bars in the container fittings and near the supports, on the supports near the spacer bars,

and in other areas according to the structural features of the container in accordance with [9].

7.6 The strength tests for the bearing structure of the container with elastic interaction of the container fittings and fixed fittings are conducted in the dynamic mode at various impact speeds in the interval and conditions specified in the standards [1 – 3]. The stresses in the bearing structure of the container are determined with consideration of elastic interaction of the container fittings and fixed fittings.

## 8. TEST INTERPRETATION

8.1 The data on the static loading are processed with automated data processing complexes. The stresses during the static tests are determined as the difference of indications of the measuring equipment before the flat car frame is lifted and after it [10]

$$\sigma_{\text{exp}} = (\Delta - \Delta_0) \cdot K \quad (1)$$

where  $\Delta$  – indications of the measuring equipment when the test item is loaded;

$\Delta_0$  – indications of the measuring equipment when the test item is empty;

$K$  – calibrating coefficient of the measuring equipment determined by formula (2)

$$K = \frac{R_x}{R_{\text{ш}} \cdot A_{\text{ш}}} \quad (2)$$

where  $R_x$  – resistance of the strain gage, Ohm;

$R_{\text{ш}}$  – resistance of the calibration shunt, Ohm;

$A_{\text{ш}}$  – amplitude (discrepancy) of the process, measured during the calibration, B.

8.2 The stresses  $\sigma$  MPa, in the elements of the structure at the areas of the strain gages are determined by formula (3)

$$\sigma = a \cdot \frac{R_x}{R_{\text{ш}} \cdot A_{\text{ш}}} \cdot \frac{E}{K_{\text{ш}}} \quad (3)$$

where  $a$  – amplitude (deflection) of the process, B;

$R_{\text{ш}}$  – resistance of the strain gage, Ohm;

$R_{\text{м}}$  – resistance of the calibration shunt, Ohm;

$A_{\text{м}}$  – amplitude (discrepancy) of the process, measured during the calibration, B.

$E$  – elastic modulus of the material of the test detail, MPa;

$K_{\text{м}}$  – sensitivity coefficient of the strain gage.

8.3 The stress state of the structural elements of the car in operation is estimated by testing modes I and II:

- total stresses for mode I calculated by formula [8]

$$\sigma_{\text{веп}} + \sigma_{\text{нпо}} + \sigma_{Pz} + \sigma_{Pn} < [\sigma]_I, \quad (4)$$

where  $\sigma_{\text{веп}}$  – stresses from the vertical loading of the gross weight, MPa;

$\sigma_{\text{нпо}}$  – stresses from the longitudinal loading of the gross weight, MPa;

$\sigma_{Pz}$  – vertical component of the dynamic force to the bogie from the longitudinal inertia force, MPa;

$\sigma_{Pn}$  – transverse component of the longitudinal quasi-static force, MPa;

$[\sigma]_I$  – allowable stresses in the car elements during mode I, MPa.

- total stresses for mode III are calculated by formula [8]

$$\sigma_{\text{веп}} + \sigma_{\text{нпо}} + \sigma_{\text{дин}} + \sigma_{P\text{ч}} < [\sigma]_{III}, \quad (5)$$

where  $\sigma_{\text{веп}}$  – stresses from the vertical loading of the gross weight, MPa;

$\sigma_{\text{нпо}}$  – stresses from the longitudinal loading of the gross weight, MPa;

$\sigma_{\text{дин}}$  – stresses from the vertical dynamic increment, MPa;

$\sigma_{P\text{ч}}$  – stresses from the lateral force, MPa;

$[\sigma]_{III}$  – allowable stresses in the car elements during mode III, MPa.

8.4 The strength of the structure according to the results of the impact tests is estimated by formula [8]

$$(\sigma_{\text{вep}} + \sigma_{\text{ylo}}) \leq \sigma_m, \quad (6)$$

where  $\sigma_{\text{вep}}$  – stresses from the vertical loading of the gross weight, MPa;

$\sigma_{\text{нpo}}$  – stresses from an impact force of 3.5 MPa;

$\sigma_{\text{дun}}$  – yield limit of the material, MPa.

8.5 The results of the running dynamic tests are determined on the basis of data (measurements, calculations, control, observation) taken during the measurements.

The preliminary analysis and processing of the data taken during the running dynamic tests are made by computer in real time and after the testing with the mathematical statistic data processing software for dynamic processes. The processing and estimation of the test results are made according to the requirements [1, 11, 12].

The dynamic processes registered during the tests are processed by the program for calculation of instantaneous amplitudes of the process. The discretisation frequency of the dynamic processes recorded is chosen as over 128 Hz; it allows determining the values in the required frequency range. The characteristics of the processes and their maximum values are calculated at the probability corresponding to the normative values. The final values in each speed range are obtained by choosing the mean value for each realization. Finally, one value for an indicator within each speed range with an interval of 10-20 km/h beginning with a speed of 30-40 km/h is determined. These values are used for the basic conclusions of the running dynamic characteristics of the test cars.

The strength of a wheel against derailment is determined for the most dangerous cases when the lateral interaction wheel/rail force combines with a low vertical loading on this wheel. If this external combination of the forces continues for some time, the wheel flange can roll on the rail head which results in derailment.

8.6 The test results are recorded.

The test protocol and all the materials on the testing are stored in UkrSURT on a basis of confidentiality.

8.7 Processing of the running dynamic test data.

8.7.1 The processing of the running dynamic test data includes deciphering, identification, and systematization of the dynamic process values.

The data processing includes the running performance index of the car up to 20 Hz. During the computerization of the test results, the sampling frequency should exceed 100 Hz.

8.7.2 The test data are grouped by traffic speed range (10-20 km/h) according to special features of track sections (direct sections, straight sections, switches, etc.).

8.7.3 During the analysis of the processes recorded the typical oscillation types are found and the dependency of the character and intensity of the oscillations on the traffic conditions is estimated. According to the probable character of the dynamic loading of the gear parts of the cars (including the peculiarities of the technical state of the gear parts, and the transport structure) the appropriate machinery of probability theory should be applied.

8.7.4 In order to estimate the performance according to the dynamic characteristics of the car with the use of the dependencies including calibrating data, the following factors should be determined: potential maximum values of the vertical dynamic coefficients of the sprung  $K_{\text{до}}$  and unsprung  $K_{\text{нн}}$  car weights, lateral (frame) forces, horizontal dynamic coefficient  $K_{\text{дт}}$ , and values of the coefficient of the strength reserve against derailment  $K_{\text{yc}}$ .

The maximum values of the coefficients of vertical and horizontal dynamics and frame forces are determined with a confidence probability of 0.999 (by amplitude value) and 0.001 (by instantaneous value), and the minimal values of the coefficients of strength reserve against derailment with a confidence probability of less than 0.001.

The value of lateral (frame) forces is taken as the sum of the frame forces acting simultaneously to the frame from each box of one wheel set.

8.7.5 The technique for calculation of the coefficient of strength reserve against derailment when the wheel flange rolls on the rail due to the dynamic forces during the motion, the coefficient of vertical dynamics of the sprung and unsprung weights of the car is presented below. Generally, the coefficient of vertical dynamics is determined as follows

$$K_{\text{д}}^c = \frac{\sigma_{\text{д}}}{\sigma_{\text{ст}}}, \quad (7)$$

where  $\sigma_{\text{д}}$  – dynamic stresses from the vertical loading in the section of a given element;  
 $\sigma_{\text{ст}}$  – static loading from the vertical loading in the same section.

The coefficients of vertical dynamics are determined for the sprung ( $K_{\text{ср}}$ ) and unsprung ( $K_{\text{нср}}$ ) weights of the bogies.

The horizontal dynamic coefficient (the frame force in fractions of the axial loading)  $K_{\text{гп}}$  is determined by the formula

$$K_{\text{гп}} = \frac{H_{\text{гп}}}{P_{\text{с}}} \quad (8)$$

where  $H_{\text{гп}}$  – horizontal lateral frame force;  
 $P_{\text{с}}$  – vertical static loading from the axle to the rail.

The coefficient of strength reserve against derailment is calculated with the integral coefficient for the range of operational speeds at a probability of 0.001.

The wheel stability against derailment is estimated by the formula

$$K_{\text{yc}} = \frac{t_{\text{г}}\beta - \mu}{1 + \mu t_{\text{г}}\beta} \cdot \frac{Q_{\text{м}} \left( \frac{2(b - a_1)}{l} - K_{\text{н}}^{\text{н}} \frac{2b - a_1}{l} + K_{\text{н}}^{\text{нн}} \frac{a_2}{l} \right) + q \frac{b - a_1}{l} + \frac{r}{l} H_{\text{гп}}}{\mu Q_{\text{м}} \left( \frac{2(b - a_1)}{l} + K_{\text{н}}^{\text{н}} \frac{a_1}{l} - K_{\text{н}}^{\text{нн}} \frac{2b - a_1}{l} \right) + \mu q \frac{b - a_1}{l} + (1 - \frac{r}{l}) H_{\text{гп}}}, \quad (9)$$

where  $\beta$  — gradient of the generatrix of the wheel flange to the horizontal axle;  $\beta = 60^\circ$ ;

$\mu$  – friction coefficient, = 0.25;

$q$  – gravity force of the unsprung weights to a wheel set, N;

$2b$  – distance between the middle parts of the axle necks of a wheel set, m;

$a_1, a_2$  – design distance from the contact points of the wheels with the rails to the middle of the corresponding (leading and non-leading) axle necks of a wheel set are taken 0.250 and 0.220 m, respectively;

$r$  – wheel rolling radius,  $r=0.45\text{m}$  (for an average worn-out wheel), or according to the results of measurements of the wheels of the test sample;

$K_{\text{н}}^{\text{н}}$  – vertical dynamics coefficient on the leading wheel; the coefficient values are taken positive for unloaded wheels;

$K_{\text{н}}^{\text{нн}}$  – vertical dynamic coefficient for a leading wheel; the coefficient values are taken positive for unloaded wheels;

$H_{\text{гп}}$  – horizontal lateral frame force.

$Q_{\text{м}}$  – gravity force of the bolster parts of the car, applied to the axle neck of a wheel set, kN; determined by the formula

$$Q_{\text{ш}} = \frac{Q - n \cdot Q_{\text{кг}}}{2n_0}, \quad (10)$$

where  $Q$  – weight of the car, kN;

$Q_{\text{кг}}$  – gravity force of the unsprung parts, applied to a wheel set, kN;

$n$  – number of the car axles;

$K_{\text{д}}^{\text{л}}$  – vertical dynamic coefficient for a leading wheel;

$K_{\text{д}}^{\text{н}}$  – coefficient of vertical dynamics for a non-leading wheel;

$H_{\text{п}}$  – horizontal lateral frame force.

The value  $H_{\text{п}}$  is taken positive if it is directed to the leading wheel, and  $K_{\text{д}}^{\text{л}}$  and  $K_{\text{д}}^{\text{н}}$  – if the wheels are unloaded.

The dynamic characteristics of the flat car are estimated by comparing the dynamic values obtained with the rating scale for performance of a rail car in accordance with [1, 2], and also with the corresponding characteristics of the model car.

8.8 The deformations measured in the locations of the strain gages are converted to stresses by formula [11].

For single strain gages

$$\sigma = E \cdot \varepsilon, \quad (11)$$

where  $E$  – elasticity modulus of the 1<sup>st</sup> type, MPa;

$\varepsilon$  – relative deformation.

For a T-shape socket at  $\mu = 0.3$  and a known direction of the main stresses (the direction of  $\sigma_x$  and  $\sigma_y$  correspond to  $\varepsilon_1$  and  $\varepsilon_2$ ).

$$\sigma_x = 1,1 \cdot \varepsilon_1 \cdot E + 0,33 \cdot \varepsilon_2 \cdot E, \text{ MPa} \quad (12)$$

$$\sigma_y = 1,1 \cdot \varepsilon_2 \cdot E + 0,33 \cdot \varepsilon_1 \cdot E, \text{ MPa} \quad (13)$$

where  $\varepsilon_1$  and  $\varepsilon_2$  – relative deformations.

If the direction of the main stresses is not known, spread sockets of three strain gages are recommended.

The deformations measured by the strain gages mounted along the axle of the object have the “a” index, across the axle – the “σ” index, under the angle of 45° – the “B” index.

For spread sockets it is recommended to determine the deformations along the main stresses by the formula

$$\varepsilon_{1,2} = \frac{\varepsilon_a + \varepsilon_b}{2} \pm \frac{\sqrt{2}}{2} \sqrt{(\varepsilon_a - \varepsilon_b)^2 + (\varepsilon_c - \varepsilon_d)^2} \quad (14)$$

The values of deformations determined by formula (14) are put to formulae (12) and (13) for determination of the main stresses in the test point.

The equivalent stresses are determined through the main stresses in each point by the formula

$$\sigma = \sqrt{\sigma_x^2 + \sigma_y^2 - \sigma_x \sigma_y}, \text{ MPa} \quad (15)$$

During the strength impact tests the results are processed with the method of maximum amplitude values. The amplitude value is multiplied by the scale – m, MPa/mV, determined by calibrating with the formula

$$m = \frac{R_o \cdot E}{R_u \cdot A_u \cdot K}, \quad (16)$$

where  $R_o$  – resistance of a strain gage, Ohm;  
 $E$  – elasticity modulus, MPa;  
 $R_u$  – shunt resistance, Ohm;  
 $A_u$  – unbalance of the measuring diagram with the shunt resistance, mV;  
 $K$  – coefficient of strain sensitivity of a strain gage.

The test results of leading speeds for the hammer car, impact forces to the coupler, and stresses in the test points are used for building dot diagrams of the dependencies between impact force to the coupler and impact speed, and dependencies between stresses in the test points and leading speed of the hammer car; the approximating curves of these values for a free flat car with the



test container and the flat car with a supported container are added to these diagrams.

The diagrams obtained can be used for determination of the leading speed for the hammer car, which corresponds to an impact force of 3.5 MN and the values of stresses in each point at an impact force of 3.5 MN –  $\sigma_{y0}$ .

## 9 REQUIREMENTS FOR PERSONNEL

The testing can be conducted only by those over 18 years of age, by those who have taken appropriate training, have the exam on safety passed, and have the appropriate certificate.

## 10 RESPONSIBILITIES AND ACCOUNTABILITY

10.1 The test manager and the executive officer are appointed by the director of the Center for Diagnostics of Transport Facilities under UkrSURT.

10.2 The test manager is in charge of:

- preparation of the program and the test schedule;
- provision of the needed documents for the test car;
- arrangement of the needed documents for the testing;
- preparation of the test car for the testing in a set period;
- performance of the tests scheduled;
- record of the test results on the basis of the actual and factual information regarding the characteristics of the test cars needed for evaluating the state according to the standards;
- preparation of the protocol of the test results; and
- provision of the safe traffic for the test car.

10.3 The executive officer is responsible for:

- preparation of the test units and measuring equipment for the testing;
- record of all the measuring values and their processing;
- determination of the characteristics by the results of measurement;
- preparation of the test protocol according to the results of the test measurements;
- provision of the safety for all personnel participating in the testing on the test car.

## 11 SAFETY REQUIREMENTS

11.1 The safety requirements should be observed during preparation, conduction, and completion of the tests. These requirements are presented in

- Occupational Safety Rules during technical service and repair of freight cars and refrigerating rolling stock, НПАОП 63.21–1.24 –03;
- Fire safety regulations on the railway transport, НАПБА 01.001–2004.
- Occupational safety and health training according to the requirements НПАОП 0.00–4.12–05;

11.2 Occupational safety and health training according to the requirements НПАОП 0.00–4.12–05.

11.3 Before the testing all personnel should be instructed and trained on the occupational safety with appropriate registration in the test sheet.

11.4 The work on preparation and testing should be supervised and controlled by the test manager. The measuring equipment and instruments should be safe in use.

11.5 Persons under 18 are not allowed for the testing;

11.6 The testing should be done only during the daytime;

11.7 The persons involved in the tests should have special uniform, personal protections items, and means of communication.

11.8 The testing under the test car can be conducted only with the permission of the test manager.

11.9 The mounting of the measuring equipment, commutation, adjustment, and regulation can be done by those certified for this work.

11.10 The mounting of the measuring equipment on the external surfaces of the test car can only be done when the test cars are secured against motion.

11.11 The work under the test car and on its body on the station and main tracks is prohibited. This work can be done only on the territories of regional enterprises, when the car enclosed, and on the tracks of a noncontact network.

11.12 The devices and communication means installed should not exceed the dimensions of the rolling stock and hamper the normal interaction of all the elements of the test rolling unit. They should be securely fixed.

11.13 Only certified specialists with appropriate permission can work with the testing equipment.

## REFERENCES

- 1 . DSTU 7598-2014 “Vagoni vantazhni. Zagalni vimogi do rozrahunkiv ta proektuvannya novih i modernizovanih vagoniv kolii 1520 mm (nesamohidnih)”.
- 2 . DSTU GOST 33211:2017 “Vagoni vantazhni. Vimogi do micnosti ta dinamichnih yakostej”.
- 3 . OST 32.55-96 “Sistema ispytaniy podvizhnogo sostava. Trebovaniya k sostavu, soderzhaniyu, oformleniyu i poryadku razrabotki programm i metodik ispytaniy i attestacii metodik ispytaniy”.
- 4 . CV-0142 Vagoni vantazhni zaliznic Ukraini kolii 1520 (1524) mm. Nastanova z depovskogo remontu. Zatverdzheno nakazom Ukrzaliznici vid 26.12.2013 №468-C/od.
- 5 . CV-0016 Vantazhni vagoni zaliznic Ukraini kolii 1520 mm. Pravila kapitalnogo remontu, priynyato nakazom Ukrzaliznici vid 20.06.2006 №242-C.
- 6 . Morskoy Registr Sudohodstva. Pravila izgotovleniya kontejnerov, Sankt-Peterburg, 2002.
- 7 . 002-2009 PKB CV Albom-spravochnik “Gruzovye vagony zheleznyh dorog kolei 1520 mm”. OAO “RZhD”, filial “Proektno-konstruktorskoe byuro vagonnogo hozyajstva”. – 741 s.
- 8 . Normy dlya rascheta i proektirovaniya vagonov zheleznyh dorog MPS kolei 1520 mm (nesamohodnyh), GosNIIV-VNIIZhT, M, 1996.
- 9 . Tekhnicheskie usloviya pogruzki i krepleniya gruzov. M., Transport, 1990.
- 10 Metodika vypolneniya izmerenij staticheskikh i dinamicheskikh deformacij pri ispytaniyah izdelij mashinostroeniya. Mariupol, 1998.
- 11 RD 24.050.37-95. “Vagony gruzovye i passazhirskie. Metody ispytaniy na prochnost i hodovye kachestva”, GosNIIV, 1995.
- 12 RD.24.050.37.95 “Vagony gruzovye i passazhirskie. Metodi ispytaniy na prochnost i hodovye kachestva (Vagoni vantazhni j pasazhirski. Metodi viprobuvan na micnist ta hodovi yakosti)”.





Oleksij Fomin, Alyona Lovska

Improved models and constructs of structural interaction in railway container transportation

